



U.S. Department
of Transportation

**Federal Highway
Administration**

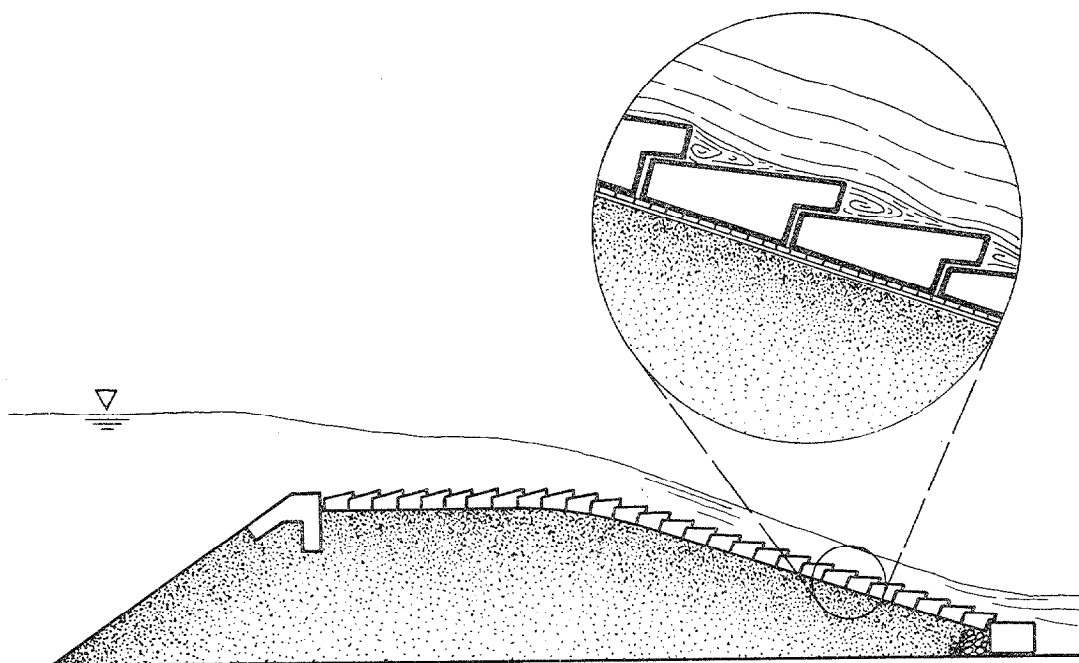
Cosponsored by:

U.S. Dept. of Interior
Bureau of Reclamation
Denver, Co. 80225

U.S. Dept. of Agriculture
Soil Conservation Service
Washington, D.C. 20013

Tennessee Valley Authority
Knoxville, Tn. 37902

HYDRAULIC STABILITY OF ARTICULATED CONCRETE BLOCK REVTMENT SYSTEMS DURING OVERTOPPING FLOW



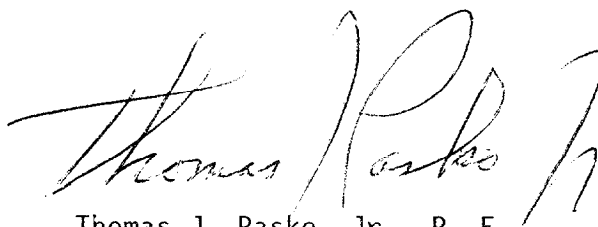
Research, Development, and Technology
Turner-Fairbank Highway Research Center
6300 Georgetown Pike
McLean, Virginia 22101-2296

Publication No. FHWA-RD-89-199
November 1989

FOREWORD

This report is the third in a series of three that describe a large scale model study of embankment damage due to flood overtopping and of performance of selected protective measures for embankments. This report describes hydraulic tests on the performance of articulated concrete block systems for protecting embankments. This report will be of interest to State highway hydraulics engineers, consultants and federal government engineers who deal with flood damage evaluations and with stability of earth embankments.

Sufficient copies of this report are being distributed by an FHWA transmittal memorandum to provide a minimum of one copy to each regional office, division office, and State highway agency. Direct distribution is being made to the division offices. Additional copies may be obtained from the National Technical Information Service, 5285 Port Royal Road, Springfield, Virginia 22161.



Thomas J. Pasko, Jr., P. E.
Director, Office of Engineering and
Highway Operations Research and Development

NOTICE

This document is disseminated under the sponsorship of the Department of Transportation in the interest of information exchange. The United States Government assumes no liability for its contents or use thereof.

The contents of this report reflect the views of the author who is responsible for the facts and the accuracy of the data presented herein. The contents do not necessarily reflect the policy of the Department of Transportation.

This report does not constitute a standard, specification, or regulation. The United States Government does not endorse products or manufacturers. Trade or manufacturers' names appear herein only because they are considered essential to the objective of this document.

1. Report No. FHWA-RD-89-199		2. Government Accession No.		3. Recipient's Catalog No. FHWA-RD-89-199	
4. Title and Subtitle HYDRAULIC STABILITY OF ARTICULATED CONCRETE BLOCK REVTMENT SYSTEMS DURING OVERTOPPING FLOW				5. Report Date Nov 1989	
				6. Performing Organization Code DC-FHA-04	
				8. Performing Organization Report No.	
7. Author(s) Paul E. Clopper, P.E.				10. Work Unit No. (TRAIS) NCP 3D32062	
9. Performing Organization Name and Address Simons, Li & Associates, Inc. 3555 Stanford Road P.O. Box 1816 Fort Collins, CO 80522				11. Contract or Grant No. DTFH61-83-C-00131	
				13. Type of Report and Period Covered Final Report Aug 1988 - July 1989	
12. Sponsoring Agency Name and Address Office of Engineering & Highway Operations R & D Federal Highway Administration 6300 Georgetown Pike McLean, VA 22101-2296				14. Sponsoring Agency Code	
15. Supplementary Notes Contracting Officer's Technical Representative: J. Sterling Jones Co-sponsoring agency: U.S. Bureau of Reclamation (HNR-10) Soil Conservation Service Tennessee Valley Authority					
16. Abstract Initial investigations of articulated concrete block revetment systems were performed as part of an overall study to examine methods of protecting earth embankments during overtopping flow. The results of the initial study are presented in Report No. FHWA-RD-88-181. The favorable performance of these earlier tests resulted in additional and more detailed investigations which are presented in this report. In this study, the hydraulic characteristics and stability of articulated concrete block revetment systems in high-velocity overtopping flow are examined. Seventeen hydraulic tests were performed on five different revetment systems, including cable and uncabled installations. Eight of the tests were conducted over a rigid concrete test embankment, while the remainder were conducted over an embankment made of highly erosive soil. Hydraulic data were collected both above and below the revetment system, the latter being accomplished through the use of a remote pressure transducer network. Relationships involving pressure, velocity, depth, and slope on the stability and resistance to flow are developed and presented.					
17. Key Words overtopping, embankment, erosion, erosion protection systems, hydraulics, shear stress, channels spillways, floods, revetment, concrete blocks			18. Distribution Statement No restrictions. This document is available to the public through the National Technical Information Service (NTIS). Springfield, VA 22161		
19. Security Classif. (of this report) Unclassified		20. Security Classif. (of this page) Unclassified		21. No. of Pages 140	22. Price

SI* (MODERN METRIC) CONVERSION FACTORS

APPROXIMATE CONVERSIONS TO SI UNITS

Symbol	When You Know	Multiply By	To Find	Symbol
--------	---------------	-------------	---------	--------

LENGTH

in	inches	25.4	millimetres	mm
ft	feet	0.305	metres	m
yd	yards	0.914	metres	m
mi	miles	1.61	kilometres	km

AREA

in ²	square inches	645.2	millimetres squared	mm ²
ft ²	square feet	0.093	metres squared	m ²
yd ²	square yards	0.836	metres squared	m ²
ac	acres	0.405	hectares	ha
mi ²	square miles	2.59	kilometres squared	km ²

VOLUME

fl oz	fluid ounces	29.57	millilitres	mL
gal	gallons	3.785	litres	L
ft ³	cubic feet	0.028	metres cubed	m ³
yd ³	cubic yards	0.765	metres cubed	m ³

NOTE: Volumes greater than 1000 L shall be shown in m³.

MASS

oz	ounces	28.35	grams	g
lb	pounds	0.454	kilograms	kg
T	short tons (2000 lb)	0.907	megagrams	Mg

TEMPERATURE (exact)

°F	Fahrenheit temperature	$5(F-32)/9$	Celsius temperature	°C
----	------------------------	-------------	---------------------	----

APPROXIMATE CONVERSIONS FROM SI UNITS

Symbol	When You Know	Multiply By	To Find	Symbol
--------	---------------	-------------	---------	--------

LENGTH

mm	millimetres	0.039	inches	in
m	metres	3.28	feet	ft
m	metres	1.09	yards	yd
km	kilometres	0.621	miles	mi

AREA

mm ²	millimetres squared	0.0016	square inches	in ²
m ²	metres squared	10.764	square feet	ft ²
ha	hectares	2.47	acres	ac
km ²	kilometres squared	0.386	square miles	mi ²

VOLUME

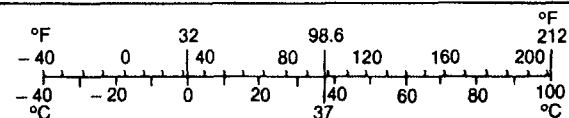
mL	millilitres	0.034	fluid ounces	fl oz
L	litres	0.264	gallons	gal
m ³	metres cubed	35.315	cubic feet	ft ³
m ³	metres cubed	1.308	cubic yards	yd ³

MASS

g	grams	0.035	ounces	oz
kg	kilograms	2.205	pounds	lb
Mg	megagrams	1.102	short tons (2000 lb)	T

TEMPERATURE (exact)

°C	Celsius temperature	$1.8C + 32$	Fahrenheit temperature	°F
----	---------------------	-------------	------------------------	----



* SI is the symbol for the International System of Measurement

(Revised April 1989)

TABLE OF CONTENTS

Page

INTRODUCTION

1. Description of Problem	1
2. Project Objectives	1
3. Organization of Report	2

DESCRIPTION OF FULL-SCALE EMBANKMENT TESTING PROGRAM

1. General	3
2. Embankment Construction and System Placement	7
3. Data Collection Procedure	10
4. Documentation of Test Conditions and Qualitative Assessment of Performance	14
a. Rigid Embankment Tests	22
(1) Armorflex Class 30 Concrete Block Protection System	22
(2) DyceI 100 Concrete-Block Protection System	29
(3) Petraflex-Vick Concrete-Block Protection System	32
(4) Construction Block Protection System	33
(5) Wedge-Shaped Concrete-Block Protection System	36
b. Erodible Embankment Tests	39
(1) Armorflex Class 30 Concrete Block Protection System	44
(2) DyceI 100 Concrete Block Protection System	46
(3) Construction Block Protection System	48
(4) Wedge-Shaped Concrete Block Protection System	54
c. Qualitative Summary of Concrete Block Mattress Performance	54
(1) Rigid Embankment Tests	54
(2) Erodible Embankment Tests	56

RESULTS OF FULL-SCALE EMBANKMENT TESTING PROGRAM

1. Determination of Test Discharges	66
2. Data Conditioning and Computation of Hydraulic Parameters	66
3. Hydraulic Analysis Methodology for Freefall Conditions	67
a. Computation of Bed Shear Stress	68
b. Computation of Flow Resistance	71
4. Hydraulic Analysis Results for Freefall Conditions	72
a. Rigid Embankment Test Results	72
b. Erodible Embankment Test Results	74

TABLE OF CONTENTS (continued)

	<u>Page</u>
5. Analysis of Transducer Data for the Freefall Tests	79
a. Rigid Embankment Test Results	79
b. Erodible Embankment Test Results	93
6. Analysis of the Pressure Data	103
7. Analysis of the Flow Resistance Data	113
 SUMMARY AND CONCLUSIONS	
1. Summary	121
2. Conclusions	-122
GLOSSARY OF TERMS	127
REFERENCES.	131

LIST OF FIGURES

<u>Figure</u>	<u>Page</u>
1 Sketch of the hydraulic testing facility	4
2 Typical embankment profiles	5
3 Sketches of the five types of concrete blocks tested	6
4 Sketch of the observation window (viewport) and instrumentation canisters	12
5 Example of hydraulic tests data reduction for storage and analysis	15
6 Embankment, water surface, and energy grade line profiles for the 4-ft (1.22 m) overtopping flow, test AR-1	18
7 Example of velocity profile data	19
8 Velocity profiles along the embankment for test CR-1	21
9 Profile of the rigid embankment	23
10 Completed rigid embankment with instrumentation canisters installed	24
11 Installation of the Armorflex Class 30 protection system on the rigid embankment	26
12 Upstream anchor system for the Armorflex Class 30 blocks on the rigid embankment	27
13 The completed Armorflex Class 30 protection system on the rigid embankment	28
14 Installation of the Dycel 100 protection system on the rigid embankment	30
15 The completed Dycel 100 protection system on the rigid embankment	31
16 The completed Petraflex-Vick protection system on the rigid embankment (without rock infill)	34
17 Block configuration for the construction block protection system	35

LIST OF FIGURES (continued)

<u>Figure</u>		<u>Page</u>
18	The completed construction block protection system on the rigid embankment	37
19	Installation of the wedge block protection system on the rigid embankment	38
20	Moisture density curves for the type I soil.	42
21	Grain-size distribution range for the type I soil	42
22	The erodible embankment, illustrating 2H:1V slope and 4H:1V crest chamfer, prior to geotextile placement and protection system installation (tests A-3 and A-4)	43
23	Installation of helix slope anchors for the Armorflex Class 30 system on the erodible embankment	45
24	The completed Armorflex Class 30 protection system on the erodible embankment (with helix slope anchors)	47
25	The completed Dycel 100 protection system on the erodible embankment (with helix slope anchors)	49
26	Construction block protection system on the erodible embankment	51
27	Profile of the completed construction block embankment protection system	53
28	Profile of the completed wedge block protection system	55
29	The wedge block protection system after testing on the rigid embankment	57
30	Erosion of the pressure transducer cable trenches beneath the Armorflex Class 30 protection system after test A-2	59
31	The Armorflex Class 30 protection system after testing on the erodible embankment (test A-4)	60
32	Failure of the Dycel 100 system after testing on the erodible embankment, looking upstream	61
33	Failure of the Dycel 100 system after testing on the erodible embankment, looking downstream	62

LIST OF FIGURES (continued)

<u>Figure</u>		<u>Page</u>
34	The construction block protection system after testing on the erodible embankment	64
35	The wedge block protection system after testing on the erodible embankment	65
36	Control volume for the test AR-1 with 4-ft (1.22 m) overtopping	69
37	Typical control volume with momentum equation parameters	70
38	Average shear stress on the downstream slope versus unit discharge for rigid embankment tests	75
39	Average flow velocity on the downstream slope versus unit discharge for rigid embankment tests	76
40	Average flow depth on the downstream slope versus unit discharge for rigid embankment tests	77
41	Average shear stress on the downstream slope versus unit discharge for erodible embankment tests	80
42	Average velocity on the downstream slope versus unit discharge for erodible embankment tests	81
43	Average flow depth on the downstream slope versus unit discharge for erodible embankment tests	82
44	Transducer data for test AR-1 (Armorflex Class 30)	83
45	Transducer data for test AR-2 (Armorflex Class 30)	85
46	Transducer data for test BR-1 (Dycel 100)	86
47	Transducer data for test BR-2 (Dycel 100).	87
48	Transducer data for test CR-1 (Petraflex-Vick)	88
49	Transducer data for test DR-1 (construction blocks)	89
50	Transducer data for test ER-1 (wedge blocks)	90
51	Transducer data for test ER-2 (wedge blocks)	91
52	Transducer data for test A-1 (Armorflex Class 30)	92

LIST OF FIGURES (continued)

<u>Figure</u>		<u>Page</u>
53	Transducer data for test A-2 (Armorflex Class 30)	94
54	Transducer data for test A-3 (Armorflex Class 30)	96
55	Transducer data for test A-4 (Armorflex Class 30)	97
56	Transducer data for test B-1 (Dycel 100)	98
57	Transducer data for test D-1 (construction blocks)	99
58	Transducer data for test D-2 (construction blocks)	100
59	Transducer data for test E-1 (wedge blocks)	101
60	Transducer data for test E-2 (wedge blocks)	102
61	Mean observed sub-block pressure versus calculated sub-block pressure, in feet of water, at station 34.0	104
62	Mean observed sub-block pressure versus calculated sub-block pressure, in feet of water, at station 37.5	105
63	Mean observed sub-block pressure versus calculated sub-block pressure, in feet of water, at station 41.5	106
64	Mean observed sub-block pressure versus calculated sub-block pressure, in feet of water, at station 44.0	107
65	Mean pressure at the block surface versus unit discharge at station 34.0	109
66	Mean pressure at the block surface versus unit discharge at station 37.5	110
67	Mean pressure at the block surface versus unit discharge at station 41.5	111
68	Mean pressure at the block surface versus unit discharge at station 44.0	112
69	Manning's n versus unit discharge for all freefall tests .	115
70	Darcy-Weisbach f versus unit discharge for all freefall tests.	116

LIST OF FIGURES (continued)

<u>Figure</u>		<u>Page</u>
71	Boundary rugosity k_s calculated using the Bathurst relationship for all freefall tests.	118
72	Boundary rugosity k_s calculated using the Mussetter relationship for all freefall tests.	119

LIST OF TABLES

<u>Table</u>		<u>Page</u>
1	Geometric configuration and hydraulic conditions for the rigid embankment tests	8
2	Geometric configurations and hydraulic conditions for the erodible embankment tests	9
3	Engineering properties of embankment soil	40
4	Hydraulic analysis results for freefall conditions for the rigid embankment tests	73
5	Hydraulic analysis results for freefall conditions for the erodible embankment tests	78
6	Coefficients a and exponents b resulting from the pressure versus unit discharge regression analysis	114
7	Summary of critical velocity and shear stress for various protection measures.	123

INTRODUCTION

1. Description of Problem

The quantitative understanding of erosion and failure processes of earth embankments and their protection systems during overtopping flow is incomplete. Previous studies have provided general insight concerning hydraulic conditions of failure for both protected and unprotected earth embankments, and the characteristic failure mechanisms. In particular, a 1988 study by the United States Department of Transportation, in coordination with the U.S. Bureau of Reclamation, investigated the performance of protected and unprotected embankments under various hydraulic conditions.⁽¹⁾ Two soils with distinctly different erosional characteristics were investigated, along with six categories of embankment erosion protection systems.

The systems investigated in the 1988 study included three proprietary concrete block products, known in the industry as articulating cable-tied concrete block revetment mattresses. Test results illustrated that, while these block systems as a category have significant promise for effective erosion protection, the performance of specific systems varied dramatically. While a general understanding of failure mechanisms for concrete block protection systems was developed through the 1988 study, specific causal factors influencing system stability could not be distinguished given the nature and scope of testing. The need for further investigation and characterization of the efficacy of concrete block systems for protection of embankments during overtopping flow was acknowledged.

2. Project Objectives

This study seeks to provide the detailed testing and analysis required to better understand and quantify the processes causing failure of concrete block embankment protection systems during overtopping flow conditions. In addition to the three concrete block systems previously investigated, two other systems were included in this study. Specifically, the objectives of this project were to:

- Conduct full-scale tests of five different types of concrete block protection systems on both rigid and erodible embankments in order to obtain a qualitative understanding of failure mechanisms, and to provide a quantitative assessment of hydraulic conditions at the failure threshold of the protection systems (if this threshold can be exceeded by the capacity of the testing facility).
- Investigate the hydrodynamic pressure field under various conditions of overtopping flow at selected locations, and correlate, where possible, the resulting uplift forces which may lead to separation of the protection system from the embankment subgrade.
- Develop, where possible, preliminary design recommendations for the protection of embankments against erosion and uplift induced by overtopping flow.

3. Organization of Report

This report documents the conduct and results of the full-scale hydraulic tests. The first section of the report provides a description of the test facility, documentation of embankment construction procedures and installation of protection systems, description of data collection procedures, and testing methodology. A qualitative discussion of the performance of each protection system is also included.

The second section of the report presents the methodology used to determine hydraulic parameters and analyze hydraulic conditions based on the test data. Summaries of test results are provided, and include both the results of the hydraulic analysis and the data obtained from the pressure transducer data acquisition system.

Summary and conclusions based on the hydraulic tests and data analyses are provided in the third section of the study report. These are presented within the context of the foregoing developments and are based on theoretical considerations, results of controlled experimental research, and field experience.

DESCRIPTION OF FULL-SCALE EMBANKMENT TESTING PROGRAM

1. General

The testing program was conducted in the same 90-ft (27.4 m) long by 4-ft (1.22 m) wide flume used for the earlier 1988 U.S. Department of Transportation and U.S. Bureau of Reclamation embankment overtopping study. A sketch of the hydraulic testing facility is shown in figure 1. The flume was modified from the 1988 study by adding a 42-in (105 cm) long by 30-in (75 cm) high plexiglass observation window in one side of the flume.⁽¹⁾ This window allowed observation of flow and embankment behavior during testing. The observation room which was constructed to allow access to the window also housed the data collection hardware associated with the transducers used to collect pressure, block displacement and velocity data under the protection systems.

A diagram of typical embankment profiles is given in figure 2. Note that the embankment shoulder was located at station 36 for all tests. The location of the toe of the embankment varied depending on the downstream slope of the embankment and whether a 4H:1V chamfer was added at the shoulder of the embankment.

The testing program was divided into five general categories based on the type of concrete-block protection system used. These categories were:

1. Armorflex Class 30 cabled blocks (longitudinal and lateral cable tunnels).
2. Dycel 100 closed-cell cabled blocks (longitudinal cable tunnels).
3. Petraflex-Vick cabled blocks (longitudinal and lateral cable tunnels).
4. Concrete construction blocks (noncabled).
5. Concrete wedge-shaped, overlapping blocks (noncabled).

A dimensional drawing of each of these concrete blocks is provided in figure 3, which also provides the representative unit weight of each system.

Test designations and nomenclature conventions were established according to the system being tested and the type of embankment subgrade used. For example, the second test of the Armorflex system on an erodible (soil) embankment

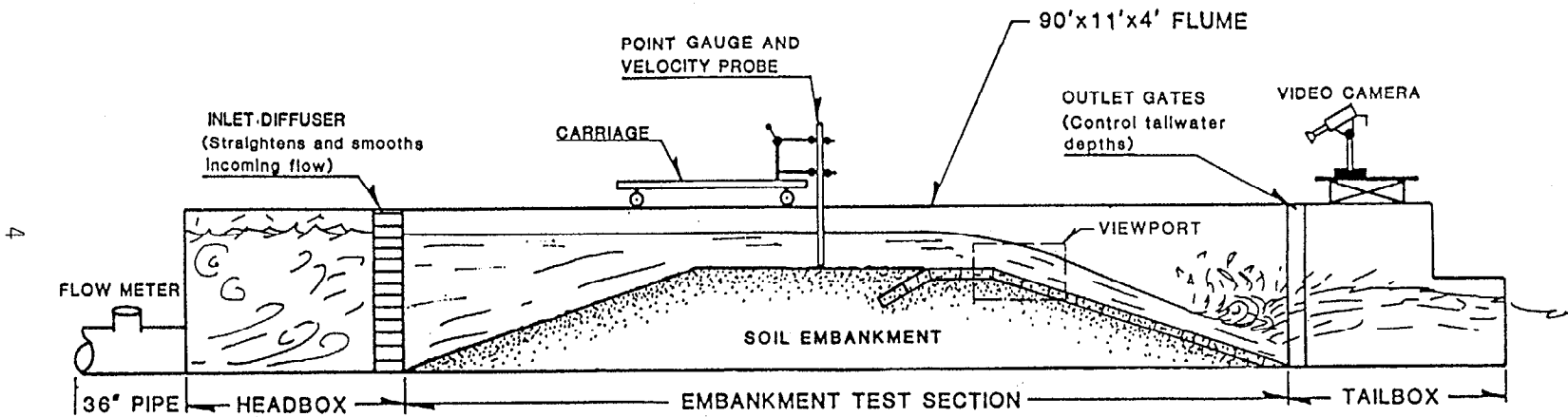


Figure 1. Sketch of the hydraulic testing facility.

5

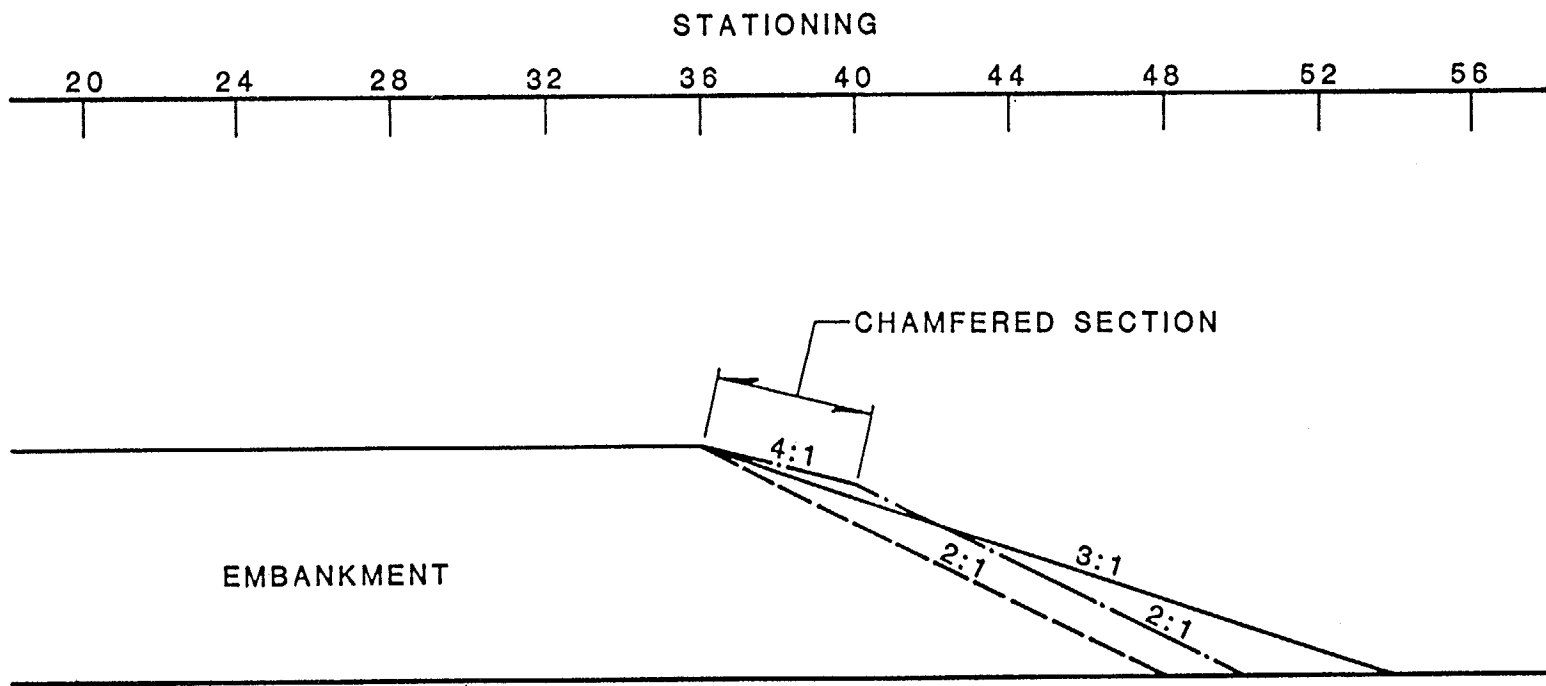
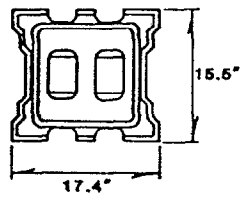
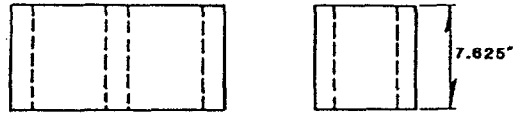
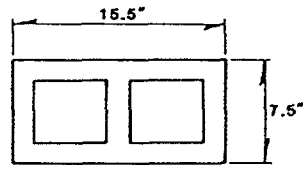


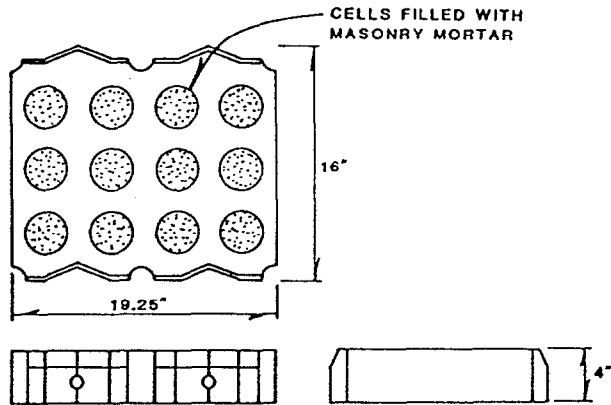
Figure 2. Typical embankment profiles.



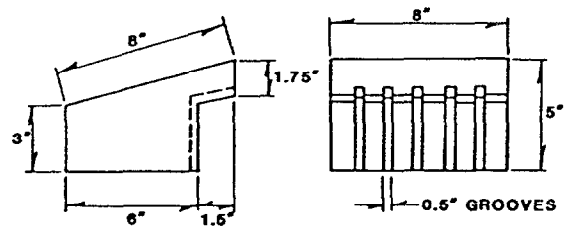
A.



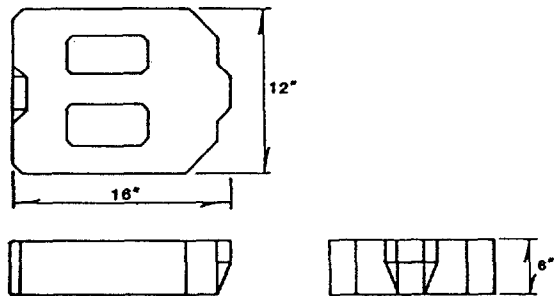
D.



B.



E.



C.

SYSTEM	UNIT WEIGHT WITHOUT GRAVEL FILL (LB/FT ²)
A. ARMORFLEX CLASS 30	36
B. DYCEL 100	42
C. PETRAFLEX-VICK	42
D. CONSTRUCTION BLOCK	40
E. WEDGE BLOCK	48

Figure 3. Sketches of the five types of concrete blocks tested.

is identified as "A-2." Tests which utilized a rigid (concrete surfaced) embankment were given an additional letter designation of "R." Continuing the example, the first Armorflex test using a rigid embankment is identified as "AR-1."

The testing program consisted of 17 hydraulic tests: 8 utilizing the rigid embankment and 9 utilizing a soil embankment. Each test was run for a total duration of 8 hours, and up to 4 separate overtopping conditions were imposed on each system during that time. As an example, test A-1 included both 1-ft and 2-ft (0.30 and 0.61 m) overtopping depths for Armorflex placed on an erodible embankment, while test BR-2 involved the Dycel 100 system placed on a rigid embankment, with 4-ft (1.22 m) overtopping conditions for both freefall and tailwater conditions. Overtopping depths, tailwater conditions, and embankment slopes for all tests are summarized in tables 1 and 2.

It should be noted that each protection system was tested at least once with tailwater conditions. The tailwater elevation did not submerge the embankment crest, but instead was held near midslope in every case. This resulted in a plunging flow condition along the downstream face of the embankment. Although water-surface and pressure data were collected for these tests, velocities in the tailwater zone could not be measured accurately with the electromagnetic flow meter due to the 3-dimensional nature of the highly turbulent flow condition. Consequently, the data collected for these tests were limited, and complete hydraulic analyses were not performed.

2. Embankment Construction and System Placement

A 6-ft (1.8 m) high embankment with a crest width of 20 ft (6.1 m) was constructed in the 4-ft (1.22 m) wide flume for each test. Construction of the rigid embankment began with the placement and compaction of a soil core with a crest height of 5.2 ft (1.58 m). A 6-in (15 cm) thick concrete shell was placed over the soil core to ensure nonerodibility. For the tests using an erodible embankment, soil was placed to specified embankment dimensions and compacted in accordance with U.S. Department of Transportation and U.S. Bureau of Reclamation procedures. The embankments for tests A-3 and A-4 included a 4H:1V chamfer at the shoulder of the embankment (refer to figure 3).

Table 1. Geometric configurations and hydraulic conditions
for the rigid embankment tests.

Product	Test Number	Duration (hr)	Embankment Slope	Nominal Overtopping Depth (ft)	Tailwater Condition	Comments	
Armorflex Class 30	AR-1	2	2:1	1.0	freefall		
		2	2:1	2.0	freefall		
		4	2:1	4.0	freefall		
	AR-2	4	2:1	4.0	freefall	lateral cables removed	
		4	2:1	4.0	tailwater	lateral cables removed	
	Dycel 100	BR-1	4	2:1	1.0	freefall	
4			2:1	2.0	freefall		
BR-2		4	2:1	4.0	freefall		
		4	2:1	4.0	tailwater		
Petriflex-Vick		CR-1	2	2:1	1.0	freefall	
			2	2:1	2.0	freefall	
	2		2:1	4.0	freefall		
	2		2:1	4.0	tailwater		
Construction Blocks	DR-1	2	2:1	1.0	freefall		
		2	2:1	2.0	freefall		
		2	2:1	4.0	freefall		
		2	2:1	4.0	tailwater		
Wedge Blocks	ER-1	2	2:1	0.5	freefall		
		2	2:1	1.0	freefall		
		2	2:1	1.5	freefall		
		2	2:1	2.0	freefall		
	ER-2	2	2:1	3.0	freefall		
		2	2:1	3.5	freefall		
		2	2:1	4.0	freefall		
		2	2:1	4.0	tailwater		

Table 2. Geometric configurations and hydraulic conditions for the erodible embankment tests.

Product	Test Number	Duration (hr)	Embankment Slope	Nominal Overtopping Depth (ft)	Tailwater Condition	Comments
Armorflex Class 30	A-1	4	2:1	1.0	freefall	
		4	2:1	2.0	freefall	
	A-2	4	2:1	4.0	freefall	erosion and soil piping along electronic cable trenches
		4	2:1	4.0	tailwater	
	A-3	4	2:1*	1.0	freefall	embankment rebuilt with cables deeply buried and trenches well compacted
		4	2:1*	2.0	freefall	
	A-4	4	2:1*	4.0	freefall	tailwater
		4	2:1*	4.0	tailwater	
Dycel 100	B-1	1	2:1	1.0	freefall	failure due to shallow soil slip
Construction Blocks	D-1	4	3:1	1.0	freefall	loss of granular filter near toe
		4	3:1	2.0	freefall	
	D-2	2	3:1	2.0	freefall	embankment rebuilt with revised toe installation
		3	3:1	4.0	freefall	
		3	3:1	4.0	tailwater	
Wedge Blocks	E-1	4	3:1	1.0	freefall	
		4	3:1	2.0	freefall	
	E-2	4	3:1	4.0	freefall	tailwater
		4	3:1	4.0	tailwater	

*With 4H:1V chamfer (see figure 2)

Prior to placing the concrete block protection system on the embankment, a dual-layer geosynthetic system was laid down. The lower layer was a 2-dimensional woven monofilament geotextile (Nicolon 40/30) for soil retention. On top of this was laid a 3-dimensional nylon mesh fabric (Enkamat 7020) approximately 3/4-in (1.9 cm) thick for subsystem drainage and pressure relief. The concrete blocks were then placed by hand, ensuring that any mechanical interlock and/or cabling requirements were fully established. In the case of the cabled systems, the cables were affixed to helical soil anchors within a terminal trench located at station 20 within the flume. This procedure was followed for the rigid embankment tests as well as for the erodible embankment tests.

3. Data Collection Procedure

Hydraulic data collected during testing included embankment elevation, water-surface elevation, and flow velocities at predetermined stations along the centerline of the flume. Embankment and water-surface elevations were measured using a point gauge attached to a carriage which moved along the length of the flume (refer to the profile of the testing facility shown in figure 1). Velocities were measured with a Marsh-McBirney Model 201 portable electromagnetic water current meter at three relative depths (20, 60, and 80 percent of the total flow depth) at each predetermined station, provided that the flow depth was great enough to submerge the probe.

Both embankment and water-surface elevations, as well as velocities, were measured at the beginning and end of each period of constant discharge. The velocities and flow depths measured during the data collection process defined the hydraulic characteristics for each test and allowed the calculation of water discharge, energy grade line, shear stress, Darcy-Weisbach friction factor, and Manning's n . The determination of these parameters will be described in the section entitled, "Results of Full-Scale Embankment Testing Program."

In addition to the manually collected flow data described above, a computerized data acquisition system was used to collect data below the geotextile underlayment at the interface between the protection system and

embankment subgrade. Hydrodynamic pressure was measured at four locations along the embankment centerline. Deflections of a centerline block located 1.5 ft (0.46 m) downstream from the shoulder, along with corresponding velocities of flow beneath the same block, were also recorded. Data were collected automatically at 30-second intervals at each of the six probes for the entire duration of each test. The automatic data acquisition system was utilized for both the rigid embankment and the soil embankment series of tests.

The locations of the data collection instrument boxes (canisters) are shown in figure 4. The furthest upstream data collection canister was installed at station 34, located 2 ft (0.61 m) upstream of the embankment shoulder. This box contained a Data Instruments Model AB semiconductor strain-gauge pressure transducer with a pressure range of 0 to 15 lb/in² (0 to 0.72 kN/m²). This type of pressure transducer is typical of those used throughout the testing program.

The second instrumentation box was located at station 37.5 [1.5 ft (0.46 m) downstream from the shoulder]. It contained a model AB pressure transducer, a total displacement transducer, and a differential pressure transducer. The displacement transducer was a Celesco Model PT801, a variable resistance underwater transducer with a maximum displacement of 10 in (25.4 mm). A Schvaevitz Model P3061 differential pressure sensor was used to measure the flow velocity beneath the various block systems by reporting the difference between static and kinetic (i.e., stagnation) pressures. The P3061 has a differential pressure range of 0 to 2 lb/in² (0 to 0.10 kN/m²).

The third and fourth instrument canisters were installed at stations 41.5 and 44, respectively. These two canisters contained model AB pressure transducers identical to that at station 34.

All of the transducers were controlled by a Campbell Scientific Inc. (CSI) CR7X automated data acquisition system. The CR7X interrogated each of the six transducers at 30-second intervals and stored the data in its internal memory. The CR7X was programmed to convert the transducer output voltages, via the proper calibration equation, to equivalent engineering units. When the memory buffer was filled, the data were then transferred to an audio cassette tape. At the end of each test, data on the cassette tape were downloaded into an IBM-

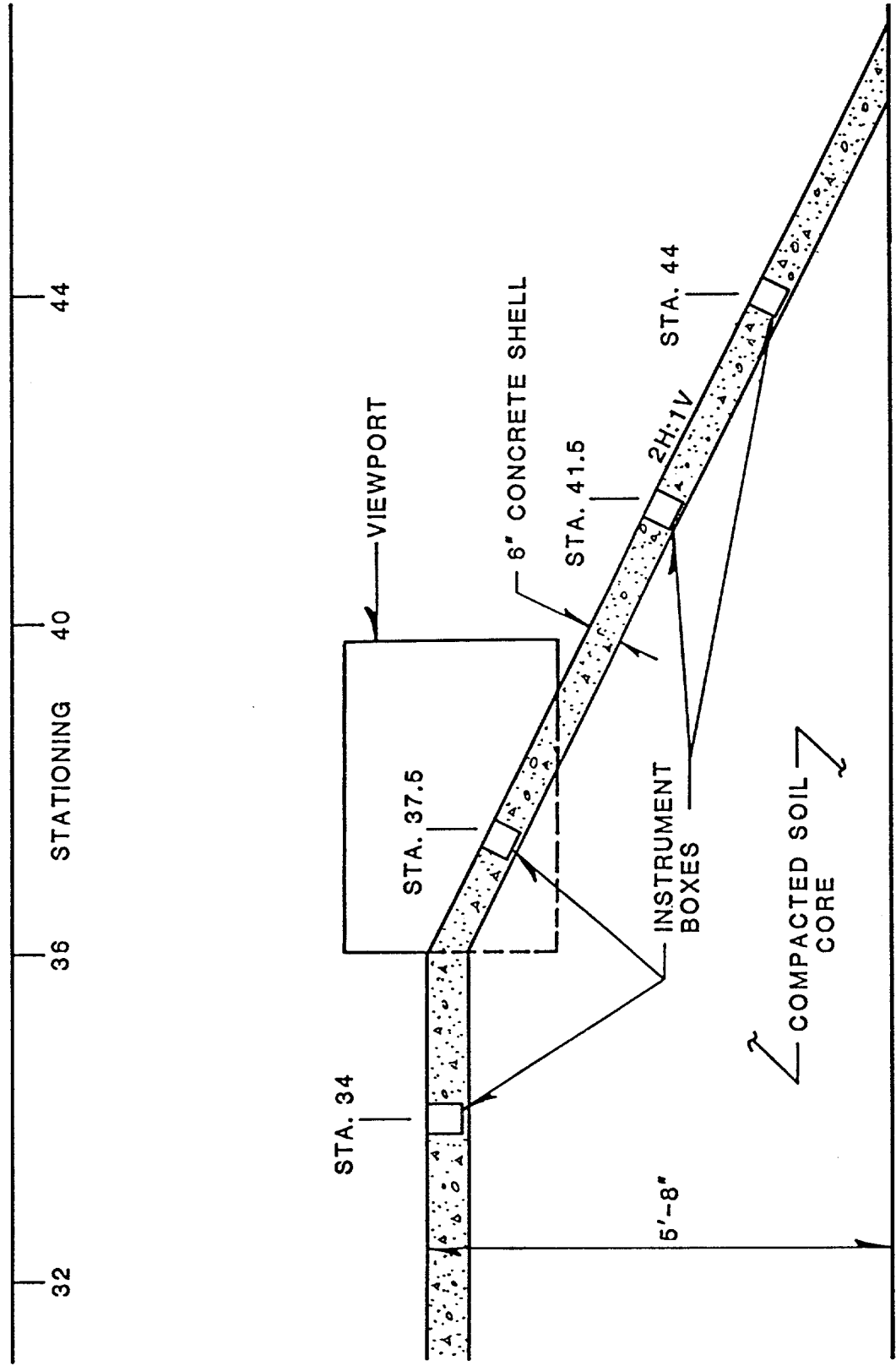


Figure 4. Sketch of the observation window (viewport) and instrumentation canisters.

compatible microcomputer using a CSI Model C20 cassette tape interface to encode an ASCII file with the data in column format.

A unique aspect of the data collection program was the visual inspection of the protection system and the underlying embankment soil throughout the duration of each test. It also aided in contrasting the hydraulic characteristics of each concrete block system. Unfortunately, the viewing range was limited to the first row of blocks [approximately 12 to 15 in (30 to 38 cm)] directly in front of the window due to the turbidity of the water passing through the flume.

The general testing procedure was similar for all test categories. Water was introduced to the flume and an overtopping depth was established. The overtopping depths were normally 1, 2, or 4 ft (0.30, 0.61, or 1.22 m), although the wedge blocks were also tested with depths of 0.5, 1.5, 3.0 and 3.5 ft (0.15, 0.46, 0.91 and 1.07 m). After establishment of the overtopping depth, which typically required from 3 to 10 minutes, the tailgate louvres were adjusted to achieve either freefall conditions (no tailwater) or to establish and maintain the tailwater elevation at midslope. Adjustment of the tailgate louvres typically required an additional 3 to 5 minutes.

Immediately after establishing steady hydraulic conditions, the point gauge was used to measure water-surface and embankment elevations along the embankment. In addition, flow velocities were measured beginning at station 16 and continuing downstream to the embankment toe. Elevations and velocities were measured at the beginning and at the end of each "step" of the discharge hydrograph. A typical test consisted of two to four separate overtopping flow conditions imposed on the protection system over an 8-hour period.

Videotapes and photographs were taken to document system performance and erosion scour growth, if any, beneath the geotextile fabric, as visually determined by observation through the viewport.

The bed and water-surface elevations were entered into an IBM-compatible PC using R:base 5000, a relational data-base management software package. These data were placed in a data block within R:base named EMBANK. R:base was then

used to analyze the EMBANK data by computing flow depths, corrected flow depths (i.e., adjusted for the embankment slope), average velocities (based on corrected flow depths), and energy grade line elevations. An example of the tabular output from the R:base analysis of EMBANK data is shown in figure 5, which illustrates a complete listing for test AR-1. This was a test of Armorflex blocks on a rigid embankment with a 2H:1V slope and 1-, 2- and 4-ft (0.30, 0.61, and 1.22 m) overtopping depths with freefall conditions. Both the beginning and ending data sets are shown for each overtopping depth. A plot of the results for the 4-ft (1.22 m) overtopping flow for test AR-1 is shown in figure 6. These forms of data reduction, tabulation, and graphical presentation are typical and were performed for each of the 17 tests conducted during this investigation. These data are available from the author and the FWHA upon request.

The velocity profiles, as measured with the portable electromagnetic current meter, were also entered into R:base. These data were placed in a data block within R:base named VEL268. An example of the organization of these data is shown in figure 7. This figure contains, in tabular form, the 3-point velocity profile information for test CR-1, which documents the measured velocities at the beginning and end of each step of the discharge hydrograph during the course of this test. The 3-point velocity profiles corresponding to these data are plotted in figure 8.

4. Documentation of Test Conditions and Qualitative Assessment of Performance

The performance of five types of concrete block embankment protection systems were investigated. All five block systems were initially tested on a rigid (concrete-covered) embankment in order to establish baseline hydraulic information for each system without incurring the risk of deformation or failure during the test. The rigid embankment was later replaced with an erodible (soil) embankment. Embankment construction, protection system descriptions and installation procedures, and hydraulic test conditions are described in the following sections.

Meas. Set	Discharge (cfs)	Station Number	Embankment Elev. (ft)	Water Surface Elev. (feet)	Meas. Flow Depth (ft)	Corr. Flow Depth (ft)	Ave Vel (ft/s)	EGL Elev. (ft)
3.0	34.9	16	6.07	7.72	1.65	1.65	5.289	8.154
3.0	34.9	18	6.06	7.45	1.39	1.39	6.279	8.062
3.0	34.9	20	5.99	7.24	1.25	1.25	6.982	7.997
3.0	34.9	22	5.98	7.20	1.22	1.22	7.154	7.995
3.0	34.9	24	5.96	7.31	1.35	1.35	6.465	7.959
3.0	34.9	26	5.95	7.54	1.59	1.59	5.489	8.008
3.0	34.9	28	5.95	7.48	1.53	1.53	5.704	7.985
3.0	34.9	30	5.95	7.34	1.39	1.39	6.279	7.952
3.0	34.9	32	5.92	7.21	1.29	1.29	6.766	7.921
3.0	34.9	34	5.93	7.14	1.21	1.21	7.213	7.948
3.0	34.9	36	5.92	7.02	1.10	1.10	7.934	7.997
3.0	34.9	38	5.07	6.13	1.06	0.95	9.210	7.447
3.0	34.9	40	3.98	4.81	0.83	0.74	11.762	6.958
3.0	34.9	42	2.96	3.73	0.77	0.69	12.678	6.226
3.0	34.9	44	2.13	2.82	0.69	0.62	14.148	5.928
3.0	34.9	46	1.13	1.82	0.69	0.62	14.148	4.928
3.0	34.9	48	0.58	1.20	0.62	0.55	15.746	5.050
4.0	34.7	16	6.07	7.74	1.67	1.67	5.187	8.158
4.0	34.7	18	6.06	7.44	1.38	1.38	6.277	8.052
4.0	34.7	20	5.99	7.26	1.27	1.27	6.821	7.982
4.0	34.7	22	5.98	7.19	1.21	1.21	7.159	7.986
4.0	34.7	24	5.95	7.29	1.34	1.34	6.465	7.939
4.0	34.7	26	5.95	7.40	1.45	1.45	5.974	7.954
4.0	34.7	28	5.94	7.46	1.52	1.52	5.699	7.964
4.0	34.7	30	5.95	7.40	1.45	1.45	5.974	7.954
4.0	34.7	32	5.90	7.22	1.32	1.32	6.563	7.889
4.0	34.7	34	5.94	7.13	1.19	1.19	7.279	7.953
4.0	34.7	36	5.92	6.98	1.06	1.06	8.172	8.017
4.0	34.7	38	5.06	6.14	1.08	0.97	8.972	7.390
4.0	34.7	40	3.99	4.83	0.84	0.75	11.535	6.896
4.0	34.7	42	2.98	3.75	0.77	0.69	12.584	6.209
4.0	34.7	44	2.11	2.76	0.65	0.58	14.907	6.211
4.0	34.7	46	1.20	1.87	0.67	0.60	14.462	5.118
4.0	34.7	48	0.58	1.13	0.55	0.49	17.617	5.949
5.0	83.6	16	6.07	9.05	2.98	2.98	7.013	9.814
5.0	83.6	18	6.06	8.80	2.74	2.74	7.628	9.703
5.0	83.6	20	5.99	8.50	2.51	2.51	8.327	9.577
5.0	83.6	22	5.98	8.45	2.47	2.47	8.462	9.562
5.0	83.6	24	5.94	8.35	2.41	2.41	8.672	9.518
5.0	83.6	26	5.95	8.20	2.25	2.25	9.289	9.540
5.0	83.6	28	5.94	8.20	2.26	2.26	9.248	9.528
5.0	83.6	30	5.95	8.10	2.15	2.15	9.721	9.567
5.0	83.6	32	5.92	8.15	2.23	2.23	9.372	9.514

Note : A value of -0- indicates data point not taken

Figure 5. Example of hydraulic tests data reduction for storage and analysis (continued).

Meas. Set	Discharge (cfs)	Station Number	Embankment Elev. (ft)	Water Surface Elev. (feet)	Meas. Flow Depth (ft)	Corr. Flow Depth (ft)	Ave Vel (ft/s)	EGL Elev. (ft)
5.0	83.6	34	5.94	8.05	2.11	2.11	9.905	9.573
5.0	83.6	36	5.91	7.75	1.84	1.84	11.359	9.753
5.0	83.6	38	5.15	6.80	1.65	1.48	14.169	9.917
5.0	83.6	40	3.96	5.85	1.89	1.69	12.369	8.226
5.0	83.6	42	2.94	4.68	1.74	1.56	13.436	7.483
5.0	83.6	44	2.04	3.60	1.56	1.39	14.986	7.087
5.0	83.6	46	1.11	2.56	1.45	1.30	16.123	6.596
5.0	83.6	48	0.56	1.89	1.33	1.19	17.578	6.688
6.0	87.5	16	6.07	9.20	3.13	3.13	6.986	9.958
6.0	87.5	18	6.06	8.90	2.84	2.84	7.700	9.821
6.0	87.5	20	5.99	8.60	2.61	2.61	8.378	9.690
6.0	87.5	22	5.98	8.45	2.47	2.47	8.853	9.667
6.0	87.5	24	5.92	8.30	2.38	2.38	9.188	9.611
6.0	87.5	26	5.95	8.20	2.25	2.25	9.719	9.667
6.0	87.5	28	5.95	8.20	2.25	2.25	9.719	9.667
6.0	87.5	30	5.95	8.10	2.15	2.15	10.171	9.706
6.0	87.5	32	5.92	8.15	2.23	2.23	9.806	9.643
6.0	87.5	34	5.94	8.20	2.26	2.26	9.676	9.654
6.0	87.5	36	5.97	7.75	1.78	1.78	12.285	10.094
6.0	87.5	38	5.12	6.75	1.63	1.46	15.006	10.247
6.0	87.5	40	3.96	5.83	1.87	1.67	13.080	8.487
6.0	87.5	42	2.94	4.64	1.70	1.52	14.388	7.855
6.0	87.5	44	2.09	3.61	1.52	1.36	16.092	7.631
6.0	87.5	46	1.17	2.56	1.39	1.24	17.597	7.368
6.0	87.5	48	0.56	1.80	1.24	1.11	19.726	7.842

Note : A value of -0- indicates data point not taken

Figure 5. Example of hydraulic tests data reduction for storage and analysis (continued).

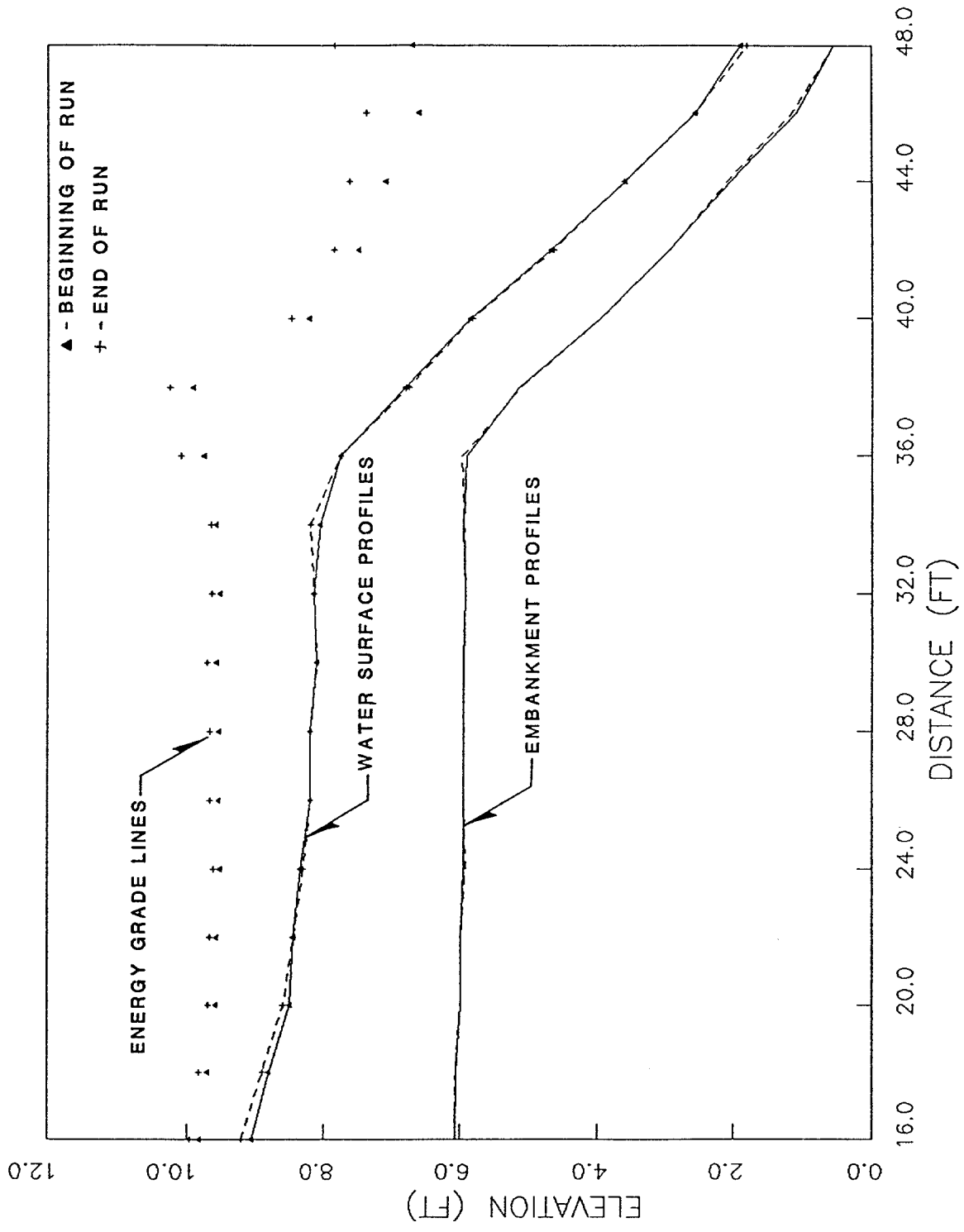


Figure 6. Embankment, water surface, and energy grade line profiles for the 4-ft (1.22 m) overtopping flow, test AR-1.

Meas. Set	Station Number	Velocity (ft/s)		
		0.2 depth	0.6 depth	0.8 depth
5.0	16	7.00	5.80	4.50
5.0	20	7.70	6.50	5.70
5.0	24	9.10	8.20	6.80
5.0	28	9.80	9.00	7.80
5.0	32	9.30	9.40	8.20
5.0	36	11.50	11.30	11.10
5.0	40	14.70	14.60	-0-
5.0	44	18.10	17.70	-0-
5.0	48	20.00	19.50	-0-
6.0	16	7.40	6.60	4.70
6.0	20	8.10	7.10	5.70
6.0	24	9.50	9.00	7.40
6.0	28	9.20	9.30	7.80
6.0	32	10.10	9.60	8.10
6.0	36	11.50	11.30	10.80
6.0	40	15.10	14.70	14.70
6.0	44	18.30	18.30	17.60
6.0	48	20.00	19.60	-0-
7.0	16	6.60	5.30	4.20
7.0	20	8.50	8.10	7.40
7.0	24	9.50	8.10	7.10
7.0	28	9.50	8.90	7.30
7.0	32	9.90	9.40	8.20
7.0	36	11.50	10.90	10.30
7.0	40	14.50	14.40	14.00
7.0	44	12.00	13.50	13.00
8.0	16	6.60	5.50	4.50
8.0	20	8.00	7.10	6.30
8.0	24	9.40	8.30	7.30
8.0	28	9.50	8.60	7.50
8.0	32	9.90	9.00	7.90
8.0	36	11.40	11.00	10.40
8.0	40	14.50	13.90	13.50
8.0	44	13.80	13.80	13.20

Note : A value of -0- indicates data point not taken

Figure 7. Example of velocity profile data (continued).

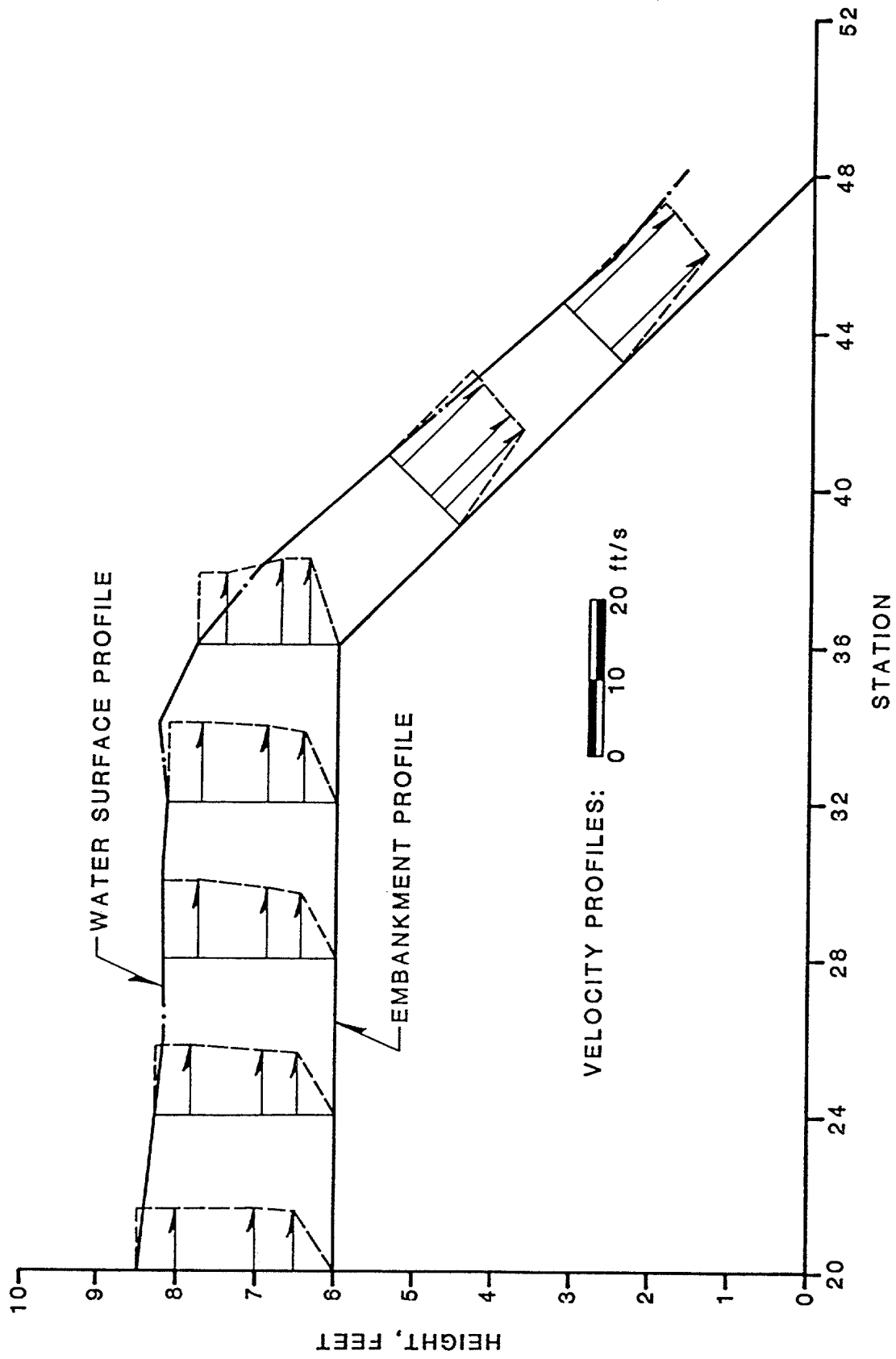


Figure 8. Velocity profiles along the embankment for test CR-1 [4-ft (1.22 m) overtopping conditions shown].

a. Rigid Embankment Tests

Soil was used to construct the embankment core for the rigid embankment. The soil was placed in 4- to 6-in (10 to 15 cm) lifts and compacted, with a jumping jack compactor, to between 95 and 100 percent of standard Proctor density. The downstream embankment face was prepared at a 2H:1V slope. A 6-in (15 cm) thick concrete shell was then placed on the soil core. Between stations 16 and 20, an additional 6 in (15 cm) of concrete was placed on top of the 6-in (15 cm) cover in order to provide a continuous bed elevation and smooth transition between the concrete shell and the protection system. Two helix anchors were installed at station 20 to afford a location to fasten the cables for those systems requiring them. In addition, preformed cavities were constructed in the concrete shell at stations 34, 37.5, 41.5, and 44 for the installation of instrumentation canisters. Figure 9 illustrates the configuration of the rigid embankment. Figure 10 is a photograph of the rigid embankment with instrumentation canisters in place, prior to the placement of a protection system.

(1) Armorflex Class 30 Concrete Block Protection System. The Armorflex Class 30 block system tested in this program consisted of concrete blocks which interlocked in a staggered pattern in the plane of the embankment slope. The system was integrated with two longitudinal (down the embankment slope) cables and one lateral (across the embankment slope) cable running through each block. The system used in the testing program is an open-cell block having an open area of 25 percent and a unit weight of approximately 36 lb/ft² (1.72 kN/m²). Each full-sized block exhibited a gross footprint area of 1.87 ft² (0.18 m²). Half-sized blocks of standard manufacture were also used to abut the flume walls at every other row of the system.

Nicolon 40/30 geotextile was used as the geotextile underlayer for all the rigid embankment tests. This geotextile underlayer is a woven polyester monofilament fabric with an effective opening sieve (EOS) of 40-50, a unit weight of 5.8 oz/yd² (1.93 N/m²), and a 20 to 30 percent open area. Enkamat 7020 fabric was then installed over the geotextile fabric to provide a drainage path beneath the revetment system. Enkamat 7020 is a 3-dimensional fabric made of nylon

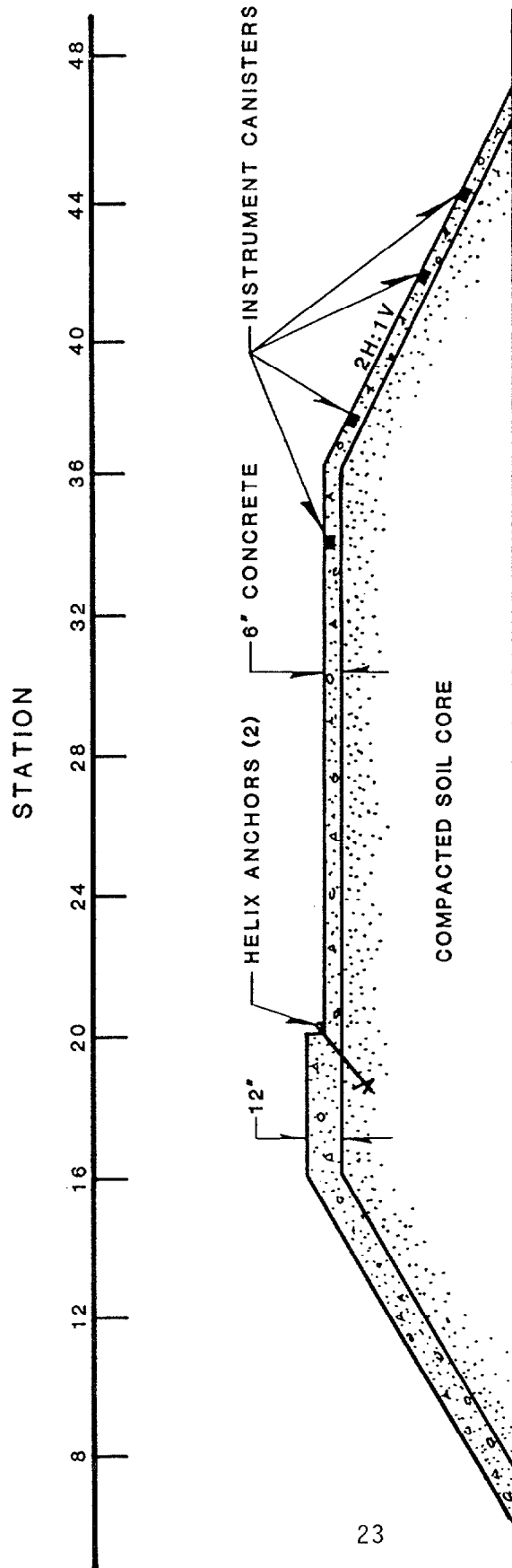


Figure 9. Profile of the rigid embankment.

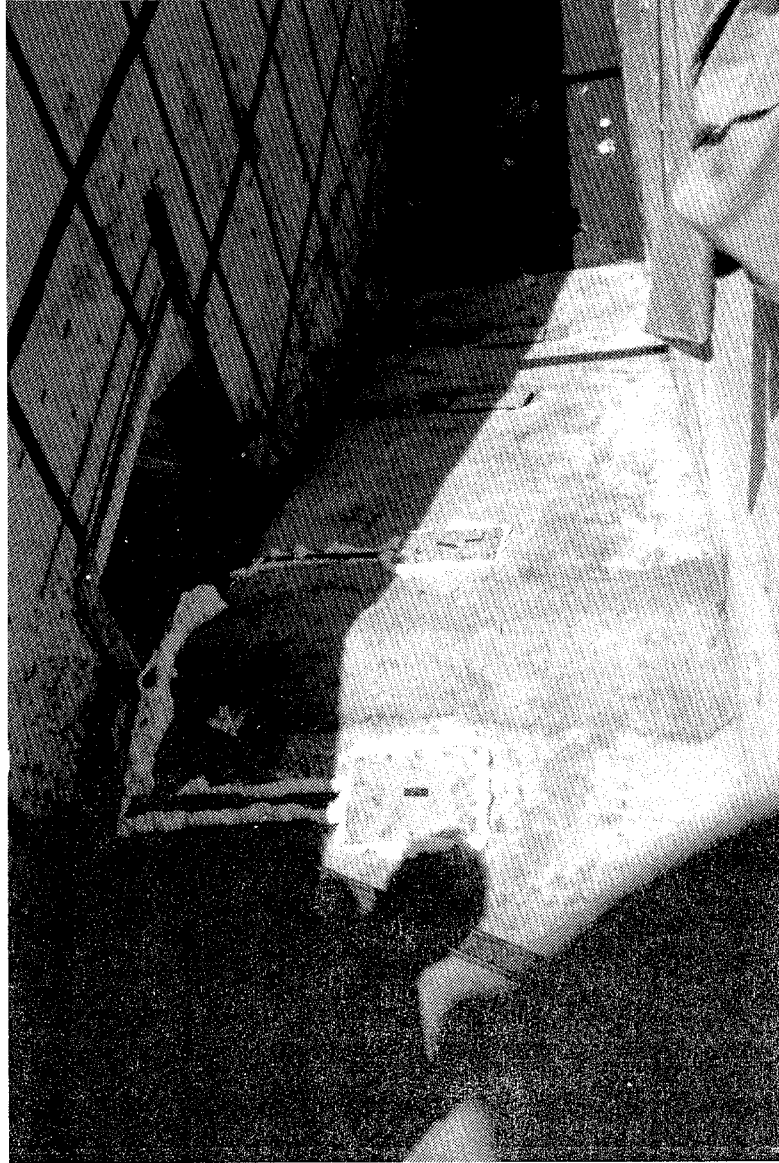


Figure 10. Completed rigid embankment with instrumentation canisters installed.

filaments fused at their intersections. It has a total thickness of approximately 3/4 in (1.9 cm), and has a 90 percent open area.

Prior to installing the system, the pressure, displacement, and differential pressure transducers were prepared for testing. This included bleeding the pressure transducers and testing for response from each of the six transducers.

The Armorflex blocks were cabled together, using the lateral cable ducts, into 4-ft (1.22 m) wide rows. The rows were then placed in the flume beginning at station 48 (the downstream embankment toe) and terminating at station 20. This process is shown in **figure 11**. Each concrete block was placed in its interlocking position allowing the longitudinal cables to be passed through the cable tunnels, two per block. During the placement of each row of blocks, the cables were pushed through the two cable ducts in each block leaving a loop in each cable at the downstream end of the mattress. Once block placement was complete, the cable ends were secured to the helix anchors at station 20. The anchor system is shown in **figure 12**. A steel bar was installed at station 48 to provide a toe anchor for the system. The wire associated with the displacement transducer was affixed to the exposed upper surface of a single block at station 37.5 by passing it through a small hole drilled vertically through the block. Finally, the open cells in the Armorflex mattress were filled with 1- to 2-in (2.5 to 5.1 cm) gravel. After installation, a gap approximately 3/4-in (1.9 cm) wide existed between the block system and the flume wall. This gap was filled with gravel having a slightly smaller median diameter. **Figure 13** shows the completed Armorflex embankment protection system.

Two 8-hour tests were performed on the Armorflex Class 30 block system. Test AR-1 subjected the system to 2 hours with a 1-ft (0.30 m) overtopping depth, 2 hours with a 2-ft (0.61 m) overtopping and lastly 4 hours with a 4-ft (1.22 m) overtopping. All 8 hours of this test were conducted under freefall conditions.

Upon completion of test AR-1, the lateral cables were removed from the system, thereby leaving only the longitudinal cables within the block matrix. As a significant amount of the gravel fill had been lost, especially on the downstream slope, the system was re-graveled prior to the next test. Test AR-



Figure 11. Installation of the Armorflex Class 30 protection system on the rigid embankment.

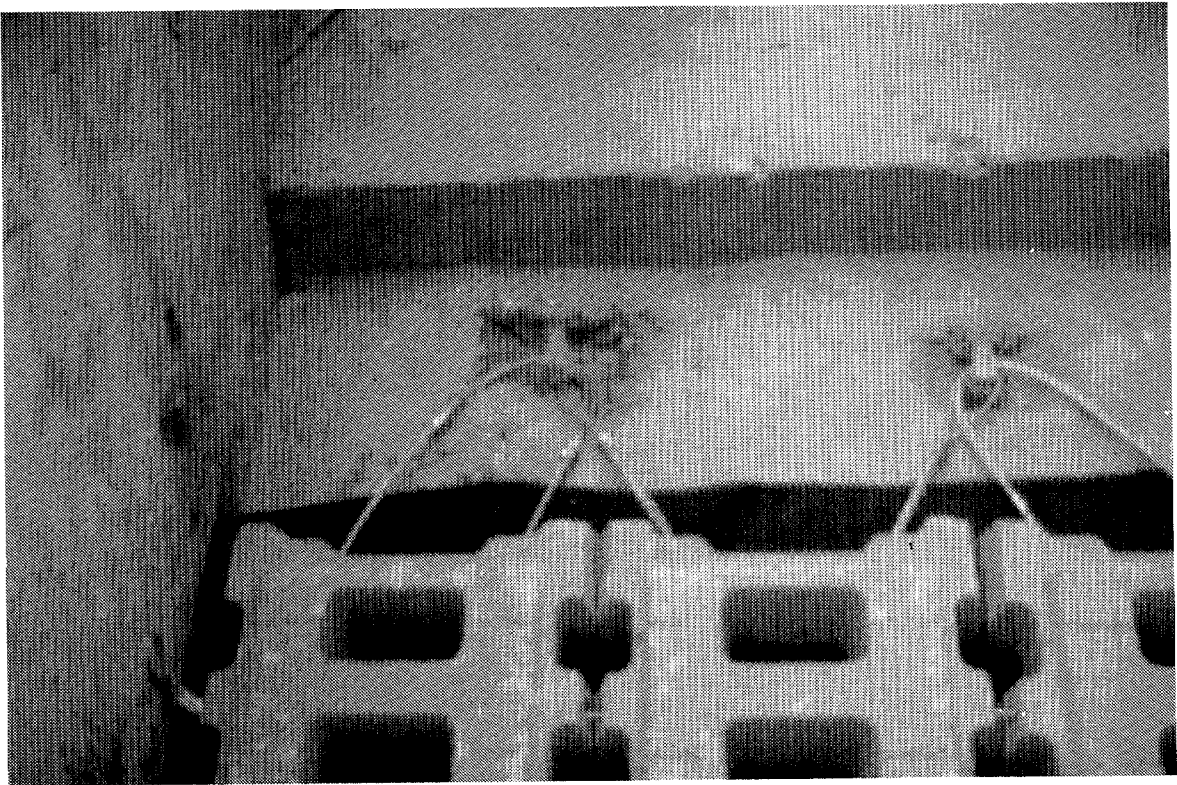
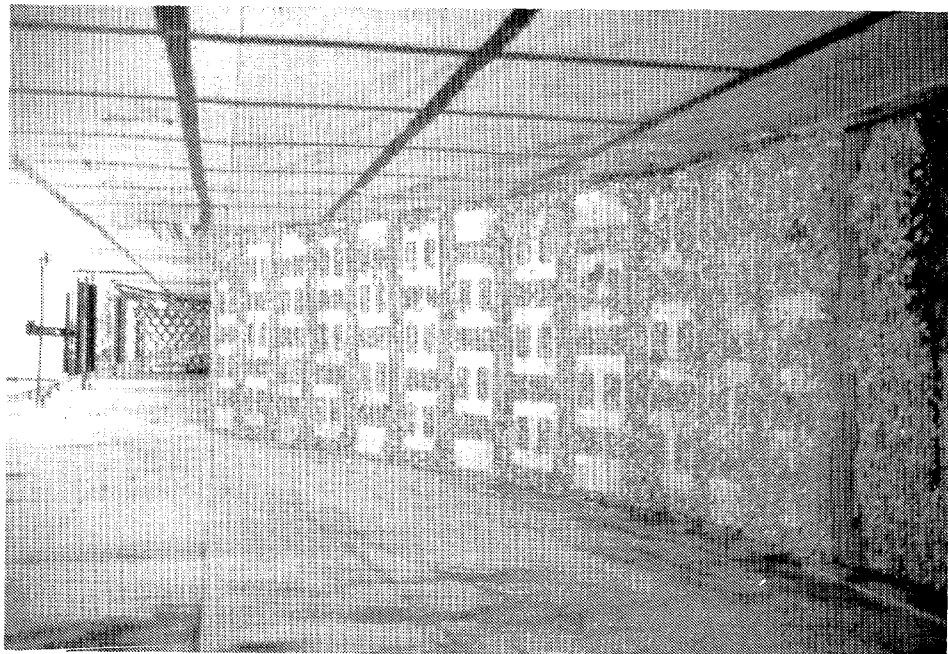
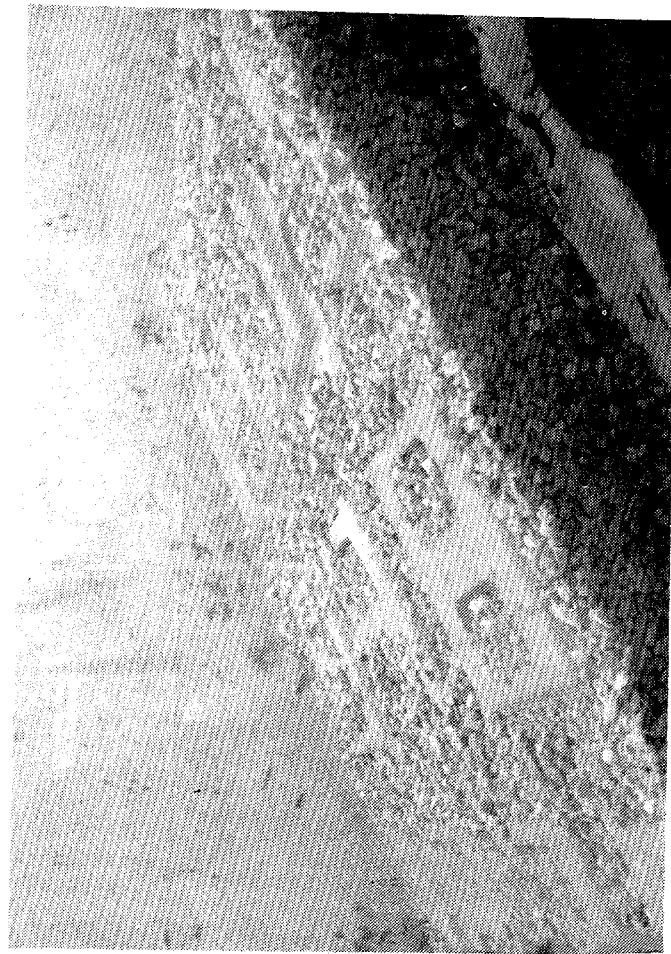


Figure 12. Upstream anchor system for the Armorflex Class 30 blocks on the rigid embankment.



a. Looking upstream



b. Looking through the observation window

Figure 13. The completed Armorflex Class 30 protection system on the rigid embankment.

2 then subjected the system to 4 hours of 4-ft (1.22 m) overtopping under freefall conditions and 4 hours of 4-ft (1.22 m) overtopping depth with 5 ft (1.52 m) of tailwater.

(2) Dycel 100 Concrete-Block Protection System. The Dycel system consisted of interlocking concrete blocks with longitudinal cables running through each block. The block type used in this test series was Dycel 100. Open cells of the blocks were filled with a low-strength masonry mortar to increase the system's unit weight. Consequently, the unit weight was increased from 33 lb/ft² (1.58 kN/m²) to approximately 42 lb/ft² (2.01 kN/m²). Because the cells were filled with mortar, the effective open area of the system was estimated to be less than 5 percent. The gross footprint area for a full-sized block is 2.14 ft² (0.22 m²). Half-sized blocks of standard manufacture were used to abut the flume walls at every other row of the system. The geotextile fabric and drainage layer configuration used for the Armorflex system (Nicolon 40/30 and Enkamat 7020) was also used beneath the Dycel 100 system.

Prior to installing the Dycel 100 blocks, the pressure, displacement, and differential pressure transducers were prepared for testing. The Dycel blocks were placed individually starting at station 48 (the downstream toe of the embankment) and proceeded upstream to station 20. This process is shown in figure 14. During block placement the longitudinal cables were pushed through the cable ducts in each individual block. The cables were inserted allowing them to be looped at the downstream end of the mattress. Upon completion of the installation, the cable ends were secured to the helix anchors located at the base of the anchor trench. A steel bar was welded to the flume walls at station 48 to provide a system anchor at the toe of the slope. The wire for the displacement transducer was affixed to the upper surface of a Dycel block at station 37.5 after threading it through a small hole drilled through the block. Figure 15 shows the Dycel 100 system after placement of the 1- to 2-in (2.5 to 5.1 cm) gravel fill material.

The Dycel 100 concrete block mattress was subjected to four separate hydraulic conditions. Test BR-1 was an 8-hour test and consisted of 4 hours with a 1-ft (0.30 m) overtopping depth and 4 hours with a 2-ft (0.61 m) overtopping depth, both of which were conducted under freefall conditions. Test



Figure 14. Installation of the Dycel 100 protection system on the rigid embankment.



Figure 15. The completed Dycel 100 protection system on the rigid embankment.

BR-2 subjected the system to a 4-ft (1.22 m) overtopping depth for 8 hours. The first half of the test was conducted under freefall conditions while the second 4 hours maintained a tailwater depth of 5 ft (1.52 m).

(3) Petraflex-Vick Concrete-Block Protection System. The Petraflex-Vick system consisted of interlocking concrete blocks reinforced with two longitudinal cables and one lateral cable running through each block. Each block had a unit weight of 42 lb/ft² (2.01 kN/m²), with an open area of 20 percent. Each full-sized block exhibited a gross footprint area of 1.33 ft² (0.13 m²). Because the method of block interlock does not utilize a stagger pattern, half-blocks were not used in the construction of the system. The geotextile underlayer system was identical to that used with the Armorflex and Dycel systems.

Lateral cables were used to connect the Petraflex-Vick concrete blocks together in rows of three. Blocks were placed in the flume starting at station 48 and ending at station 26, 10 ft (3.0 m) upstream of the embankment shoulder. Due to a slight shortage of Petraflex-Vick blocks, Armorflex class 30 blocks were installed to fill in the upstream remainder of the embankment crest from station 26 to station 20.

During the placement of each row of blocks, the longitudinal cables were pushed through the two cable ducts in each block leaving a loop in each cable at the downstream end of the mattress. Once block placement was complete, the cable ends were fastened to the helix anchors at station 20. Again, a steel bar was welded to firmly secure the toe of the system at station 48.

Washed river rock with a median size of 1 to 2 in (2.5 to 5.1 cm) was placed in the open cells of the concrete block mattress. It should be noted that the rock-fill was not placed between the edges of individual blocks, but only in the cells of each block and in the opening formed at the intersection of four block corners. This was due to the nature of the mechanical interlock. Separating individual blocks to allow gravel fill would be counter-productive to this interlock. The displacement transducer's wire was affixed to the upper surface of a Petraflex-Vick block at station 37.5 once it was passed through a

small hole drilled in the block. Figure 16 shows the Petraflex-Vick embankment protection system before placement of the gravel fill material.

The Petraflex-Vick system was tested under three different hydraulic conditions. Overtopping depths of 1, 2, and 4 ft (0.30, 0.61, and 1.22 m) were investigated, all with freefall conditions. A 4-ft (1.22 m) overtopping with 5 ft (1.52 m) of tailwater was also tested. Test CR-1 was conducted in the following sequence: 2 hours at a 1-ft (0.30 m) overtopping depth, 2 hours with a 2-ft (0.61 m) overtopping depth, and 4 hours at a 4-ft (1.22 m) overtopping depth with the first 2 hours using a freefall condition, and the last 2 hours using a 5-ft (1.52 m) tailwater condition.

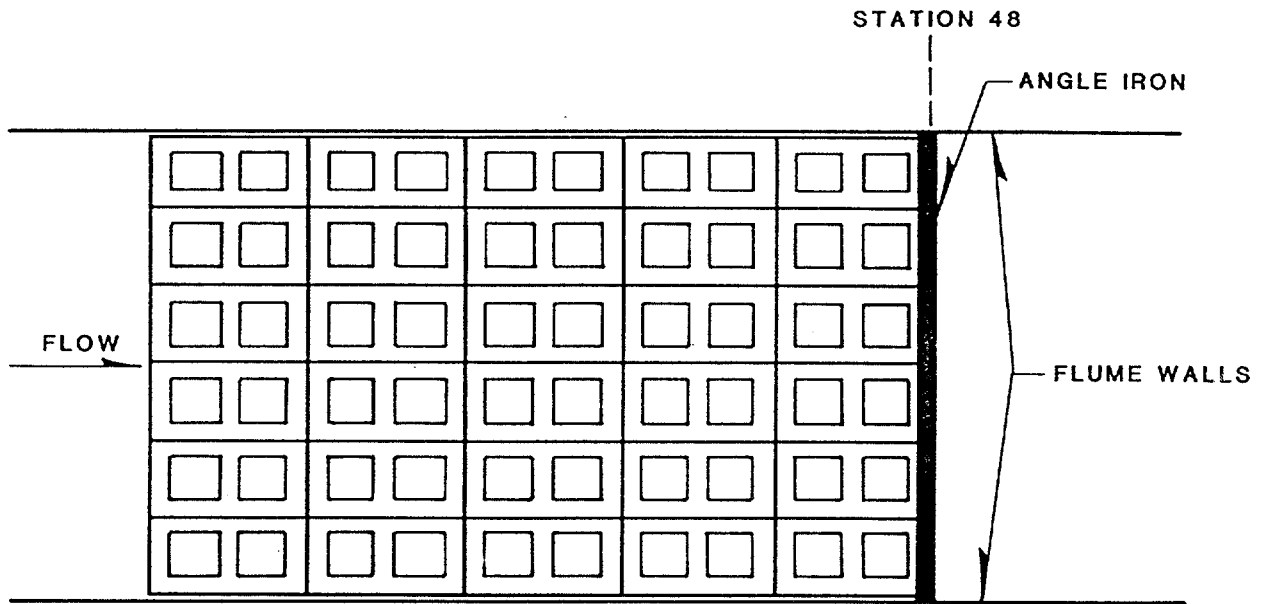
(4) Construction Block Protection System. The construction block system was comprised of conventional concrete construction blocks. The 8-by-8-by 16-in (20.3 by 20.3 by 40.6 cm) blocks had a unit weight of 40 lb/ft² (1.92 kN/m²), exclusive of any gravel fill. The open area of the system is approximately 47 percent, and each full-sized block exhibits a gross footprint area of 0.81 ft² (0.08 m²). It should be noted that these blocks have no special means for developing a mechanical interlock, except for the frictional resistance between two adjacent blocks and any additional binding caused by wedged particles of soil or fill material. When placed closely, the geometry of the block can effectively resist dislodgement by rotation. The underlying geotextile and drainage system was identical to that used for the other rigid embankment tests.

Construction blocks were placed along the embankment starting at station 48 and ending at station 20. The blocks were oriented lengthwise (i.e., the long dimension in the direction of flow) with the open cells facing up, and were aligned in rows without the use of a stagger pattern, as illustrated in figure 17. As shown in the figure, the fairly large V-shaped opening in the construction block mattress caused by the break in slope at the embankment shoulder was filled with concrete grout prior to testing. Grouting was limited to this location.

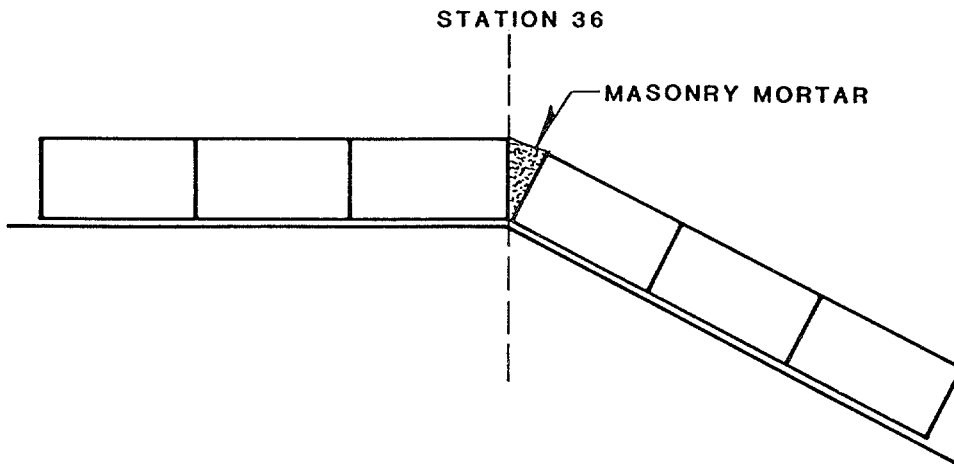
Washed river rock with a median size of 4 to 6 in (10 to 15 cm) was used to fill the open cells of the blocks. A length of angle iron was welded to the flume walls at station 48 to provide a toe anchor for the system. The



Figure 16. The completed Petraflex-Vick protection system on the rigid embankment (without rock infill).



PLAN VIEW OF TOE DETAIL



PROFILE VIEW OF SHOULDER DETAIL

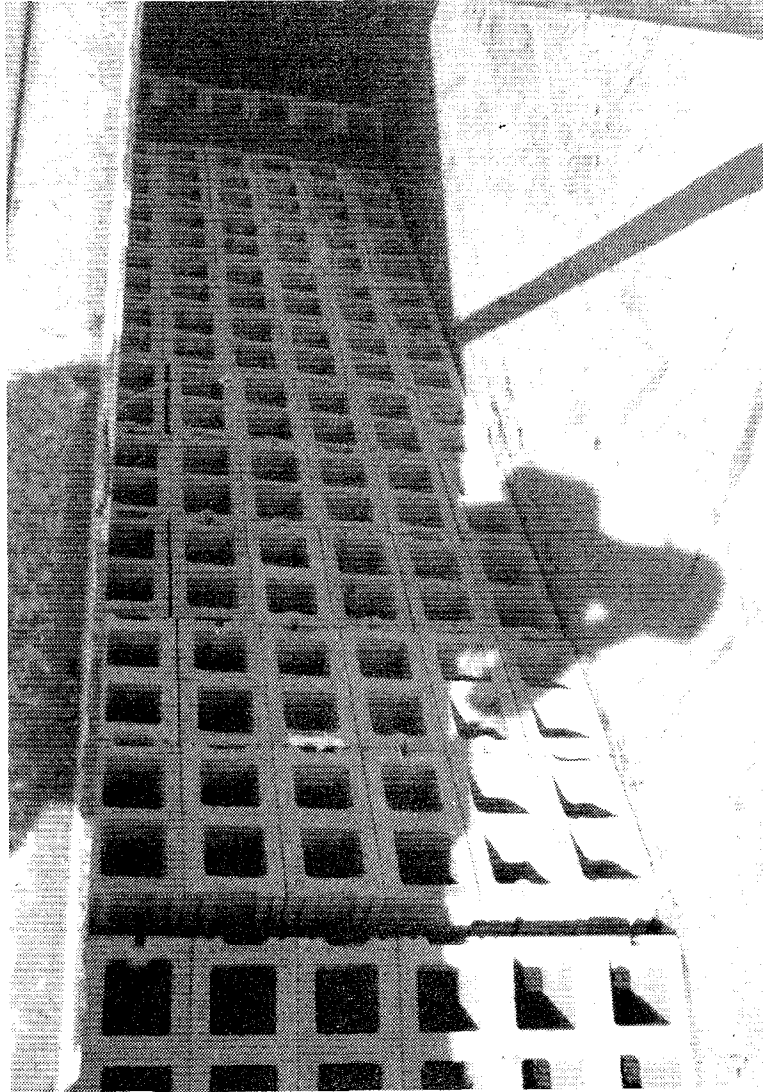
Figure 17. Block configuration for the construction block protection system.

displacement transducer's cable was affixed to the upper surface of a block at station 37.5 by passing it through one of the block's open cells. Figure 18a shows the construction block embankment protection system before grouting and placing the gravel fill. The completed system is shown in figure 18b.

One rigid embankment test was conducted on the construction block system. Test DR-1 subjected the system to a total of 8 hours of testing. The first 6 hours were conducted under freefall conditions with 2 hours each of 1-, 2-, and 4-ft (0.30, 0.61, and 1.22 m) overtopping depths. The last 2 hours of the test used a 4-ft (1.22 m) overtopping depth with 5 ft (1.52 m) of tailwater.

(5) Wedge-Shaped Concrete-Block Protection System. The wedge-shaped blocks are designed such that every transverse row of blocks overlaps the next downstream row. No cables are used in the system. Unique to this design are longitudinally-oriented drainage slots which are fabricated into the blocks along the downstream face to promote the aspiration of any water seeping beneath the embankment protection system. The blocks tested in this program exhibited a unit weight of 48 lb/ft² (2.30 kN/m²). The block system, when viewed in plan, exhibits a solid appearance with no cells or other apertures open to the flow, therefore the net open area of the system is essentially zero. Each full-sized block in the system exhibited a gross footprint area of 0.33 ft² (0.033 m²). Half-blocks were also cast for this installation, and a stagger pattern was used in the placement of the system. The geotextile fabric and drainage layer were identical to those used in previous tests.

The wedge-shaped blocks were placed along the embankment beginning at station 48 and, due to a slight shortage of blocks, terminating at station 26. The blocks were oriented such that each row of blocks overlapped the previous row, starting at the downstream edge of the block matrix. Wedge block installation is shown in figures 19a and 19b. A length of angle iron was welded across the toe of the system to anchor the terminal row of blocks. Similarly, a steel rod was installed at station 26 to restrict uplift or rotation of the most upstream row of the block system. Due to the limited quantity of wedge-shaped blocks, Dycel 100 blocks were installed from station 20 to 26 to complete the protective mattress and to provide a smooth transition from the concrete shell to the test section.

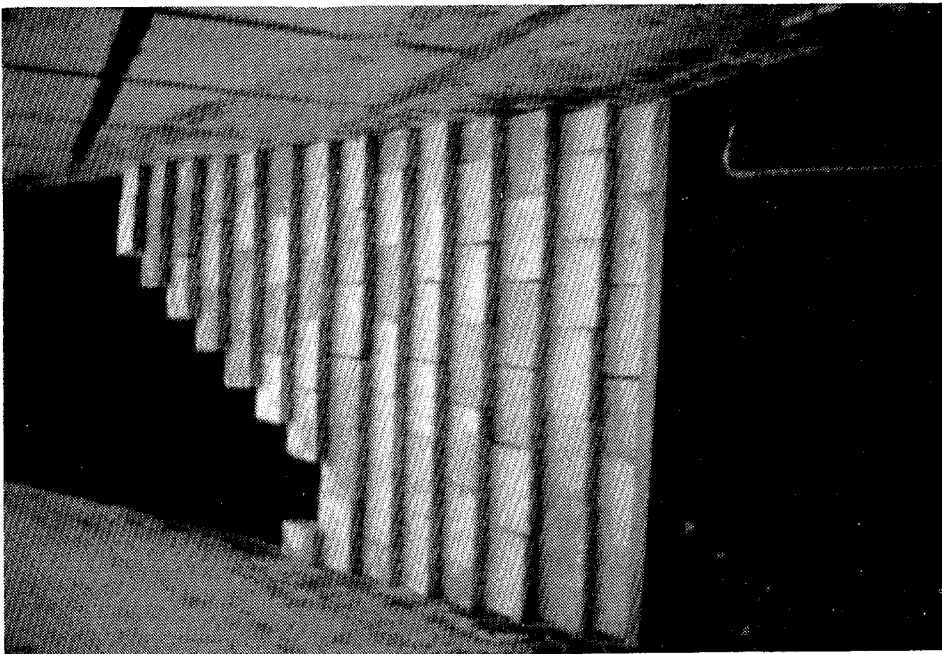


a. Before placement of the gravel fill material



b. After placement of the gravel fill material

Figure 18. The completed construction block protection system on the rigid embankment.



a. Looking upstream



b. Looking through the observation window

Figure 19. Installation of the wedge block protection system on the rigid embankment.

To assist with the sharp slope transition of the concrete shell at the embankment shoulder, a custom-fit piece of angle iron was sandwiched underneath the vertical overhang of the row of blocks at this location (station 36). It should be noted that this bar was not welded to the flume walls, but merely placed loosely so as to achieve the desired overhang effect between the rows of blocks at this location.

The cable for the displacement transducer was connected to the upper surface of a block at station 37.5 after threading it through a small channel cut in the back end of a block with a diamond-bladed saw.

Two tests were performed on the wedge-shaped block system. Test ER-1 was an 8-hour test of freefall conditions. Overtopping depths of 0.5, 1, 1.5, and 2 ft (0.15, 0.30, 0.46, and 0.61 m) were each maintained for 2 hours. Test ER-2 was also an 8-hour test. The first 6 hours were conducted under freefall conditions for overtopping depths of 3, 3.5, and 4 ft (0.90, 1.05, and 1.22 m). The final 2 hours of the test were conducted for a 4-ft (1.22 m) overtopping depth with 5-ft (1.52 m) of tailwater.

b. Erodible Embankment Tests

The second phase of the embankment testing program focused on determining the erosion protection potential of concrete block systems installed on an embankment of highly erodible soil. This phase included a total of nine tests on the Armorflex, Dycel, construction, and wedge-shaped block systems. As the Petraflex-Vick system had been tested extensively on a soil embankment during the 1988 study and was found to be stable up to the maximum flow capacity of the facility, further tests of this particular system were deemed unnecessary.

The soil used for constructing the embankment was identical to the type I soil used in the 1988 study. Field and laboratory tests were performed on the type I soil to determine its engineering properties and classification. Measured soil characteristics included Proctor density, permeability, Atterberg limits, grain-size distribution, and classification by the USCS and AASHTO system. Table 3 summarizes the key engineering properties determined for this

Table 3. Engineering properties of embankment soil.

Percent Sand: 36 to 48

Percent Silt: 34 to 40

Percent Clay: 18 to 24

Atterberg Limits: Liquid Limit 21.5 to 23.3
Plasticity Index 4.9 to 8.4

Standard Proctor Density: 118 to 122 lb/ft³ @ 11.9% moisture

Sat. Hydraulic Conductivity: 7×10^{-8} cm/s @ 95% Proctor

Unified Soil Classification: SC - SM

AASHTO Group Designation: A-4 (0)

soil. Figures 20 and 21 illustrate the moisture-density and grain size characteristics, respectively, of the embankment soil used in the testing program.

The embankment was constructed by placing soil in the flume in 4- to 6-in (15 to 20 cm) lifts. A vibrating plate compactor was used for compacting each lift. Compaction of 89 to 93 percent of standard Proctor density was achieved with six passes of the vibrating plate over each lift. The downstream slope of the embankment was prepared to a 2H:1V slope for the Armorflex and Dycel tests, and a 3H:1V slope for the construction block and wedge block tests.

Installation of the instrumentation canisters involved excavating four cubical cavities 6-in (15 cm) deep into the prepared embankment surface, along with 4-in (10 cm) deep trenches into which the electronic wiring was strung. The wiring was brought through a watertight opening in the flume wall located at station 41.5, beneath the protection system. After the wiring was connected to the CR7X data logger and tested for electrical continuity, the wiring runs and all voids surrounding the canisters were filled with soil and compacted manually. A completed erodible embankment with instrumentation canisters is shown in figure 22.

Each of the transducers were then cleaned, inspected and prepared for the ensuing test. It should be noted that shortly after test start-up, slight embankment settlement, shifting of the protection system, or initial transport of minor amounts of soil underneath the block system tended to have an undesirable effect on the functioning of some of the transducer probes. The reliability of the differential pressure transducer (station 37.5) was poor for all soil embankment tests. Soil particles moving beneath the blocks tended to plug the pitot openings of this unit, causing large variations in measured pressures. Similarly, the displacement transducer (also located at station 37.5) was occasionally jammed by soil accretion, or the block to which it was attached either settled or became wedged as the embankment shifted and settled. These difficulties sometimes resulted in inconclusive data, or data which were difficult to interpret, for these two particular probes during the course of the soil embankment tests. On the positive side, the data from the pressure transducers at the four measurement stations can be generally regarded to be of

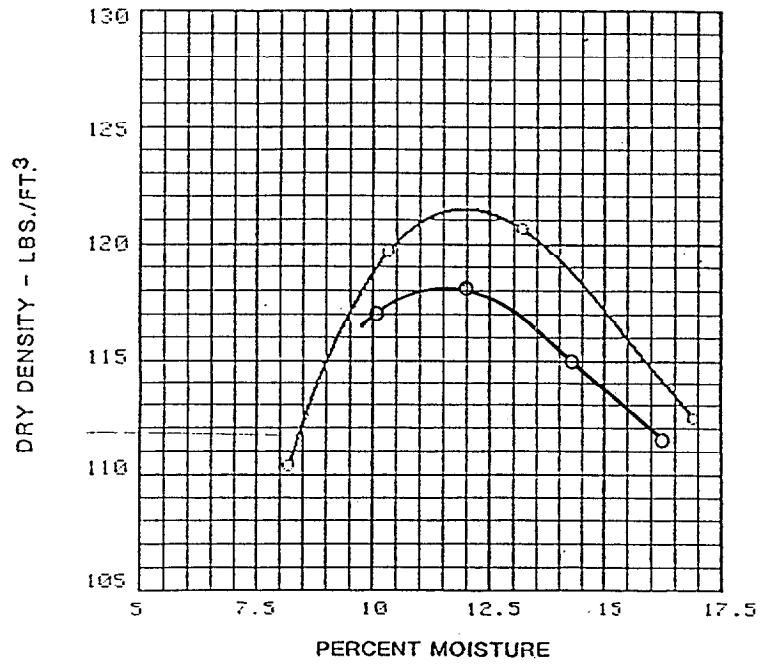


Figure 20. Moisture density curves for the type I soil.

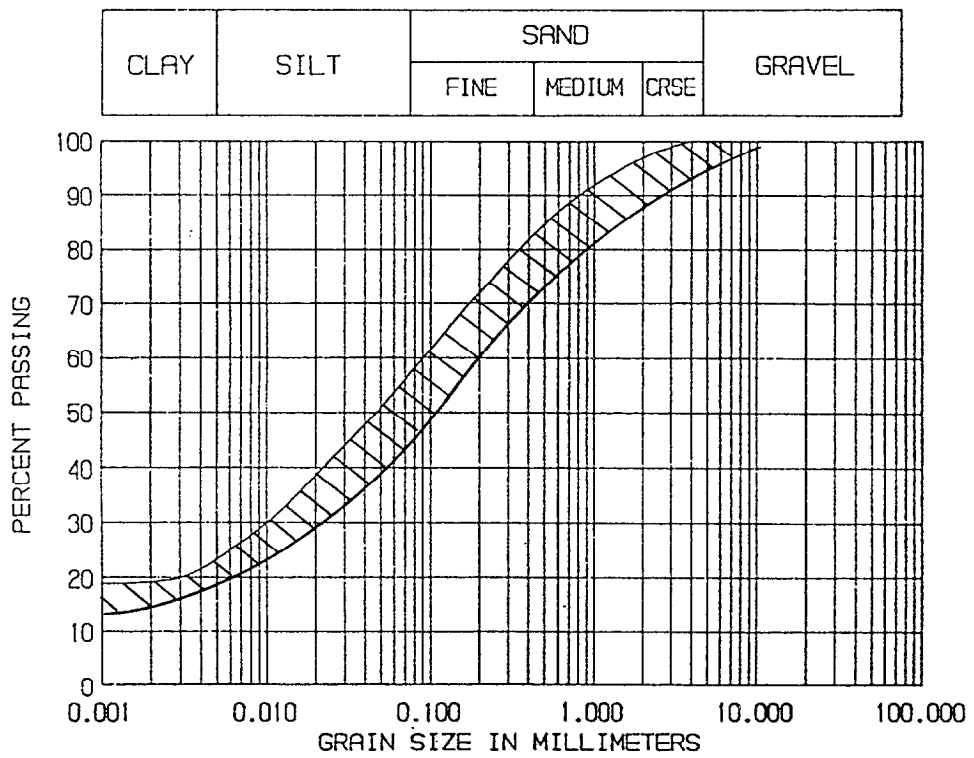


Figure 21. Grain-size distribution range for the type I soil.



a. Looking downstream



b. Looking upstream

Figure 22. The erodible embankment, illustrating 2H:1V slope and 4H:1V crest chamfer, prior to geotextile placement and protection system installation (tests A-3 and A-4).

high quality throughout the course of the soil embankment tests, except where specifically noted otherwise.

(1) Armorflex Class 30 Concrete Block Protection System. For tests A-1 and A-2, the downstream slope of the embankment was prepared with a 2H:1V slope. For tests A-3 and A-4, a 4H:1V chamfer transition from the crest to the embankment slope (extending from station 36 to 40) was constructed, with a 2H:1V slope extending from station 40 to the toe of the embankment (refer to figure 22).

Nicolon 40/30 geotextile fabric and an Enkamat 7020 drainage layer were used as the underlayer for all Armorflex tests on the soil embankment, identical to the construction technique used on the rigid embankment.

An 18-in (46 cm) deep anchor trench was prepared at a 45° angle at station 20, 16 ft (4.9 m) upstream of the embankment shoulder. Two helix anchors were installed in the foot of the trench to serve as cable anchor points. Both lateral and longitudinal cables were utilized in the construction.

The Armorflex Class 30 block system was installed on the soil embankment in the same manner as described for the rigid embankment, with the following two exceptions:

1. Two pairs of helix anchors were installed through the revetment system, one pair at station 38 and the other pair at station 42. Steel plates were mounted over the threaded stems, and secured with nuts and washers. Installation of the soil anchors is shown in figure 23.
2. Two lengths of 1/2-in (1.3 cm) rebar were placed between the block system and the flume walls between stations 20 and 48. This modification was implemented because a 3/4-in (1.9 cm) void remained between the block system and each flume wall after placement was completed. The rebar was installed in order to prevent soil scour and loss at the walls by holding the underlying geotextile and drainage fabrics in place. The gap above the rebar was then filled with angular crushed rock having a median diameter of 3/8 in (1 cm).



Figure 23. Installation of helix slope anchors for the Armorflex Class 30 system on the erodible embankment.

Figure 24 shows the completed Armorflex embankment protection system with soil anchors.

The Armorflex block system was subjected to four different hydraulic conditions on two separate embankment geometries. Overtopping depths of 1, 2, and 4 ft (0.30, 0.61, and 1.22 m) were investigated. A test of 4-ft (1.22 m) overtopping depth was also conducted with 5 ft (1.5 m) of tailwater. Test A-1 was an 8-hour test with 4 hours each at 1- and 2-ft (0.30 and 0.61 m) overtopping depths. Test A-2 was an 8-hour test using a 4-ft (1.22 m) overtopping depth, with the first 4 hours under freefall conditions and the second 4 hours using a tailwater elevation of 5 ft (1.5 m).

Upon completion of test A-2, a minor bulge in the system developed at station 42 on the slope, along with a depression from stations 37 to 39 near the crest. After removal of the block mattress and geotextile fabrics, it was observed that soil had eroded from station 37 through 39 and deposited near station 42. The areas of soil loss beneath the system were observed to be restricted to the shallow trenches in which the electronic wiring had been laid. This indicated that (a) the wiring had not been buried deep enough at points along the trenches, allowing erosion to initiate and propagate, (b) the soil in the wiring trenches had not been compacted properly, or (c) both.

Preparation for tests A-3 and A-4 included rebuilding the soil embankment as previously described, with the inclusion of the 4H:1V chamfered section at the embankment shoulder. Care was taken to bury the electronic wiring 6 in (15 cm) or deeper beneath the soil surface, and to achieve a degree of soil compaction in the trenches equal to, or slightly greater than, the rest of the embankment. Slope anchors were not used. Hydraulic conditions for tests A-3 and A-4 proceeded in the same manner as A-1 and A-2, respectively. Both of these tests were completed without any detectable erosion of the underlying embankment.

(2) Dycel 100 Concrete Block Protection System. The soil embankment was constructed using techniques previously described with a 2H:1V downstream slope. An anchor trench 18 in (46 cm) deep was prepared at station 24 and a pair of helix soil anchors embedded within it, identical to that constructed for the Armorflex tests. The geotextile fabric and drainage layer installation was



Figure 24. The completed Armorflex Class 30 protection system on the erodible embankment (with helix slope anchors).

also identical to that for the Armorflex tests. The Dycel 100 blocks were installed in the same manner as described for the rigid embankment test, except that two pairs of slope anchors were installed at stations 38 and 42 (on the face of the embankment) to provide shear and uplift resistance. The edges of the Dycel 100 system abutted closely to the flume walls with a gap width less than 1/4 in (6 mm). Therefore, the only precaution taken along the system edges was to ensure that the Nicolon 40/30 geotextile fabric was sufficiently wide to lap up along the flume walls at least 2 in (5 cm) on both sides of the system. Figure 25 shows the completed Dycel 100 system with slope anchors.

The Dycel 100 concrete block mattress was subjected to one hydraulic condition. Test B-1 used a 1-ft (0.30 m) overtopping depth with freefall conditions. This test failed within the first 45 minutes of the 1-ft (0.30 m) overtopping flow condition. The failure mode appeared to be a combination of erosion and soil liquefaction beneath the system due to an excessive ingress of water under the system. The post-failure profile of the system showed the characteristic loss of soil at the shoulder and a corresponding bulge near the embankment toe. Due to the observed rapidity of the shift from prefailure to post-failure profiles, a shallow-seated slip failure is the likely mode of embankment failure, as opposed to a more gradual scour-and-deposition process.

(3) Construction Block Protection System. Soil embankment construction and preparation techniques were identical to those described previously, with the embankment constructed to a 3H:1V downstream slope. The geosynthetic underlayer was constructed differently from the Armorflex and Dycel systems, however, in an effort to more closely replicate field procedures and design guidelines promulgated and currently utilized by the U.S. Soil Conservation Service.^(2,3,4) The field procedure involves placing a layer of leveling sand on the foundation soil to permit screeding of the surface to a uniform and true surface for subsequent placement of the geosynthetic fabric and blocks. This provides for an intimate and areally uniform contact between the fabric and the erodible foundation soil. Gradation between the foundation soil, sand, and fabric pore size is designed to prevent migration of the soil into the sand or the sand through the fabric, while providing increasing permeability toward the surface. The sand can be formed of crushed aggregate, such as rock chips, to



Figure 25. The completed Dycel 100 protection system on the erodible embankment (with helix slope anchors).

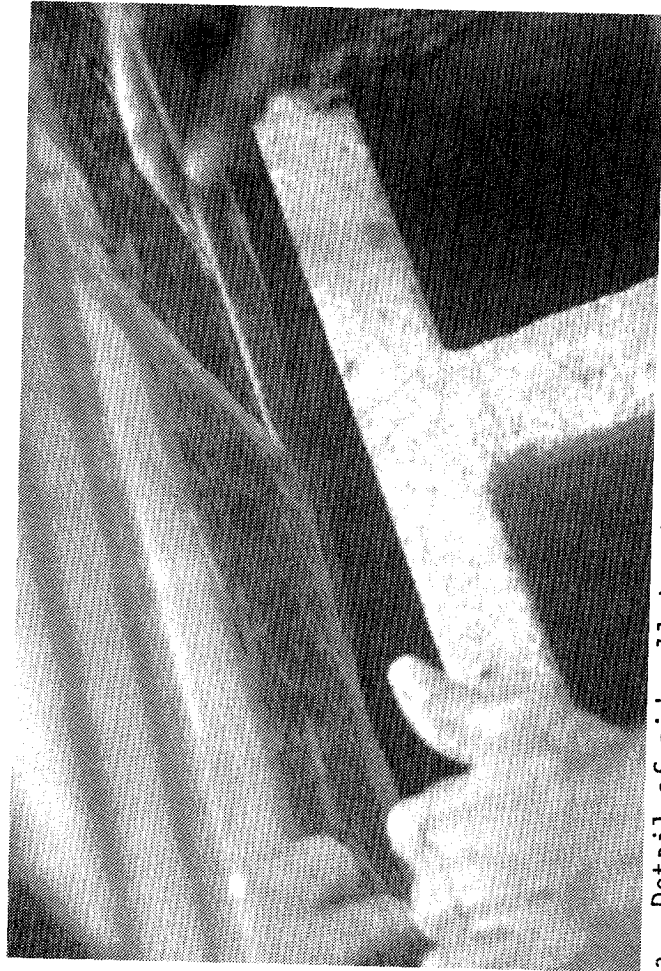
reduce permeability and increase surface stability during subsequent construction placement of the fabric and blocks.

To facilitate the placement of sand and fabric for the study, Enkamat 7020 mesh was installed directly on top of the soil, and a 3/4-in (1.9 cm) thick covering of masonry sand was used to fill the enkamat to the top of the nylon mesh. The primary purpose of the enkamat blanket in this setting was to add surface stability during subsequent placement of the geotextile fabric and blocks in the flume. Nicolon 40/30 fabric was then installed on top of the enkamat/sand layer, and the construction blocks were positioned in the same nonstaggered configuration that was used for the rigid embankment test.

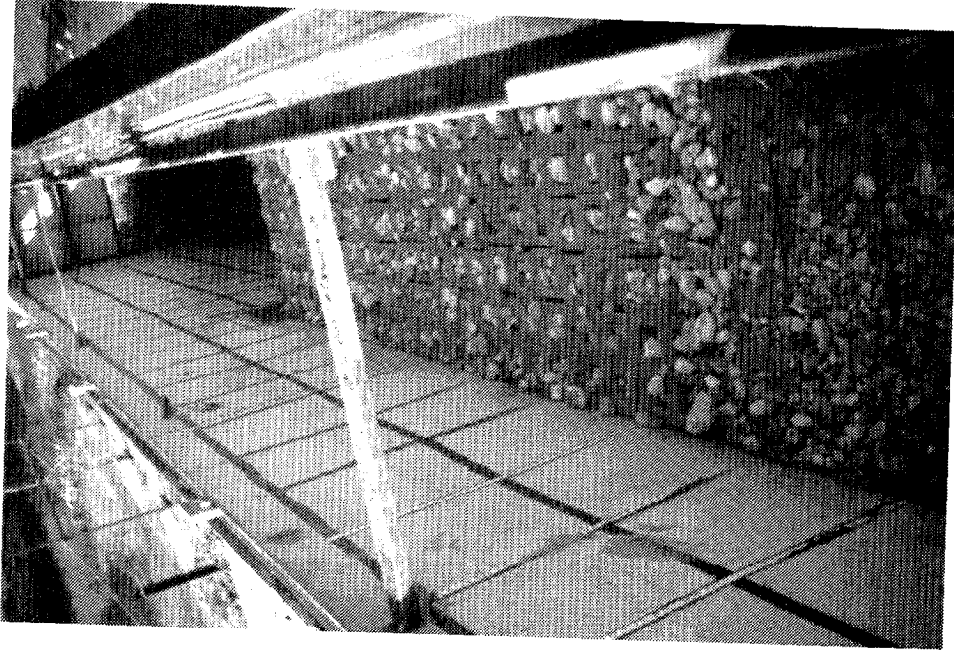
Once installed, a 1- to 1-1/2 in (2.5 to 4.0 cm) gap remained between the block system and each flume wall. Several 2-ft (61 cm) lengths of 1/2-in (1.3 cm) rebar and wood stakes were placed between the edges of the blocks and the flume walls between stations 20 and 54 to hold down the underlying geotextile fabrics and prevent scour along the walls. On top of the rebar was placed a wadding of geotextile material along both walls for the entire length of the system, and the remaining gap filled with 3/4-in (1.9 cm) crushed rock. Figure 26a shows the geotextile wadding being inserted between the block system and flume wall.

Washed river rock with a median size of 4 to 6 in (10 to 15 cm) was used to fill the open cells of the concrete construction block system. A length of angle iron was welded to the flume walls at station 52 to provide a toe anchor for the system. Figure 26b shows the completed system prior to testing.

Test D-1 subjected the system to 8 hours of testing under freefall conditions. Tests were performed for 4 hours for both 1- and 2-ft (0.30 and 0.61 m) overtopping depths. At the conclusion of this test the sand which filled the enkamat had been almost completely washed out from beneath the block system. In addition, the soil embankment along the flume walls had eroded from the toe to approximately station 32, located 4 ft (1.5 m) upstream from the embankment shoulder. Local areas of scour exceeded 6-in (15 cm) deep, with average scour depths of 3 to 4 in (7.6 to 10 cm) under much of the downstream slope. Loss of sand and soil is attributed to the ability of the material to pass unchecked



a. Detail of sidewall treatment, showing placement of geotextile wadding.



b. Completed system prior to testing (looking downstream). Note Armor-flex blocks in foreground, upstream of the tested section.

Figure 26. Construction block protection system on the erodible embankment.

through the enkammat, which itself was extended beyond the toe of the block system and provided a direct conduit for artificial (and unintentional) "piping" to occur. Interestingly, the block system did not exhibit any surface deformation, and individual blocks had become so tightly wedged in place that they bridged tightly over the voids which had propagated beneath.

The construction blocks were removed and the soil embankment was reconditioned in preparation for test D-2. Four modifications were implemented in the design and placement of the geotextile underlayment beneath the block system, as described below:

1. The Enkammat 7020 fabric was terminated at station 50, approximately 4 ft (1.22 m) upstream from the embankment toe.
2. Sand was mixed with 3/8-in (10 mm) crushed rock in equal proportions by weight. This blend was applied to the embankment to a depth sufficient to fill the enkammat to the top of the nylon mesh.
3. To prevent piping of the sand/gravel mix through the enkammat, the embankment toe was constructed over a short [6-ft (1.8 m)] length of Nicolon 40/30 geotextile fabric. This piece of fabric extended 3 ft (0.9 m) beyond the embankment toe, which allowed the fabric to be later overlapped onto the surface of the embankment.
4. Nicolon 40/30 geotextile fabric was then placed over the sand/gravel mix and was carried all the way down the embankment slope to the toe, at which point it was laid over the piece of fabric described in step 3, and secured to the steel floor of the flume with urethane foam. This prevented migration of the sand/gravel mix beyond the toe of the system.

In addition to the above precautions taken with the geotextile layers, the blocks themselves were placed so as to abut closely against the flume walls. Spaces between blocks were then distributed among interior blocks in the system, not at the edges. **Figure 27** provides a profile of the completed construction block protection system.

Test D-2 consisted of 2 hours of testing for both 2- and 4-ft (0.61 and 1.22 m) overtopping depths under freefall conditions. The test also investigated a 4-ft (1.22 m) overtopping depth under tailwater conditions for the last 4

DETAIL AT FLUME WALL

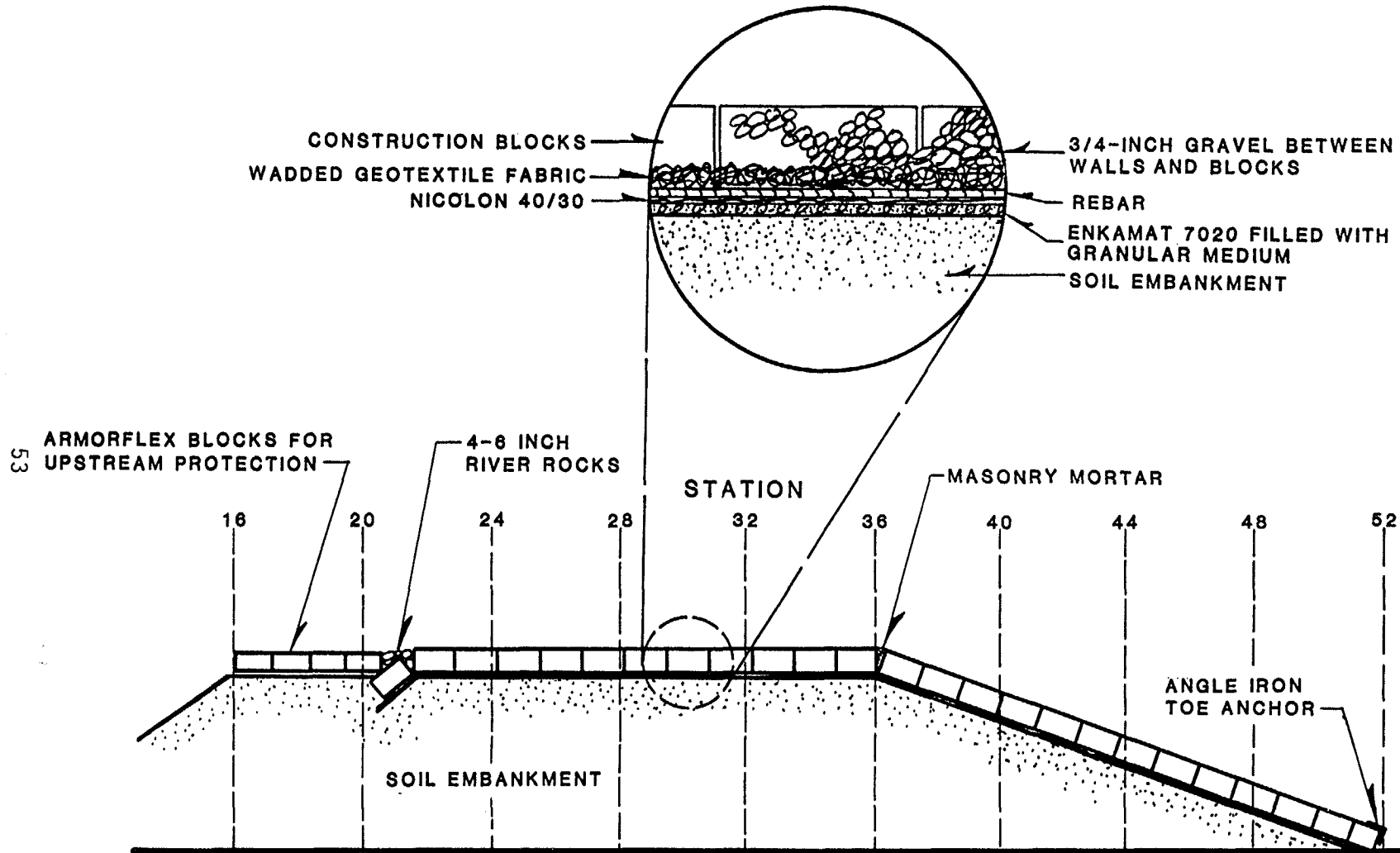


Figure 27. Profile of the completed construction block embankment protection system.

hours. This test was completed successfully, with no loss of embankment soil or deformation of the protection system noted.

(4) Wedge-Shaped Concrete Block Protection System. The soil embankment was constructed as for the other tests, and the downstream slope was built to a 3H:1V grade, which is the slope for which these blocks were designed. The geotextile fabrics were installed as they were for the Armorflex and Dycel tests: Nicolon 40/30 geotextile was placed on the soil and Enkamat 7020 was laid over the Nicolon fabric.

The wedge-shaped blocks were placed along the soil embankment in the same staggered configuration used for the earlier rigid embankment test. A rounded slope transition was used at the embankment shoulder (station 36), with a radius of vertical curvature of approximately 4 ft (1.2 m) for the finished embankment profile. The rounded transition simplified the placement of the wedge-shaped blocks, ensuring that the full overhang was developed between blocks and eliminating the need for any mechanical block support at the transition section. Figure 28 is a schematic of the completed wedge block embankment protection system.

Two tests were performed on the wedge-shaped block system. Test E-1 examined the system for 8 hours of freefall conditions--4 hours at both 1- and 2-ft (0.30 and 0.61 m) overtopping depths. Test E-2 subjected the block system to 4 hours of a 4-ft (1.22 m) overtopping depth under both freefall and tailwater conditions. Both tests were completed successfully with no loss of embankment soil or deformation of the protection system noted.

c. Qualitative Summary of Concrete Block Mattress Performance

The following two sections provide a qualitative description of the performance of the various concrete block systems investigated under this program. These descriptions are provided for both the rigid embankment tests and the soil embankment tests, respectively.

(1) Rigid Embankment Tests. All concrete block systems tested on the rigid (concrete-shelled) embankment were stable for the range of hydraulic

55

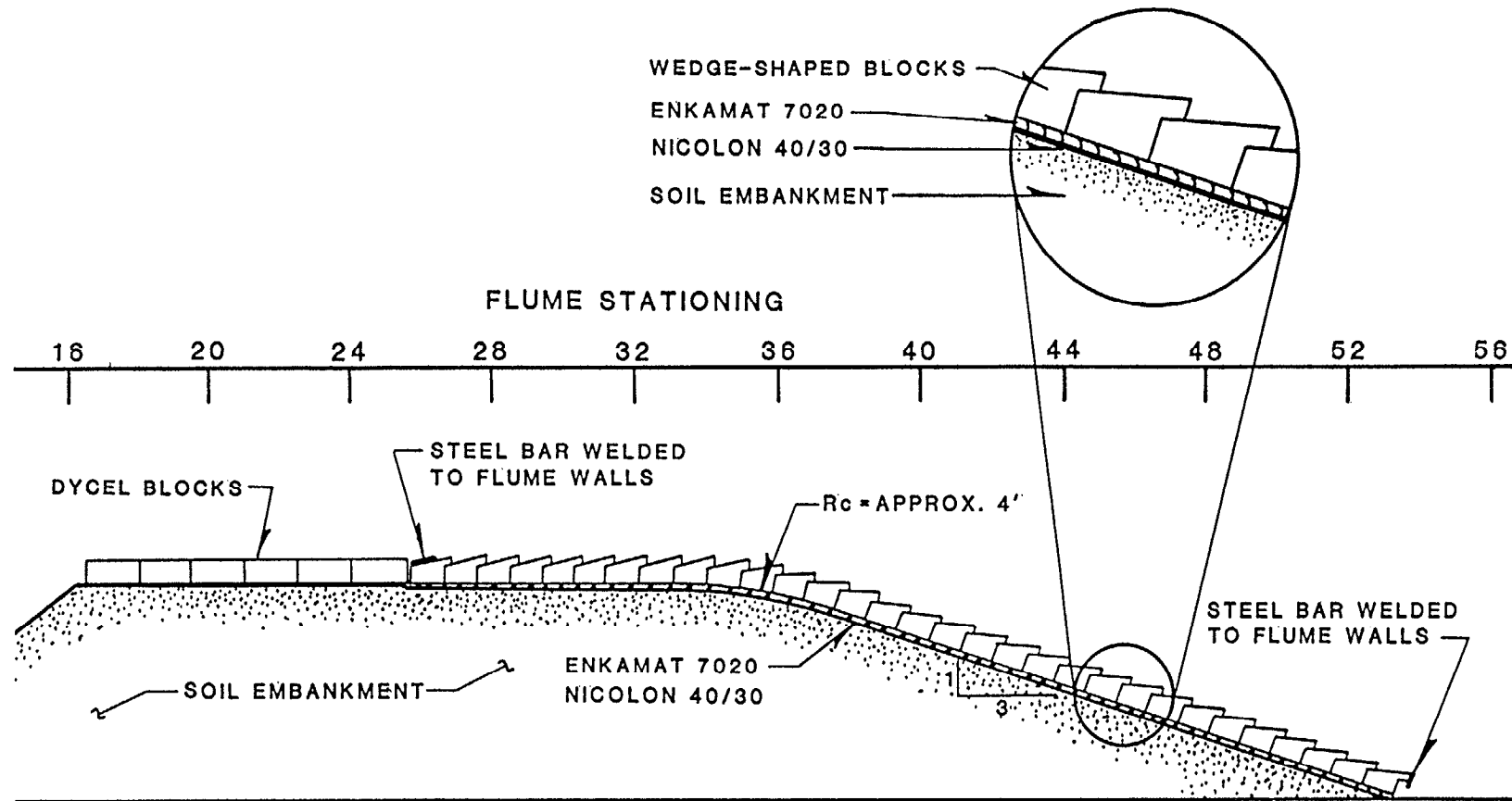


Figure 28. Profile of the completed wedge block protection system.

conditions investigated, up to and including the maximum discharge capacity of the testing facility. This was true for both the cabled systems (test series A, B, and C) and the noncabled systems (test series D and E).

Although the flow removed nearly all of the gravel fill from the Armorflex Class 30 system and the Petraflex-Vick system, no instability was indicated by either visual observation or pressure transducer data. In contrast, the Dycel 100 system, although visually appearing stable, exhibited pressure data indicating that excess hydrodynamic pressure was present near the toe of the system. The occurrence of excess pressure in this region is a result of the uncontrolled ingress of water beneath the system, and will be discussed quantitatively in the following chapter.

The construction block system was stable for all rigid embankment hydraulic conditions, despite the fact that it is a noncabled system. The system exhibited very little loss of the gravel fill material due to the large block depth and large rock size used for infill material.

Visually, the wedge block system did not give any indication of block displacement; however, the deflection transducer data showed that individual blocks in this system may tend to vibrate more than the other systems. At the same time, the differential pressure transducer revealed that less water was flowing under this system compared to other systems, thereby indicating that the self-aspirating feature of the wedge blocks appears to function as intended. These aspects will be discussed quantitatively in the next chapter. Figure 29 illustrates the wedge block system after rigid embankment testing.

(2) Erodible Embankment Tests. Three of the nine tests conducted on the soil embankment resulted in partial loss of subgrade, system deformation, or both. However, close inspection revealed that in two of the three cases, the design or installation within the testing facility was found to be at fault. Therefore, only one of the four systems tested on the erodible embankment, the Dycel 100 system, can be classified as unstable under the conditions of this testing program.



Figure 29. The wedge block protection system after testing on the rigid embankment.

The Armorflex Class 30 system was stable for 1-, 2-, and 4-ft (0.30, 0.61 m, and 1.22 m) overtopping depths. The documented failure of test A-2 was determined to be a consequence of faulty installation rather than block characteristics or system design. **Figure 30** shows the underlying soil embankment after test A-2 during which the cable trenches eroded. After reconstruction of the soil embankment which included chamfering of the shoulder, the system proved to be stable for tests A-3 and A-4, including the 4-ft (1.22 m) overtopping flow, both with and without tailwater. **Figure 31** shows the system after test A-4.

The Dycel 100 mattress was tested with a 1-ft (0.30 m) overtopping depth. The system failed within the first 45 minutes of testing. The condition of the system after testing is shown in **figures 32 and 33**. Considerable displacement of the blocks along the entire embankment profile is evident. The observed threshold of instability and mode of failure were identical to that reported in the 1988 study, despite the heavier closed-cell system.⁽¹⁾ This failure is thought to be partially due to block geometry and larger surface area per block compared to other systems. The combination of a relatively thin block with a large surface area appeared to be detrimental to block stability. Additionally, filling the cells with masonry mortar reduced the net open area, and may have hindered drainage and pressure relief. Lastly, the geometric configuration of the mechanical interlock between blocks does not appear to be as well developed as for other systems, thereby yielding small but potentially detrimental displacements at lower hydraulic stresses.

The Petraflex-Vick concrete block mattress was not tested on the soil embankment because of its success in the 1988 study.⁽¹⁾ During the previous study, the Petraflex-Vick system was tested on the same erodible soil used in the current study (type I soil), under four different hydraulic conditions with no damage. The previous study subjected this system to a total of 48 hours of testing with 28 hours at maximum flow [4-ft (1.22 m) overtopping depth]. System weight, mechanical interlock and the installation of lateral cables and slope anchors may have contributed to the success of those tests.

The construction block system was stable for 1-, 2-, and 4-ft (0.30, 0.61, and 1.22 m) overtopping depths. Test D-1 did result in erosion of the soil embankment, but like the Armorflex failure, this was a result of faulty system

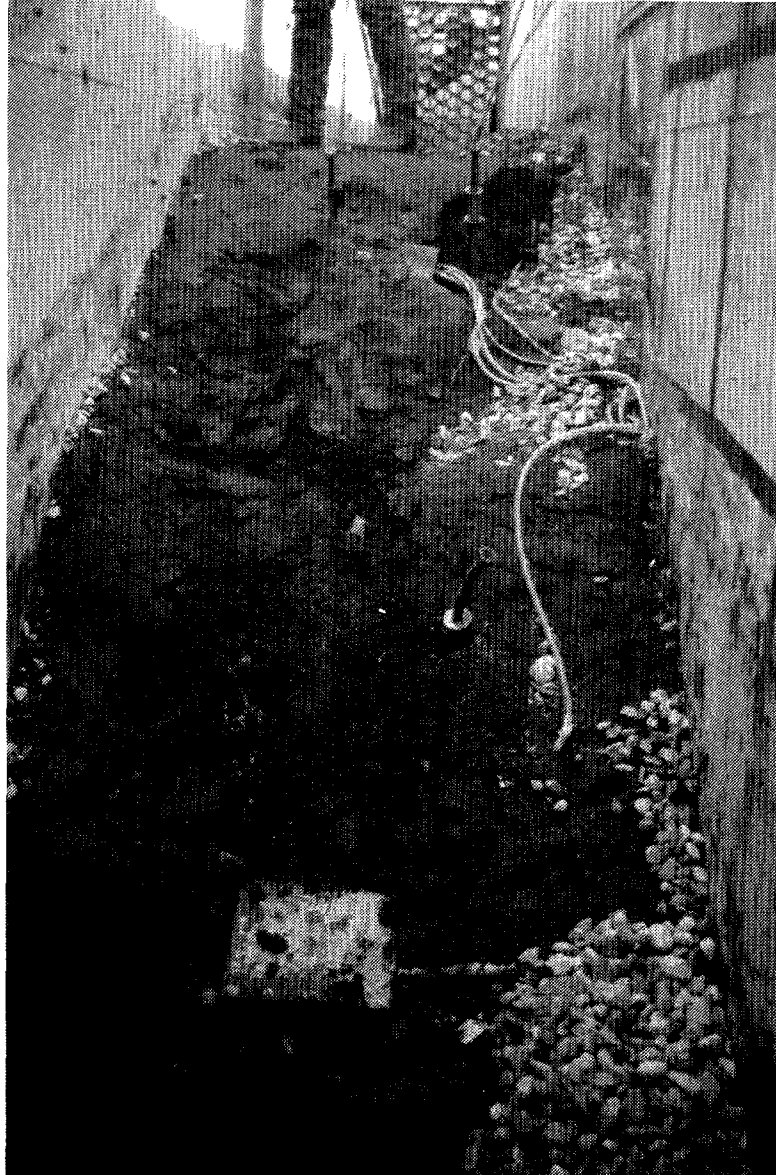


Figure 30. Erosion of the pressure transducer cable trenches beneath the Armorflex Class 30 protection system after test A-2.

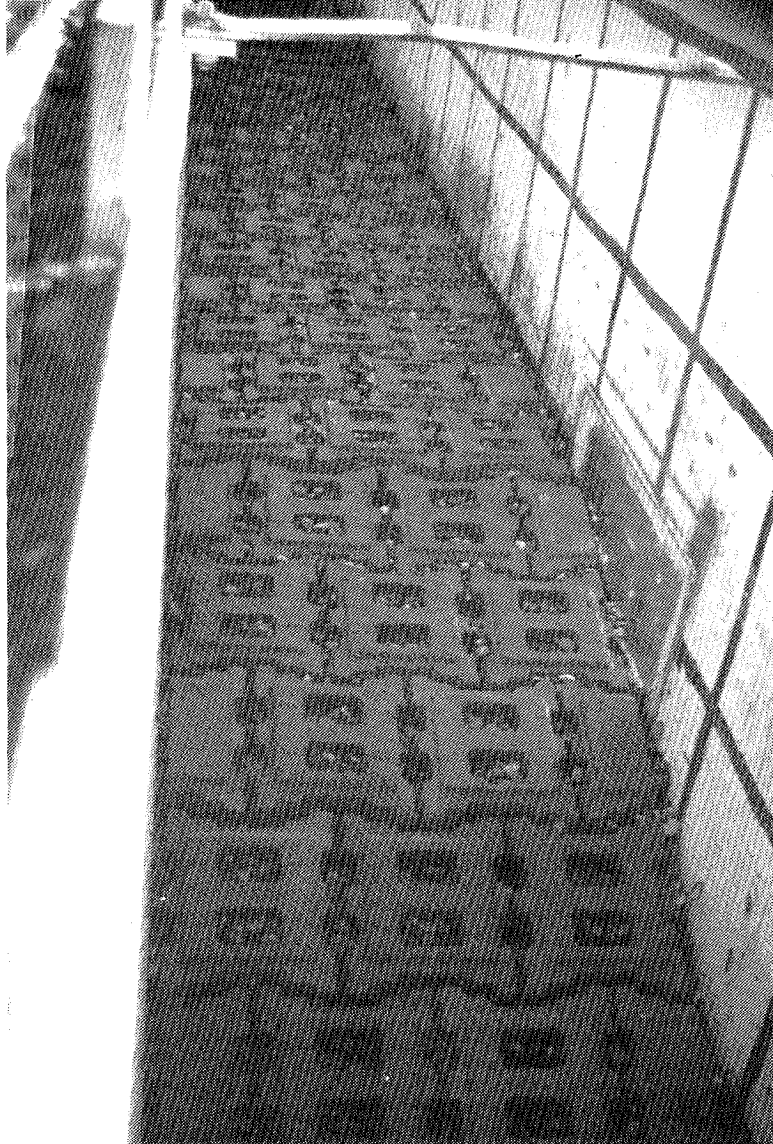


Figure 31. The Armorflex Class 30 protection system after testing on the erodible embankment (test A-4).



Figure 32. Failure of the Dycel 100 system after testing on the erodible embankment, looking upstream.



Figure 33. Failure of the Dycel 100 system after testing on the erodible embankment, looking downstream.

design and placement in the testing facility. Once these problems were resolved, test D-2 demonstrated that the construction block system is a viable method of embankment protection. This is indicated in figure 34 which shows the system after test D-2.

Tests E-1 and E-2 of the wedge-shaped block system were both successful and resulted in no detectable erosion of the underlying soil embankment or system deformation. Figure 35, which shows the system after testing, underscores this point. Note that several of the blocks appear cracked or broken in the photograph. This damage occurred due to foot traffic on the system during post-test inspection activities.

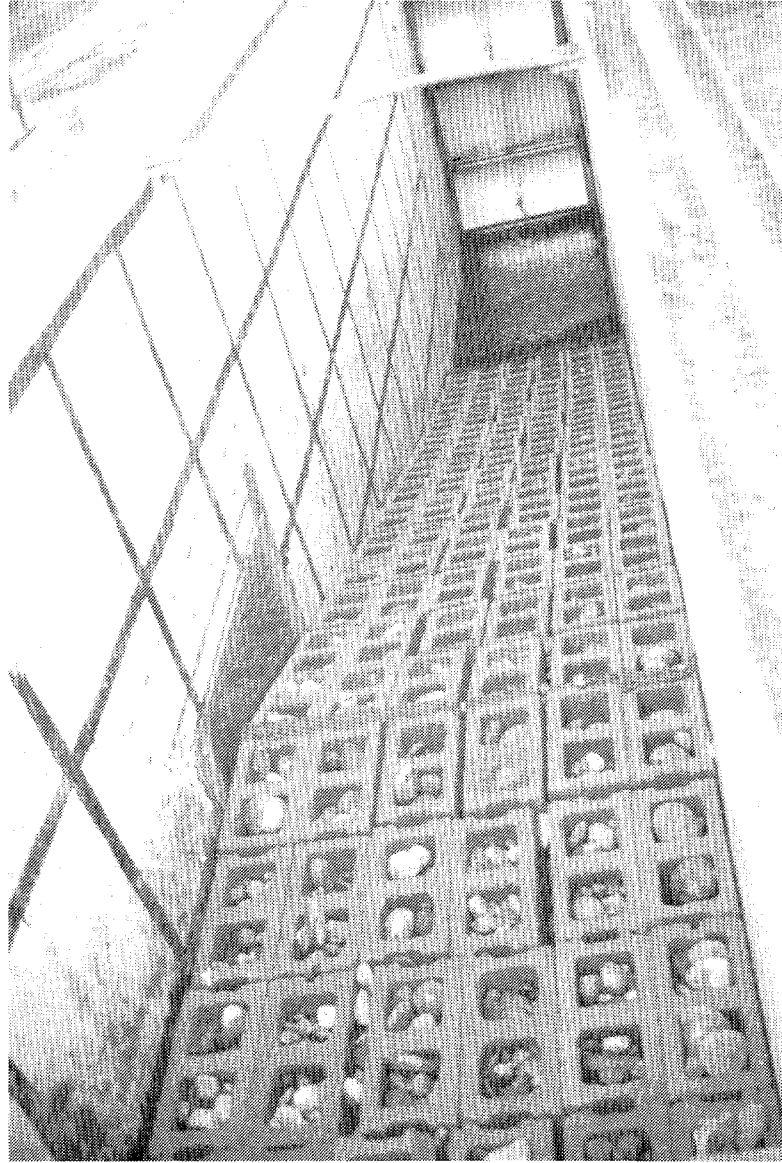


Figure 34. The construction block protection system after testing on the erodible embankment.



a. Looking downstream after Test ER-2. Note loose gravel remaining in the lee of the blocks



b. The downstream slope after Test ER-2.

Figure 35. The wedge block protection system after testing on the erodible embankment.

RESULTS OF FULL-SCALE EMBANKMENT TESTING PROGRAM

The data collection techniques and method of data organization was described in the previous chapter. This chapter will discuss the methodologies used to analyze the data and will present the results of the analyses.

1. Determination of Test Discharges

Along the horizontal portion of the embankment crest, the rate of acceleration of the (steady) overtopping flow field is gradual, allowing reliable and consistent velocity measurements to be taken. Additionally, this region exhibits flow which is non-air-entrained and is relatively less turbulent than at other locations on the embankment. For these reasons, discharges were determined based on data from this region. For each test, both the crest flow velocities and measured flow depths were averaged, and the discharge calculated using the velocity-area method. The computed discharge was then verified by comparing with the discharge given by the broad-crested weir equation. This equation is

$$Q = 3.0 L H^{3/2} \quad (1)$$

where 3.0 is the broad-crested weir coefficient for use with English units, H is the total energy head on the crest, and L is the embankment length which for the test facility is 4 ft (1.22 m). Generally, the discharges computed by these two methods agreed to within 5 percent. The nominal 1-, 2-, and 4-ft (0.30, 0.61, and 1.22 m) overtopping depths, as referred to in this report, typically correspond to approximately 13, 34, and 84 ft³/s (0.4, 1.0, and 2.4 m³/s), respectively.

2. Data Conditioning and Computation of Hydraulic Parameters

Embankment and water-surface profiles, along with the calculated position of the total energy line, were plotted for each discharge step for every test, as illustrated previously in figure 7. The profile plots were then examined as a first-level error trap in order to identify possible errors in data collection or entry.

The profile plots were also used to determine the measurement stations and data points to be used in the calculation of the friction slope on the crest and on the downstream slope of the embankment by linear regression. In some instances, this required the identification and omission of occasional data outliers. Of the total of 17 8-hour hydraulic tests conducted as part of this testing program, 34 separate hydraulic conditions corresponding to the freefall events were analyzed in this way. In three cases, the computed energy data contained a significant number of anomalies, a condition which made linear regression misrepresentative of actual flow conditions. In these three instances, the friction slope was determined graphically.

Furthermore, the profile plots provided a convenient means for identifying locations of embankment soil loss and protection system deformation. This was particularly valuable when defining control volumes for computing bed shear stress for the erodible embankment tests, as described later in this chapter.

3. Hydraulic Analysis Methodology for Freefall Conditions

Previous studies have determined that the shear stress acting on the surface of a protection system (parallel to the direction of flow), along with hydrodynamic pressure gradients causing uplift forces (normal to the embankment surface), and the transformation of velocity head into stagnation pressure at the upstream edge of a protruding element (causing rotation of the element) are the three primary destabilizing forces created during overtopping flow on an embankment.^(1,5,6) In the case of articulating concrete block revetment systems, exceeding the system's "threshold" stable stress level for any of these forces typically leads to the undesirable ingress of flow between the protection system and embankment subgrade. Unchecked, this flow can erode or liquefy the underlying soil matrix, or it can result in failure pressures further down the embankment. Consequently, determining bed shear stresses on the embankment slope, pressures along the embankment, and flow under the geotextile were primary goals of the testing, data collection, and hydraulic analysis tasks of this research program.

For design purposes it is necessary to determine the flow resistance parameters (i.e., Manning's n value, Darcy friction factor f) on the crest,

and downstream slope of the embankment. Therefore, an additional goal of this study was the evaluation of the flow resistance parameters.

a. Computation of Bed Shear Stress

Tests which involved freefall conditions were analyzed using the principle of conservation of momentum. Embankment and water-surface profile plots were evaluated and a control volume on the downstream embankment slope was defined from these data. This was done for each discharge used during each test. The control volumes were typically located beginning at station 38 and ending at station 44. In some cases it was necessary to use data at different measurement stations when inconsistencies in the data were noted. To ensure that representative conditions were utilized for the hydraulic analysis, control volumes were defined to be at least 6 ft (1.8 m) in length where data permitted. A typical control volume is shown in figure 36.

The principle of conservation of momentum may be expressed as

$$\Sigma F = \Delta(\rho VQ) \quad (2)$$

where ΣF is the sum of the forces acting on the control volume in the direction of flow, Q is the discharge, ρ is the density of water, and V is the flow velocity. The right-hand side of equation 2 represents the change in momentum across the control volume. By considering a control volume of unit width, resolving the individual force components, and taking the difference between entering and exiting momentum, equation 2 becomes:

$$W \sin \theta + P_1 - P_2 - \tau_o L = \rho q V_2 - \rho q V_1 \quad (3)$$

where W is the weight of water in the control volume, P_1 and P_2 are the forces due to pressure, τ_o is the bed shear stress, L is the length of the control volume, and q is the unit discharge. Figure 37 provides a definition sketch for the terms used in this analysis.

The shear stress term does not include wall shear because the flume walls were extremely smooth compared to the concrete blocks; therefore, flow resistance due to friction at the walls was assumed to be negligible. This assumption can be verified by computing the walls' contribution to the total shear stress force.

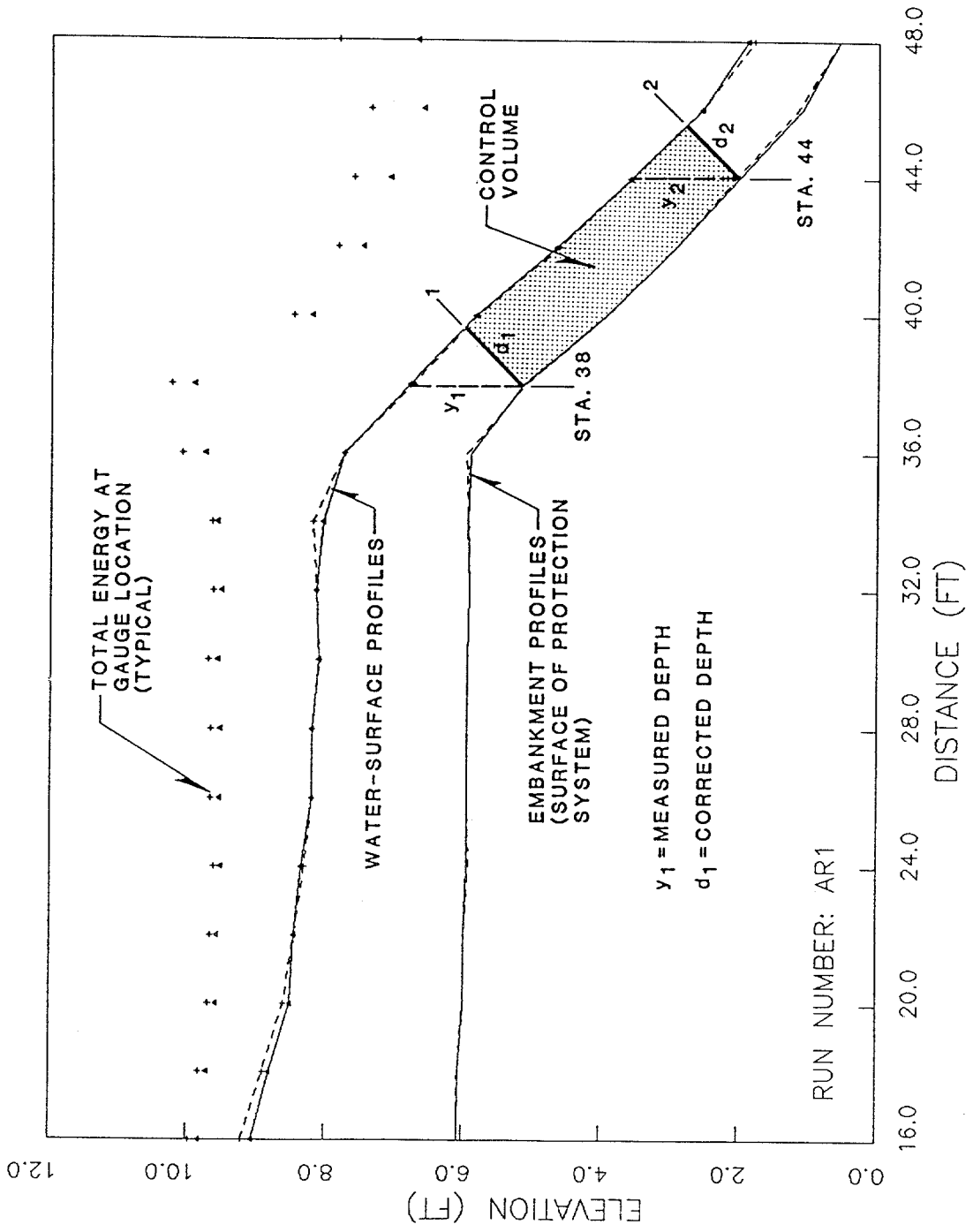


Figure 36. Control volume for the test AR-1 with 4-ft (1.22 m) overtopping.

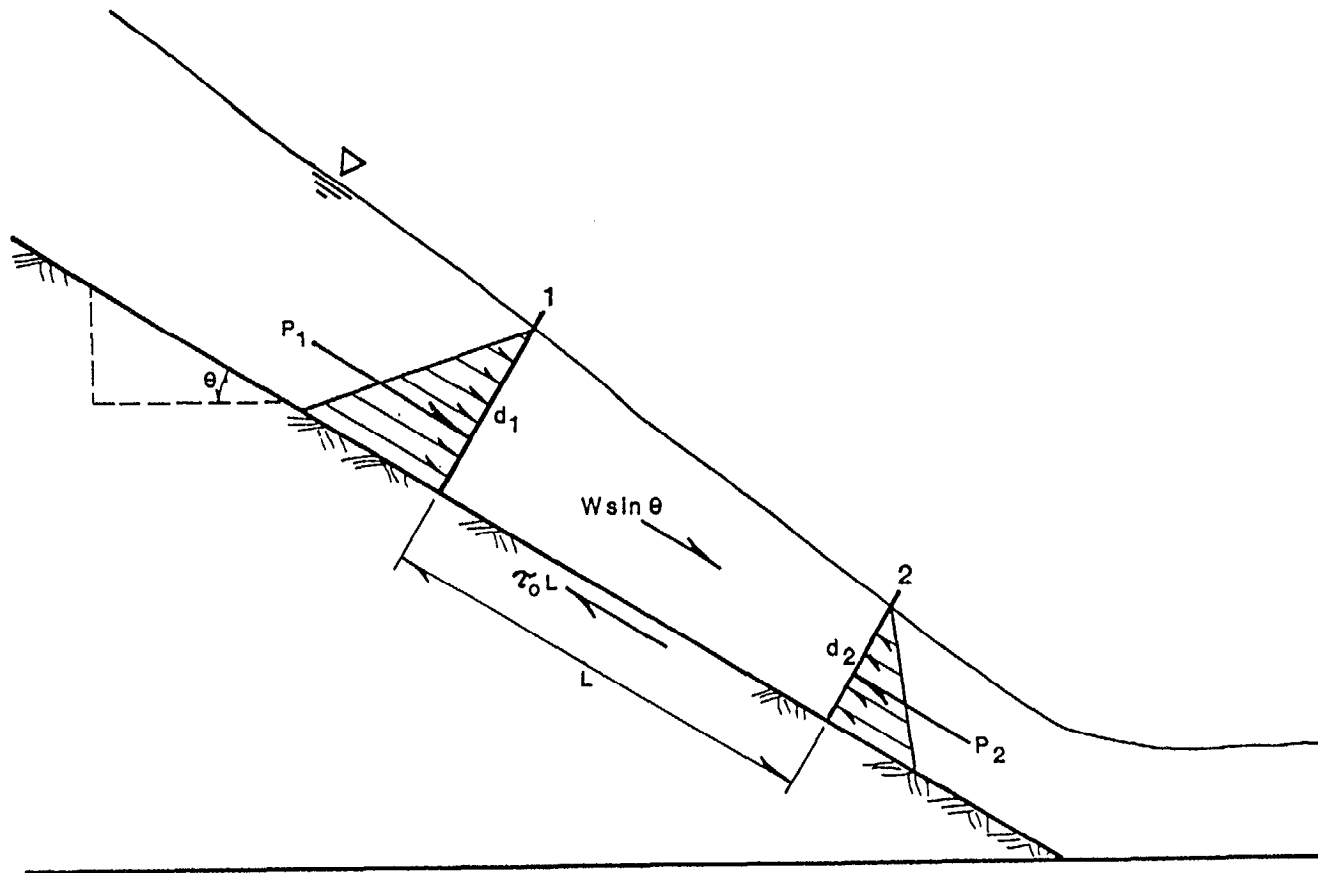


Figure 37. Typical control volume with momentum equation parameters.

Such a computation indicates that the contribution to the total flow resistance due to wall friction is less than 5 percent, for the range of flows investigated. By expanding equation 3 and rearranging to solve for the shear stress, the following equation results:

$$\tau_o = \frac{\gamma}{2} (d_1 + d_2) \sin\theta + \frac{1}{L} \left[\frac{\gamma}{2} (d_1^2 - d_2^2) - \rho q^2 \left(\frac{1}{d_2} - \frac{1}{d_1} \right) \cos\theta \right] \quad (4)$$

where γ is the unit weight of water and the remaining variables are defined in figure 37. The bed shear τ_o is the only unknown in the equation and can be computed directly. Using this equation, the bed shear stress was computed for all 34 freefall discharge conditions investigated in the testing program.

b. Computation of Flow Resistance

Flow resistance values on the crest and downstream slope of the embankment were quantified with both the Darcy-Weisbach friction factor f and Manning's roughness coefficient n . A Darcy-Weisbach friction factor was calculated for all 34 freefall discharge conditions using the computed bed shear stress, depth-averaged flow velocity, and the equation:

$$f = \frac{8 \tau_o}{\rho V^2} \quad (5)$$

where τ_o is the bed shear computed using the momentum equation, ρ is the density of water, and V is the average velocity across the control volume.

Manning's roughness coefficients were computed using Manning's equation with English units in the form:

$$n = \frac{1.49}{V} d^{2/3} S_f^{1/2} \quad (6)$$

where V is the flow velocity, d is the depth of flow, and S_f is the friction slope for a given discharge on a given protection system. This particular form of Manning's equation assumes that cross-sectional flow characteristics are hydraulically "wide," (i.e., flow resistance is due solely to the boundary characteristics of the bed, with wall friction negligible). This allows the flow depth d to be substituted for the more generally applicable hydraulic radius R . A Manning's n value can therefore be determined at each

measurement station given the observed depth and velocity, and the friction slope determined by linear regression as described previously.

4. Hydraulic Analysis Results for Freefall Conditions

Results of the quantitative hydraulic analysis for freefall conditions, including average velocities, friction slopes, shear stresses, Darcy-Weisbach friction factors, and Manning's roughness coefficients, are summarized and discussed in this section.

a. Rigid Embankment Test Results

The objective of the series of tests on the rigid embankment was to provide baseline data for conditions where embankment stability was guaranteed. This provides more reliable identification and quantification of hydraulic conditions at the failure threshold when testing on an erodible embankment. No system failures occurred during the rigid embankment tests. This enabled the collection of comprehensive hydraulic data up to and including the maximum discharge capacity of the testing facility for all the systems considered under this research program.

Results of the analysis for the rigid embankment tests are given in table 4. Bed shear stresses, friction factors and Manning's n values presented in this table are representative values derived from data taken on the downstream slope of the embankment. The results presented in table 4 indicate that the maximum shear stresses imposed on the protection systems during the 4-ft (1.2 m) overtopping tests (maximum discharge capacity) ranged from 24 to 35 lb/ft² (1.15 to 1.68 kN/m²). Darcy-Weisbach friction factors under maximum flow conditions, hence maximum hydraulic stress levels, varied from approximately 0.5 to 1.0, while Manning's n values ranged from 0.055 to 0.090.

The values obtained from this analysis appear relatively high when compared to typical values for natural stream channels. This is a result of the steep embankment slope (2H:1V) and highly turbulent conditions produced by overtopping flow. The roughness parameters were qualitatively consistent in that they tended to increase with overtopping depth, hence discharge. In addition, roughness

Table 4. Hydraulic analysis results for freefall conditions for the rigid embankment tests.

Product	Test Number	Embankment Slope	Nominal Overtopping Depth (ft)	Discharge (ft ³ /s)	Hydraulic Analysis on the Downstream Slope					
					S _f	n	f	τ (lb/ft ²)	Average Velocity (ft/s)	Maximum Velocity (ft/s)
Armorflex	AR-1	2:1	1.0	13.9	0.386	0.030	0.20	6.0	11.2	13.6
		2:1	2.0	34.8	0.304	0.045	0.41	13.7	11.7	14.5
		2:1	4.0	85.5	0.222	0.055	0.64	34.8	15.1	16.8
	AR-2	2:1	4.0	83.3	0.354	0.080	0.75	31.0	13.0	14.7
Dycel (closed cell)	BR-1	2:1	1.0	13.8	0.374	0.030	0.28	7.2	10.4	12.9
		2:1	2.0	29.7	0.344	0.050	0.44	13.3	11.2	12.8
	BR-2	2:1	4.0	68.3	0.391	0.090	1.02	32.6	11.5	13.0
Petraflex	CR-1	2:1	1.0	13.1	0.396	0.032	0.17	4.9	10.8	13.8
		2:1	2.0	34.5	0.308	0.040	0.23	9.4	13.0	15.2
		2:1	4.0	83.8	0.331	0.070	0.49	23.8	14.3	16.2
Construction Blocks	DR-1	2:1	1.0	11.7	0.475	0.040	0.25	6.1	10.2	11.1
		2:1	2.0	30.3	0.342	0.048	0.34	13.2	12.8	13.4
		2:1	4.0	81.0	0.370	0.075	0.60	28.5	14.0	15.4
Wedge Blocks	ER-1	2:1	0.5	6.9	0.428	0.045	0.45	6.6	7.7	9.2
		2:1	1.0	13.7	0.484	0.050	0.58	10.7	8.7	12.0
		2:1	1.5	22.7	0.491	0.060	0.67	14.1	9.4	14.6
		2:1	2.0	34.2	0.390	0.062	0.78	18.4	9.9	13.9
	ER-2	2:1	3.0	67.6	0.339	0.062	0.57	23.4	13.0	15.4
		2:1	3.5	73.2	0.388	0.070	0.64	27.2	13.2	15.3
		2:1	4.0	83.6	0.357	0.075	0.71	30.4	13.3	15.0

1 ft = 0.3048 m
 1 ft/s = 0.3048 m/s
 1 ft³/s = 0.0283 m³/s
 1 lb/ft² = 0.048 kN/m²

values were similar in magnitude from system to system, with the exception of the wedge blocks. Results of the hydraulic analysis for the wedge block system indicated relatively higher roughness parameters at smaller discharges. This is a result of the block geometry which, because of its stairstep configuration, causes numerous zones of small-scale flow separation, thereby producing significantly higher form roughness under conditions of shallow flow. At the higher discharges, relative roughness of the wedge blocks was approximately the same as that observed for the other systems.

Bed shear stress, flow velocity, and flow depth are plotted against unit discharge in figures 38, 39, and 40, respectively. The strong dependence of these three parameters on unit discharge is clearly indicated.

b. Erodible Embankment Test Results

The objective of these tests was to evaluate the performance of various articulating concrete block revetment systems when installed on a highly erodible embankment and subjected to overtopping flow. Because this embankment was vulnerable to failure (unlike the rigid embankment), not all overtopping flow conditions could be examined for all systems.

Results of the analysis for the erodible embankment tests are given in table 5. Bed shear stresses, friction factors and Manning's n values presented in this table are representative values derived from data taken on the downstream slope of the embankment. The results presented in table 5 indicate that the maximum shear stresses imposed on the protection systems during the 4-ft (1.22 m) overtopping tests (maximum discharge capacity) ranged from 22 to 41 lb/ft² (1.05 to 1.96 kN/m²). It should be noted that the maximum shear stress calculated for the Dycel 100 system was only 10 lb/ft² (0.48 kN/m²) because the failure threshold was exceeded by the 1-ft (0.30 m) overtopping flow, and no further testing was performed on this system. Darcy-Weisbach friction factors under maximum flow conditions, hence maximum hydraulic stress levels, varied from 0.5 to 1.0, while Manning's n values ranged from 0.05 to 0.110. The shear stress and resistance values determined for the erodible embankment tests were similar to those reported for the rigid embankment tests.

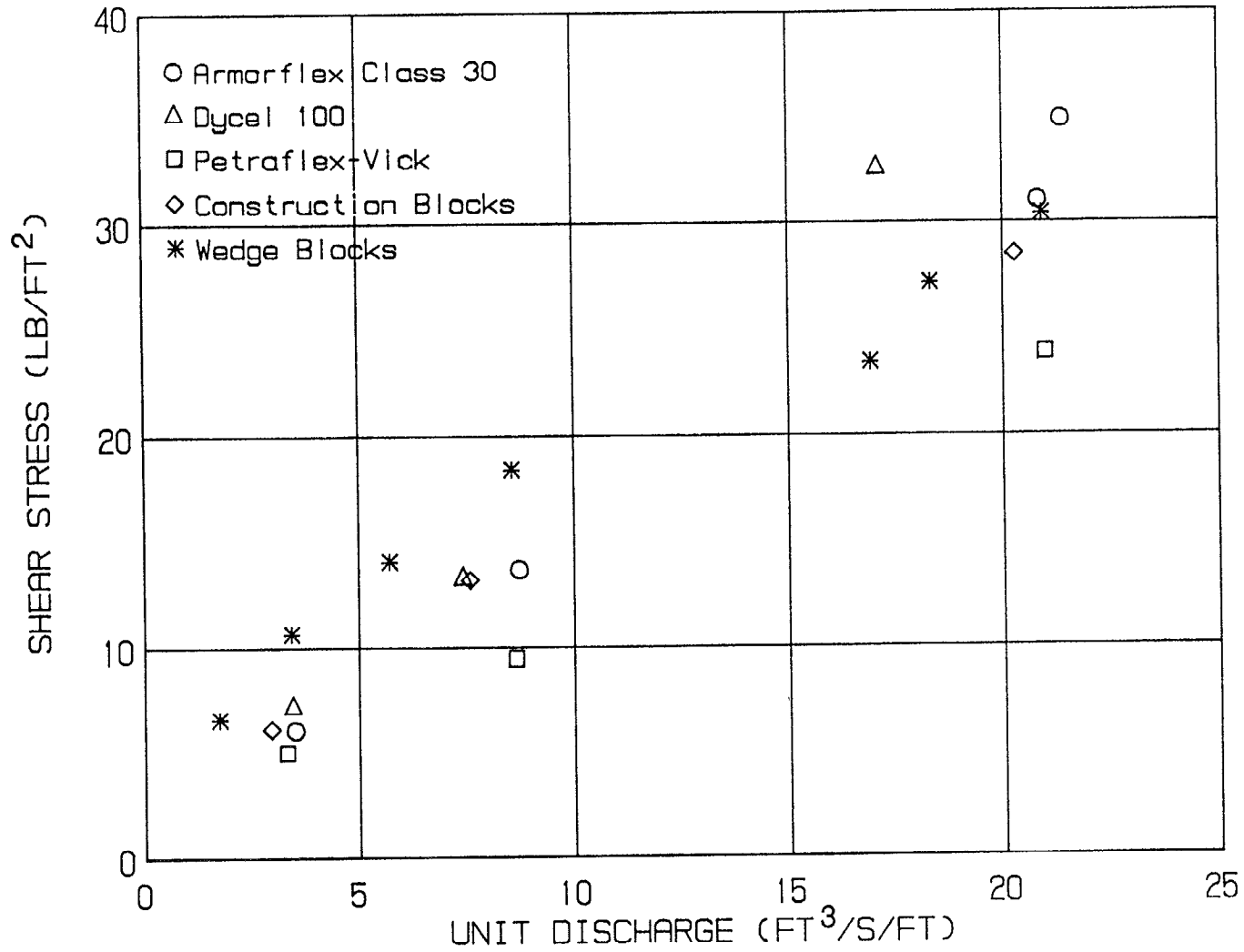


Figure 38. Average shear stress on the downstream slope versus unit discharge for rigid embankment tests.

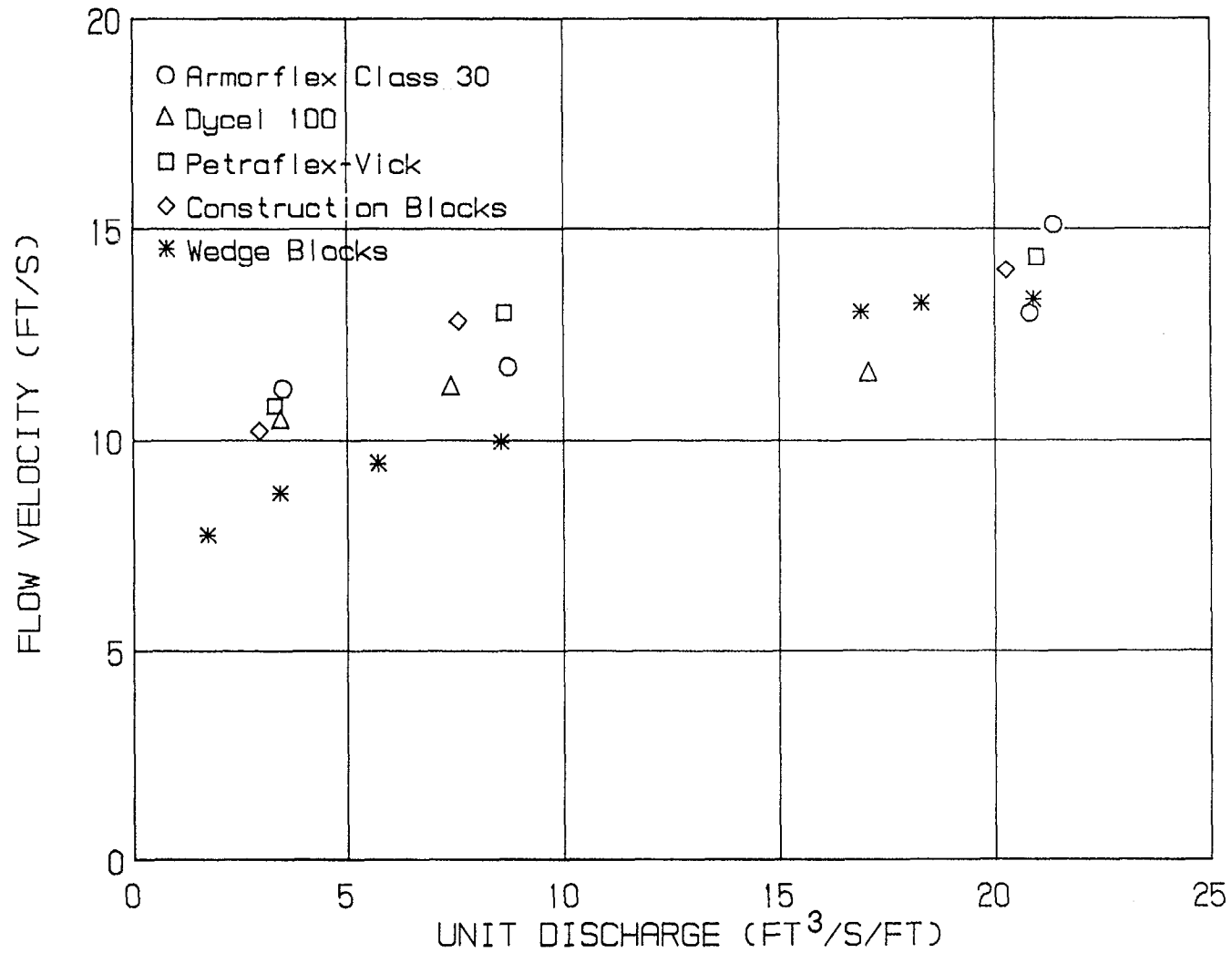


Figure 39. Average flow velocity on the downstream slope versus unit discharge for rigid embankment tests.

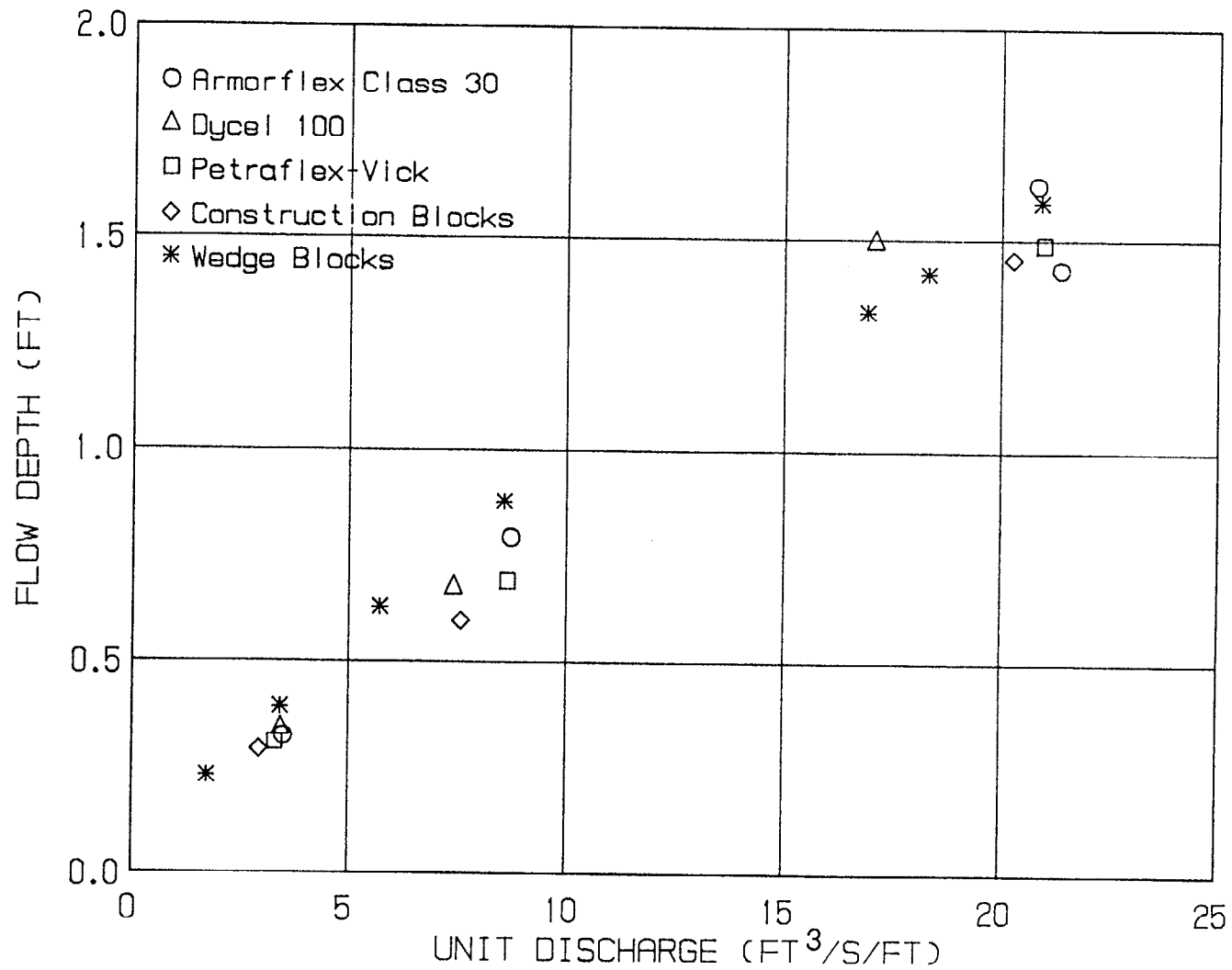


Figure 40. Average flow depth on the downstream slope versus unit discharge for rigid embankment tests.

Table 5. Hydraulic analysis results for freefall conditions for the erodible embankment tests.

Product	Test Number	Embankment Slope	Nominal Overtopping Depth (ft)	Discharge (ft ³ /s)	Hydraulic Analysis on the Downstream Slope						
					S _f	n	f	τ (lb/ft ²)	Average Velocity (ft/s)	Maximum Velocity (ft/s)	
Armorflex	A-1	2:1	1.0	15.7	0.407	0.040	0.35	9.1	10.5	11.6	
		2:1	2.0	37.3	0.293	0.050	0.30	12.1	12.9	15.4	
	A-2	2:1	4.0	83.8	0.485	0.110	1.02	40.6	12.9	13.2	
	A-3	2:1*	1.0	12.4	0.384	0.045	0.51	9.0	8.6	10.8	
		2:1*	2.0	35.4	0.429	0.065	0.63	18.9	11.1	12.2	
	A-4	2:1*	4.0	84.8	0.359	0.080	0.72	34.9	14.1	15.6	
	Dycel (closed cell)	B-1	2:1	1.0	12.5	0.389	0.030	0.35	9.7	10.7	12.5
			3:1	1.0	11.0	0.379	0.030	0.21	5.9	10.7	12.1
Construction Blocks	D-1	3:1	1.0	11.0	0.379	0.030	0.21	5.9	10.7	12.1	
		3:1	2.0	33.5	0.291	0.045	0.27	11.4	13.1	13.8	
	D-2	3:1	2.0	33.4	0.279	0.043	0.29	11.4	12.7	13.9	
		3:1	4.0	83.8	0.265	0.050	0.33	22.4	16.6	17.7	
Wedge Blocks	E-1	3:1	1.0	13.6	0.323	0.070	0.72	9.5	7.4	7.5	
		3:1	2.0	34.9	0.289	0.055	0.54	14.4	10.5	12.3	
	E-2	3:1	4.0	89.4	0.223	0.060	0.48	25.7	15.8	16.8	

*With 4H:1V chamfer

1 ft = 0.3048 m
 1 ft/s = 0.3048 m/s
 1 ft³/s = 0.0283 m³/s
 1 lb/ft² = 0.048 kN/m²

Bed shear stress, flow velocity, and flow depth are plotted against unit discharge in figures 41, 42, and 43, respectively, for the erodible embankment tests. The dependence of these three parameters on unit discharge is clearly indicated, as was for the rigid embankment tests. Figure 42 illustrates a correlation between bed shear stress and embankment slope. Tests on steeper slopes tended to exhibit higher shear stresses than on milder slopes. This results from the larger component of weight oriented in the direction of flow for a steeper embankment, as can be seen by referring to figure 37.

5. Analysis of Transducer Data for the Freefall Tests

Pressure data were collected below the Nicolon 40/30 geotextile fabric at four locations along the centerline of the embankment. Transducers were located at stations 34, 37.5, 41.5, and 44. These instruments are referred to as transducers 1 through 4, respectively. Deflections of the centerline block at station 37.5 were measured using a wireline displacement transducer, denoted transducer 2A. Subblock velocity head measurements were made using a differential pressure transducer at the same station, denoted transducer 2B. Details of the data acquisition system and data storage/retrieval and conditioning techniques have been described in the previous chapter.

a. Rigid Embankment Test Results

Data collected by the automatic data acquisition system during test AR-1 are presented in figure 44. The pressure plot (top) indicates that the pressure at station 34 (transducer 1) was higher than the other locations for all three hydraulic conditions. This was a result of station 34 being located on the crest of the embankment where flow depths were greatest. For the 1- and 2-ft (0.30 and 0.61 m) overtopping tests, average hydrodynamic pressure decreased in the downslope direction (transducers 2 and 3) due to decreasing flow depth as normal depth was approached. However, pressure at station 44 (transducer 4) remained higher than station 41.5, presumably due to an accumulation of water beneath the revetment system nearer the embankment toe.

During the 4-ft (1.22 m) overtopping flow of test AR-1, the pressure at station 37.5 was lower than the pressure at the other stations, presumably due

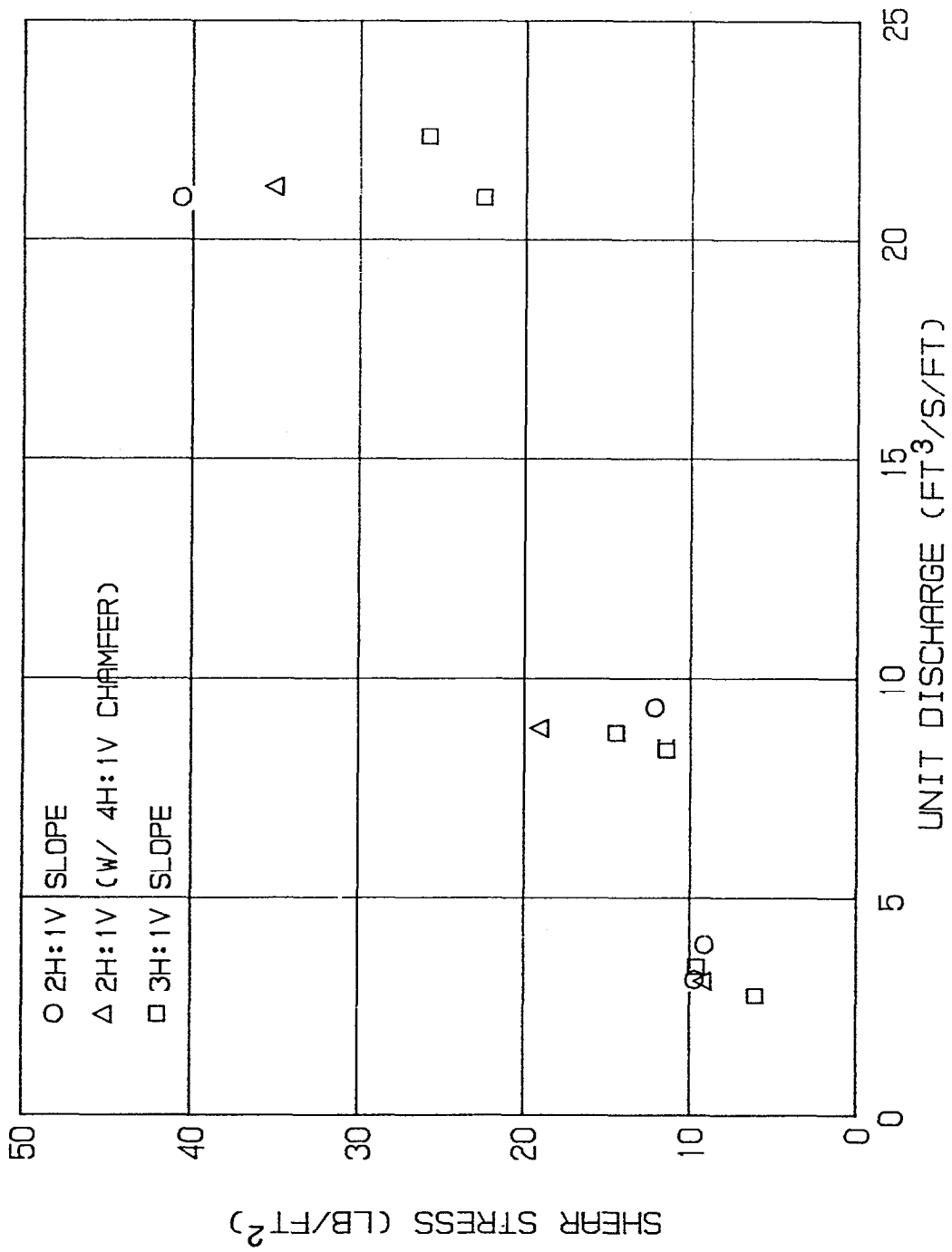


Figure 41. Average shear stress on the downstream slope versus unit discharge for erodible embankment tests.

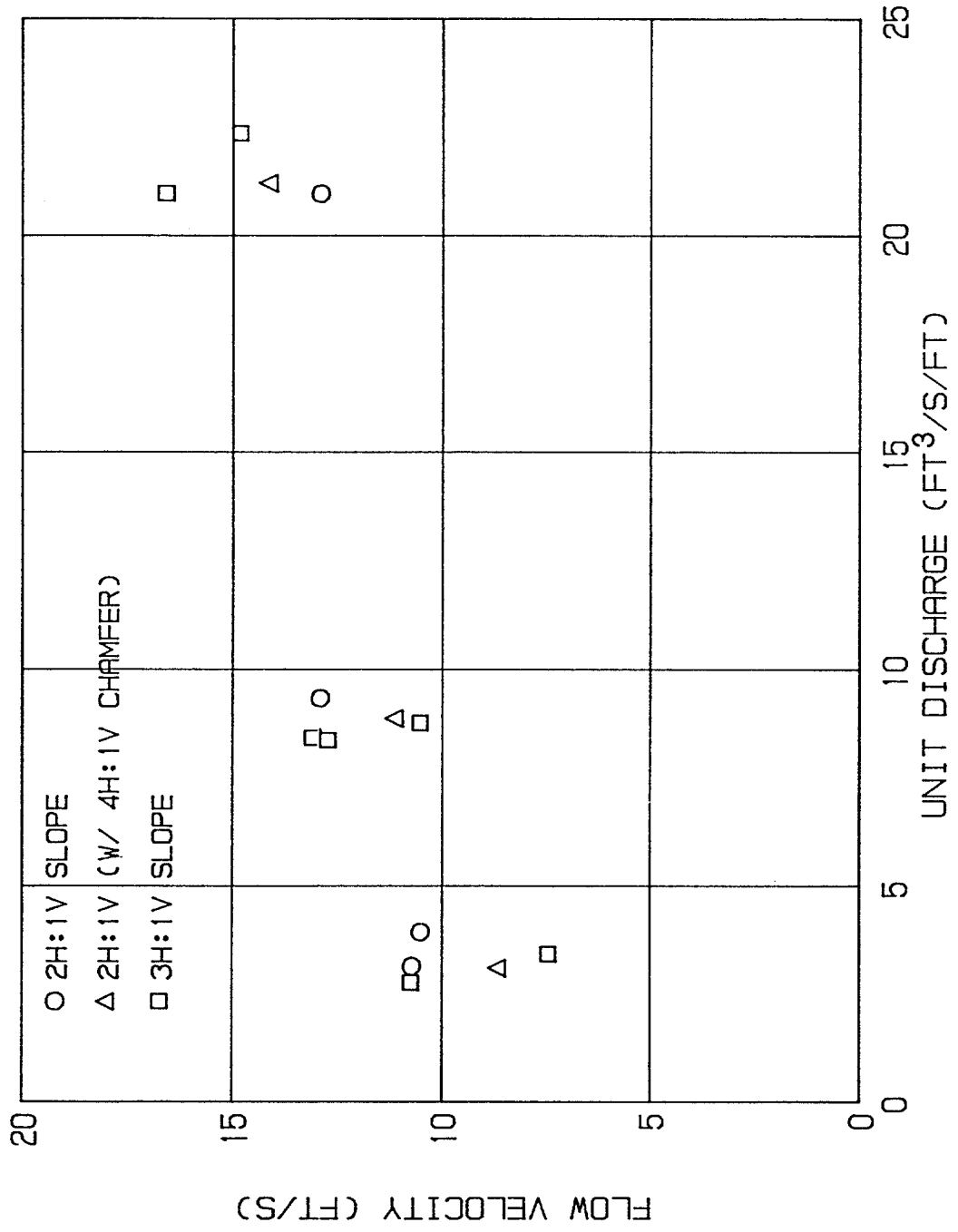


Figure 42. Average velocity on the downstream slope versus unit discharge for erodible embankment tests.

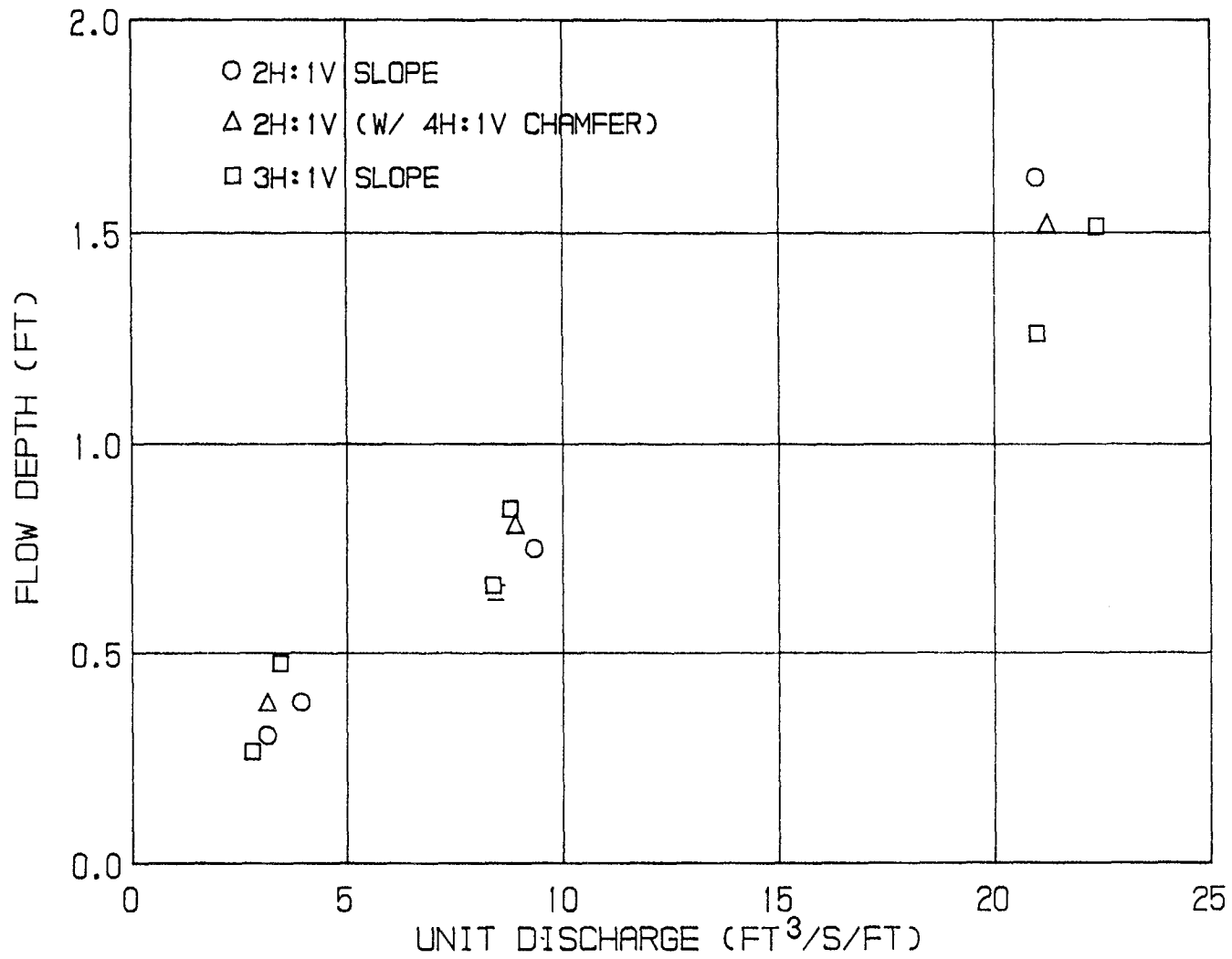


Figure 43. Average flow depth on the downstream slope versus unit discharge for erodible embankment tests.

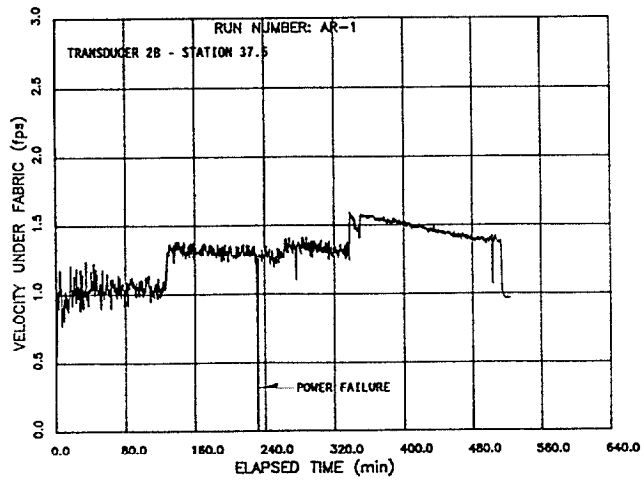
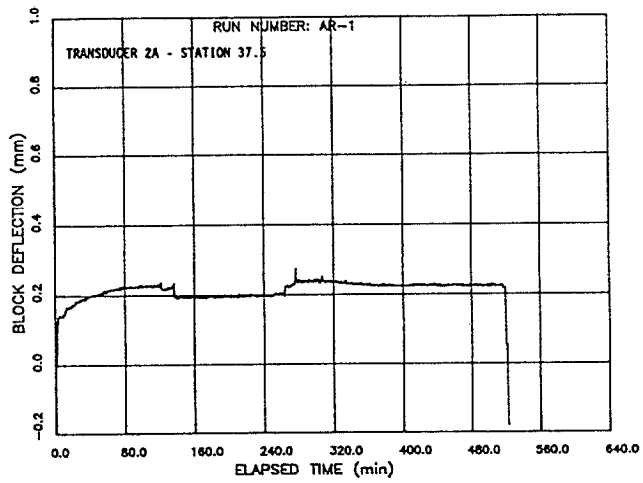
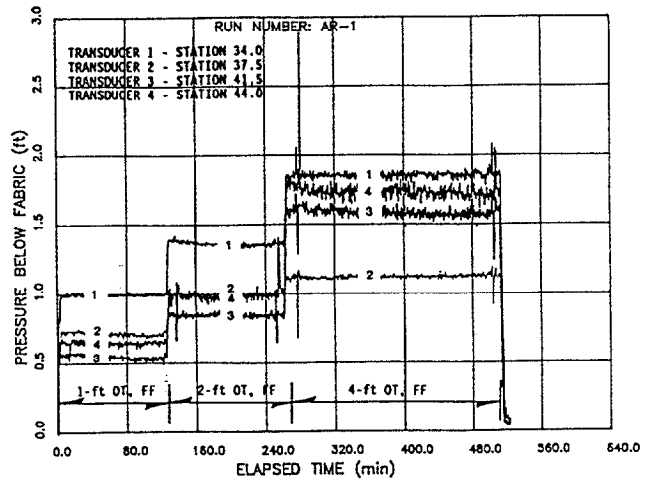


Figure 44. Transducer data for test AR-1 (Armorflex Class 30).

to the development of a low pressure zone downstream of the shoulder which resulted from separation of the flow nappe at the slope transition point. This phenomenon was described, and an analysis technique developed from a theoretical basis, in the report for the 1988 DOT/USBR study.⁽¹⁾

The block deflection plot of figure 44 (middle) shows only minor fluctuations with hydraulic conditions. Deflections generally varied between 0.008 and 0.01 in (0.2 and 0.25 mm), with negligible vibration or "chatter" observed.

The velocity plot of figure 44 (bottom) indicates that small but measurable velocities were recorded beneath the protection system at station 37.5. The measured subblock velocities increased with increasing discharge, which indicates that larger hydraulic stress levels lead to increased ingress of water beneath the system. Within the subblock environment, the measurement of increased seepage velocities with increasing discharge is in accordance with Darcy's law in that the overall head differential is greater with larger discharges. Exacerbating this effect may be the transformation of kinetic energy to stagnation pressure along transverse joints and at the downstream edges of open cells, which also increases with discharge through the agency of velocity head. Average subblock velocities observed at station 37.5 for 1-, 2- and 4-ft (0.30, 0.61, and 1.22 m) overtopping depths were approximately 1.0, 1.3 and 1.5 ft/s (0.30, 0.40 and 0.46 m/s), respectively, while velocities of overtopping flow near the upper surface of the block ranged from 9 to 15 ft/s (2.8 to 4.6 m/s).

Figure 45 presents similar data for test AR-2. The tailwater portion of this test produced large subblock pressures at stations 41.5 and 44, which were directly related to the depth of submergence beneath the tailwater pool. The range of pressure fluctuations is also quite large in this region, due to the highly turbulent, 3-dimensional flow field produced by the plunging jet.

Data collected by the automatic acquisition system for the remaining rigid embankment tests are shown in figures 46 through 52. Trends in the data recorded from the six transducers located along the embankment were generally evident in the tests of the other systems, with the exception of the Dycel 100 system. The Dycel 100 system was the exception in that, for the 4-ft (1.22 m) overtopping

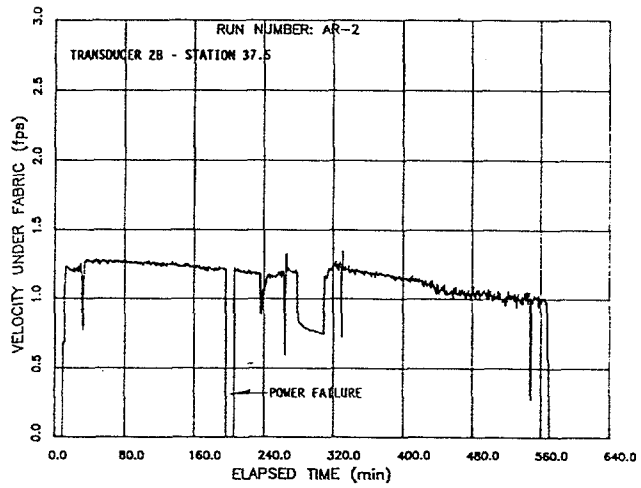
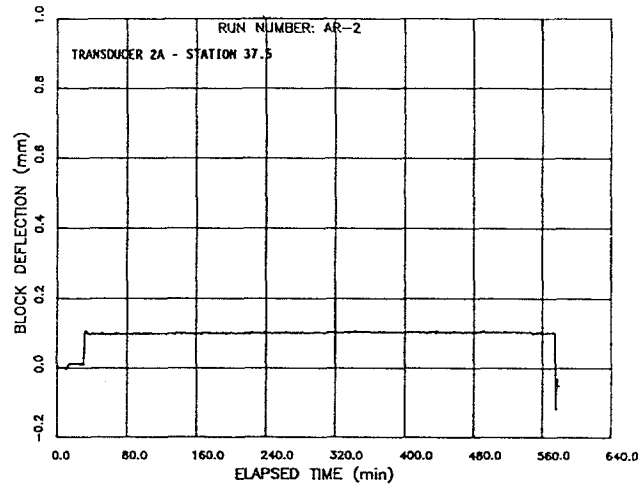
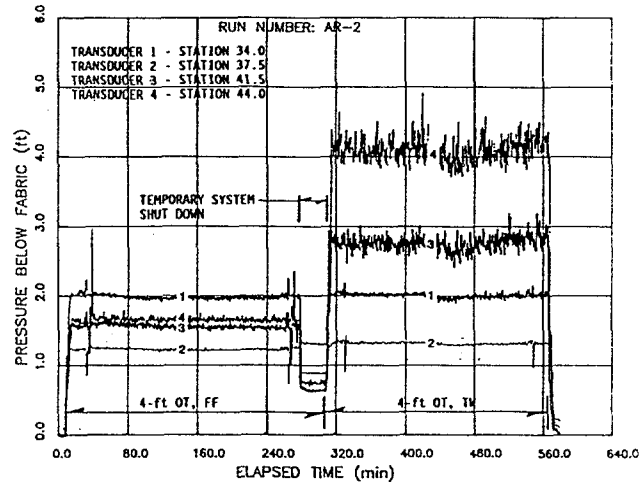


Figure 45. Transducer data for test AR-2 (Armorflex Class 30).

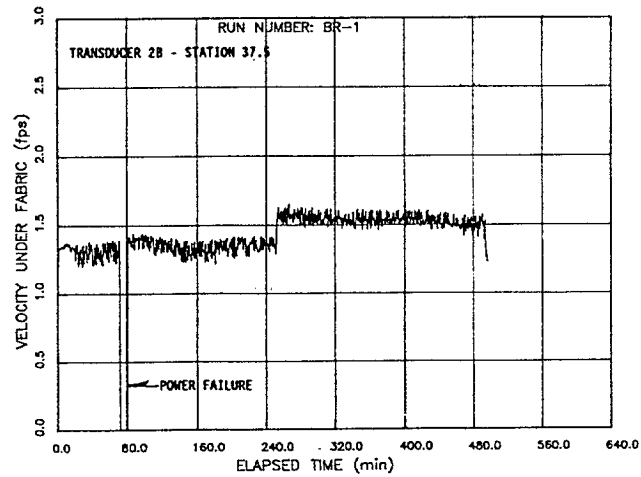
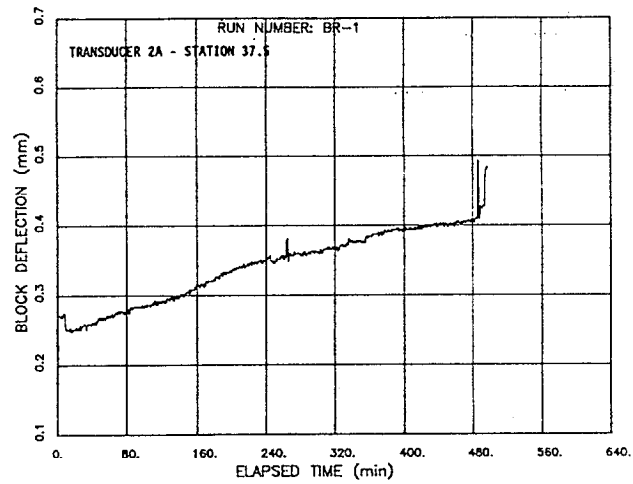
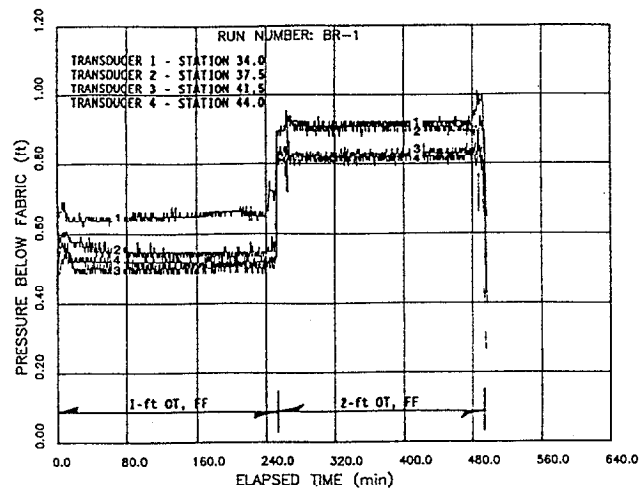


Figure 46. Transducer data for test BR-1 (Dycel 100).

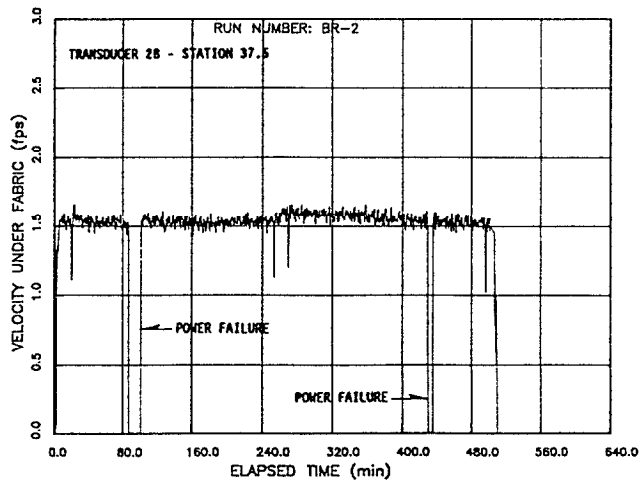
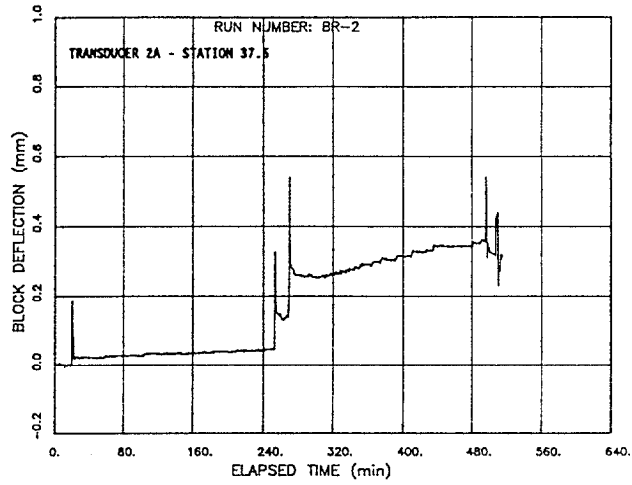
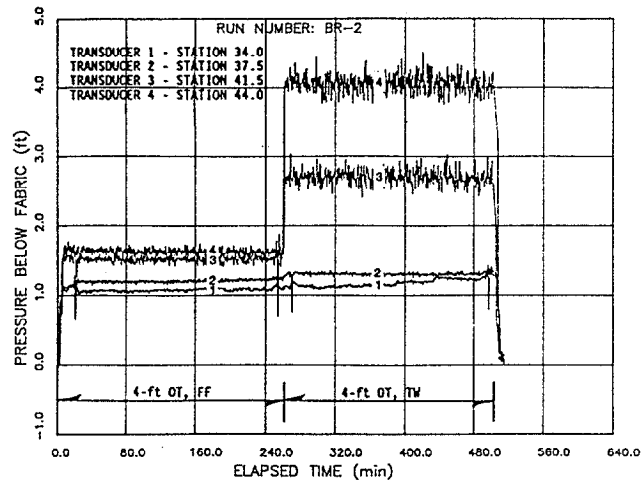


Figure 47. Transducer data for test BR-2 (Dycel 100).

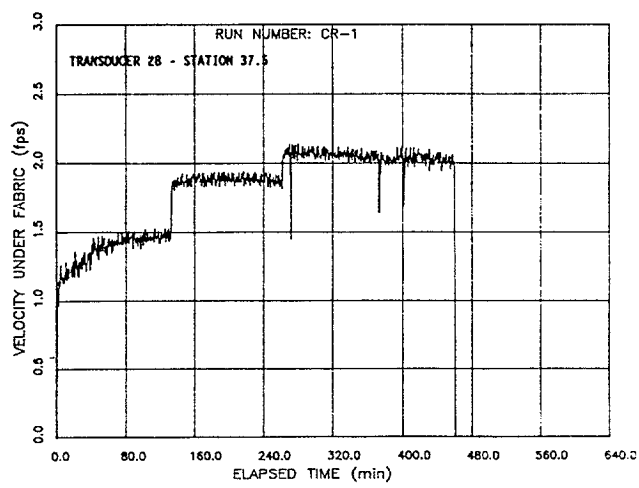
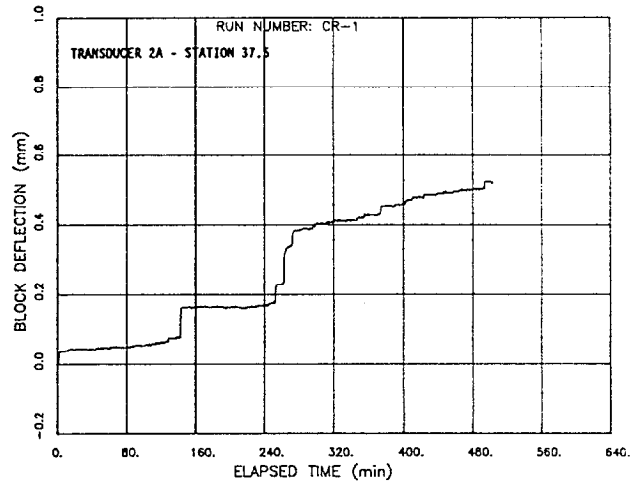
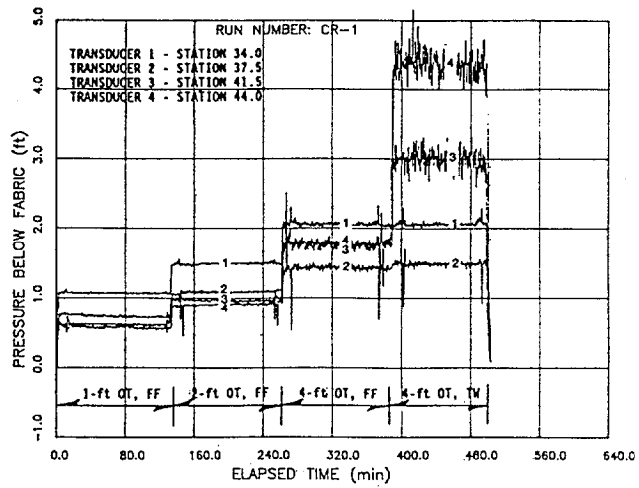


Figure 48. Transducer data for test CR-1 (Petraflex-Vick).

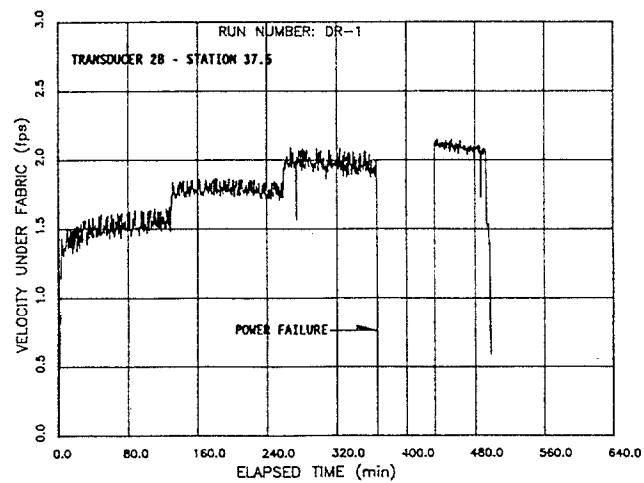
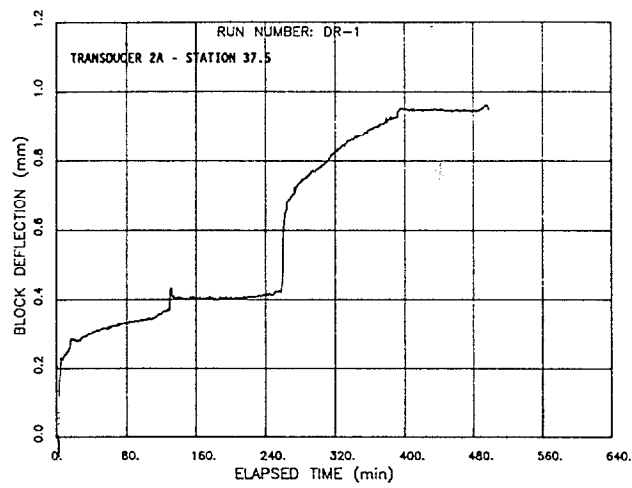
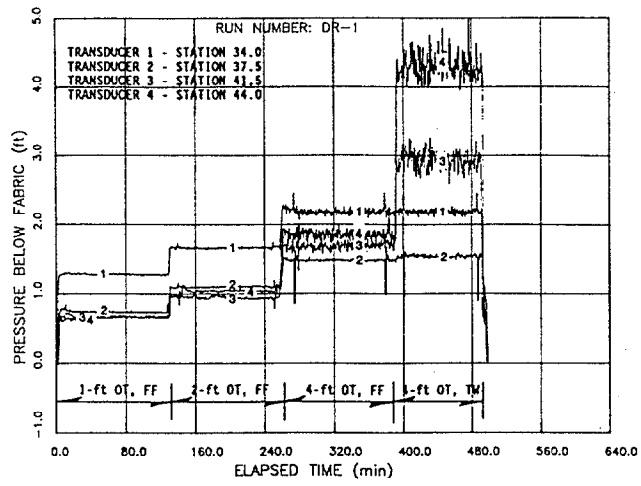


Figure 49. Transducer data for test DR-1 (construction blocks).

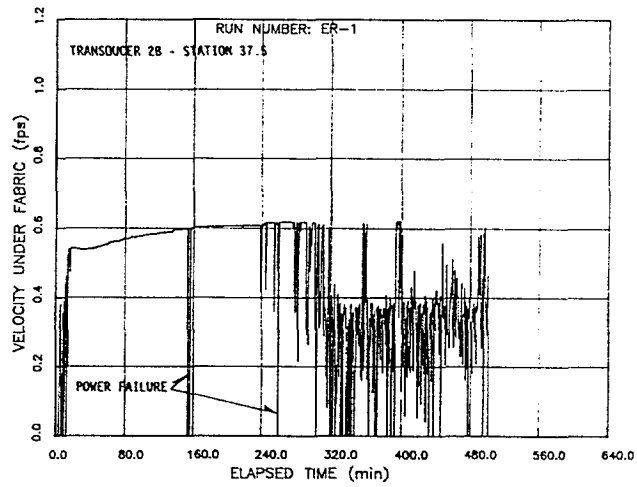
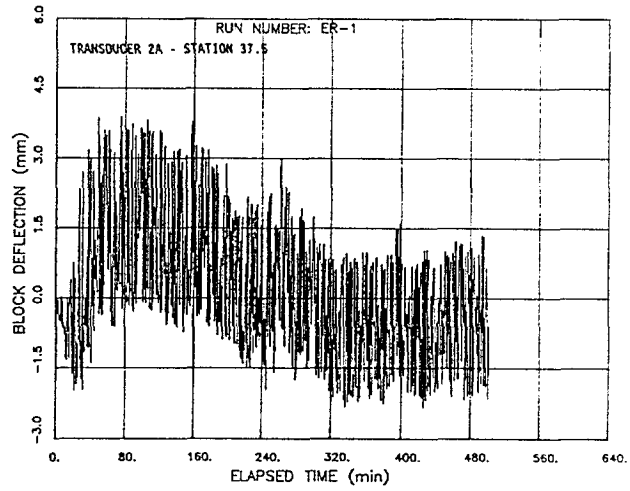
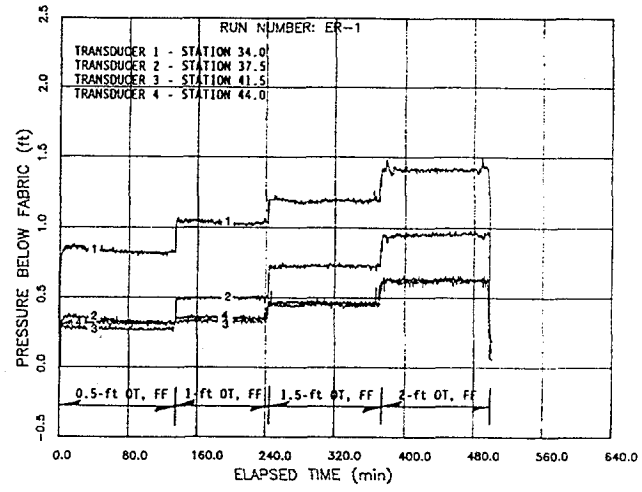


Figure 50. Transducer data for test ER-1 (wedge blocks).

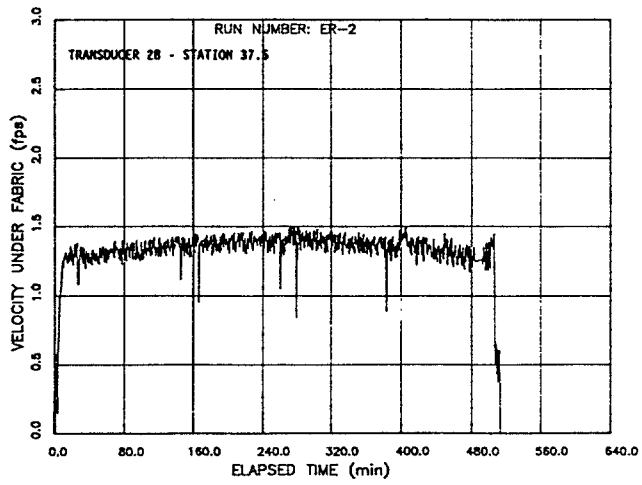
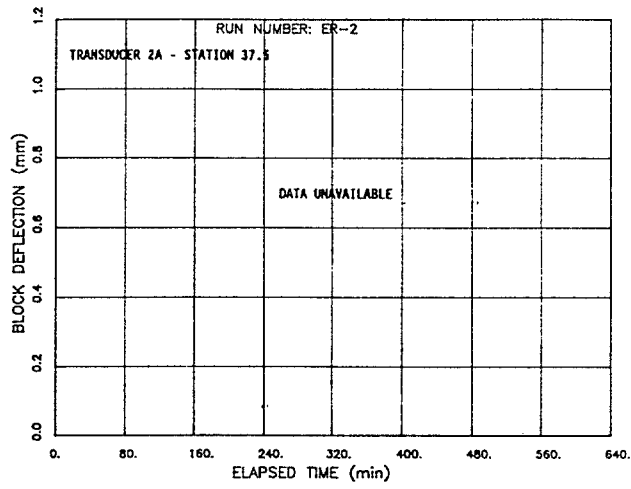
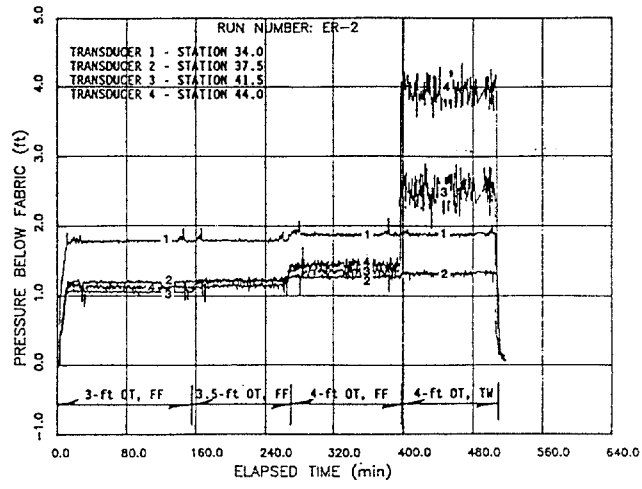


Figure 51. Transducer data for test ER-2 (wedge blocks).

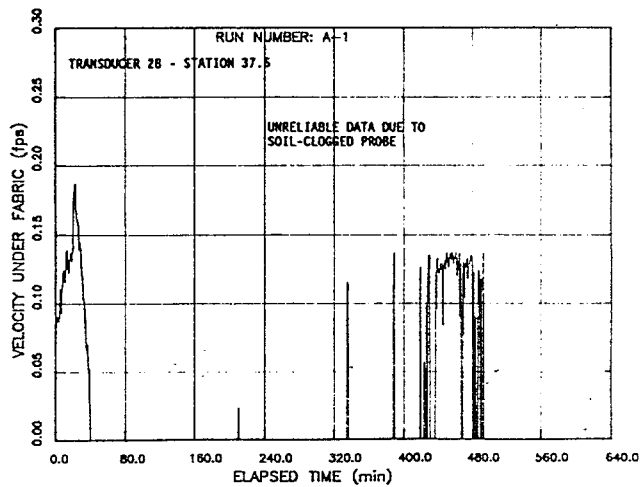
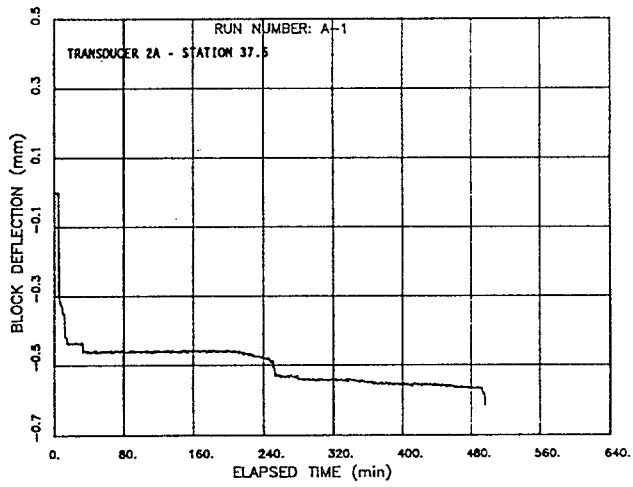
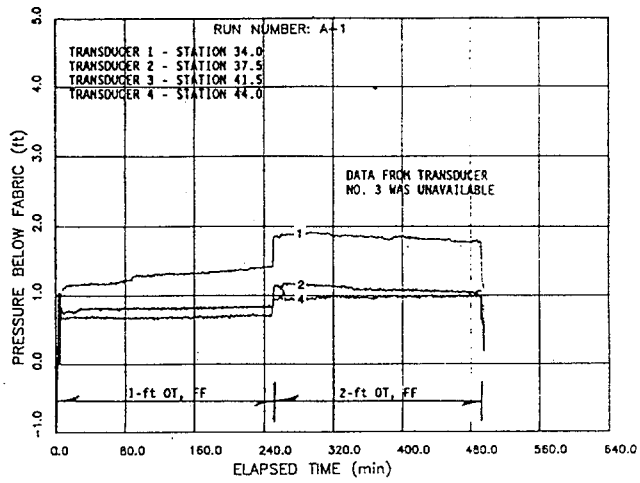


Figure 52. Transducer data for test A-1 (Armorflex Class 30).

depth the pressures at stations 41.5 and 44 were greater than at station 34. This is apparently the result of relatively large amounts of water penetrating beneath the system along the crest and shoulder regions of the embankment, accumulating under the system along the downstream slope, and resulting in relatively large subblock pressures at the middle and lower portions of the downstream slope compared to the other systems investigated in this study.

Block deflections were generally small [less than 0.04 in (1.0 mm)] and appeared to be related to overtopping discharge, hence stress level. The wedge-shaped blocks appeared to exhibit the largest magnitude of in-place vibration, with recorded deflections ranging from about -2.0 to 3.5 mm. This behavior is thought to be a result of the smaller plan area dimension of each individual wedge block compared to the other systems, coupled with the stairstepped block geometry which interacts more strongly with the high-velocity flow.

Velocities recorded beneath the block systems were dependent on overtopping discharge. For each protection system, the largest subblock velocities were observed during the period of maximum discharge of each test. Differences in measured subblock flow velocity between the protection systems were noted. The largest value of subblock flow velocity at station 37.5 was 2.1 ft/s (0.64 m/s), and was observed for both the Petraflex-Vick and the construction block systems under 4-ft (1.22 m) overtopping depths. The smallest observed subblock flow velocities for the 4-ft (1.22 m) overtopping condition were experienced with the Armorflex Class 30 and wedge block systems. These systems yielded recorded velocities in the range of 1.2 to 1.4 ft/s (0.37 to 0.43 m/s).

b. Erodible Embankment Test Results

Transducer data collected during test A-1 is presented in figure 53. Results were similar to those for the rigid embankment tests, with slightly higher pressures exhibited during the erodible embankment test. The pressure plot (figure 53, top) indicates that the pressure at station 34 (transducer 1) was higher than the other locations for all three hydraulic conditions. This was a result of station 34 being located on the crest of the embankment where flow depths were greater than on the embankment slope, and is an observation identical to that noted during the rigid embankment tests. Transducer 3

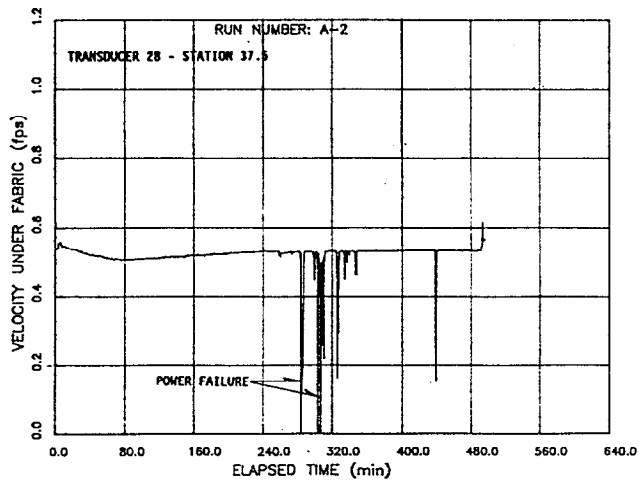
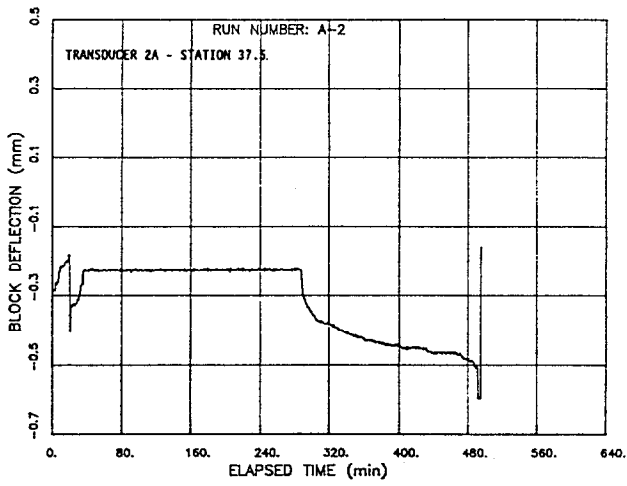
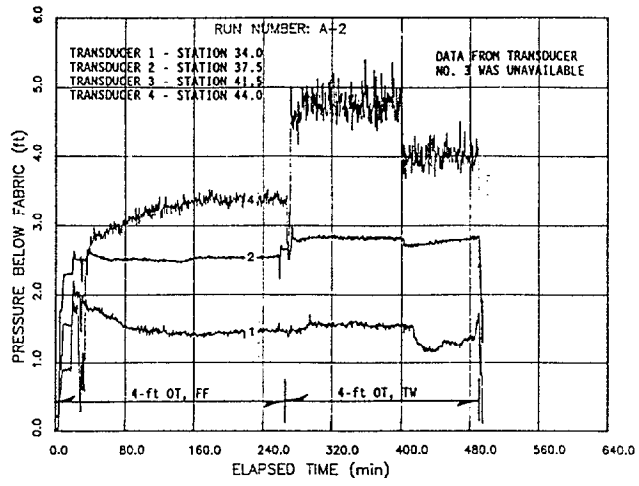


Figure 53. Transducer data for test A-2 (Armorflex Class 30).

malfunctioned so data at station 41.5 were unavailable for both tests A-1 and A-2.

Negative block deflections were measured for test A-1 (figure 53, center). This contrasts with the positive deflections recorded for the corresponding rigid embankment tests, and is most likely a result of saturation and settlement of the soil embankment during the initial stages of testing. The deflections were still relatively small, with absolute values increasing with increasing overtopping depth. Deflections during the freefall portion of test A-2 [4-ft (1.22 m) overtopping] were smaller than for the 2-ft (0.61 m) overtopping test, but fluctuations were reasonably minor (figure 54, center). However, block deflection fluctuations during the tailwater portion of the test became unusually large, probably due to the aforementioned erosion problem which affected the electronic wiring trenches and instrument canisters. Block deflection data for all erodible embankment tests should be interpreted with caution, particularly considering the very minor deflections which were measured. Erosion and settlement of the soil embankment repeatedly interfered with the proper functioning of the displacement transducer, which resulted in erroneous displacement measurements. The displacement transducer was damaged twice during the erodible embankment test series, necessitating repair or replacement and eventually making displacement data collection for some of these tests impossible.

The subblock velocity plot provided little information for test A-1 (figure 52, bottom). The corresponding plot for test A-2 (figure 53, bottom) appears to show a consistent velocity of approximately 0.53 ft/s (0.16 m/s). Inconsistent or nonexistent subblock velocity data was typical for the series of erodible embankment tests. This was a result of clogging of the pitot tube ports by loose soil during the initial stages of each test.

Data collected from the transducer network for the other erodible embankment tests are shown in figures 54 through 60. Trends similar to those observed for the rigid embankment tests were much more difficult to discern during the erodible embankment series of tests because of difficulties in measurement caused by soil clogging and settlement. This was a problem primarily with the block deflection and subblock velocity probes; the four pressure

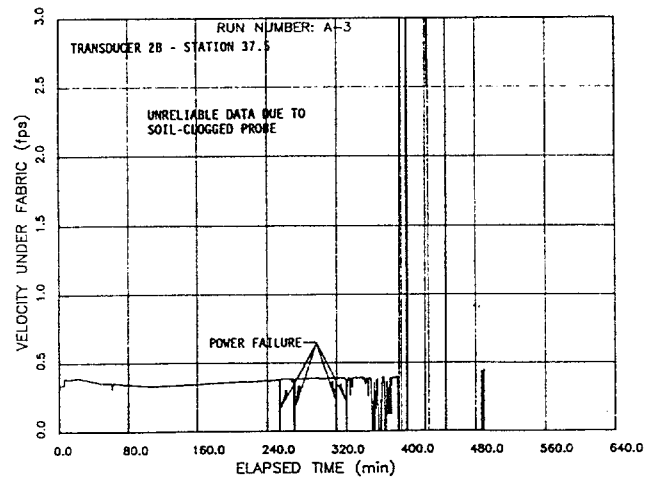
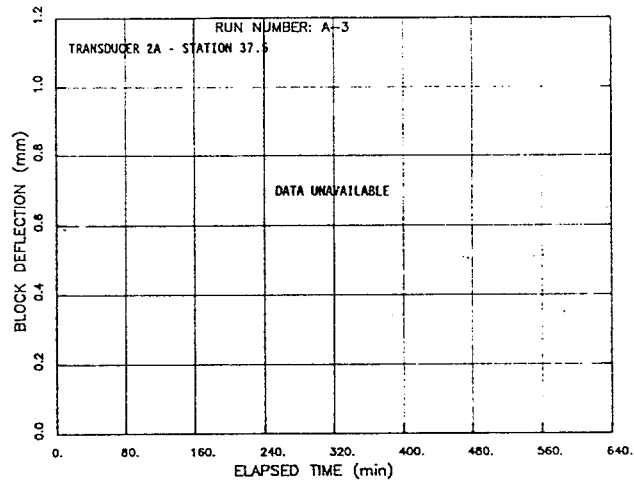
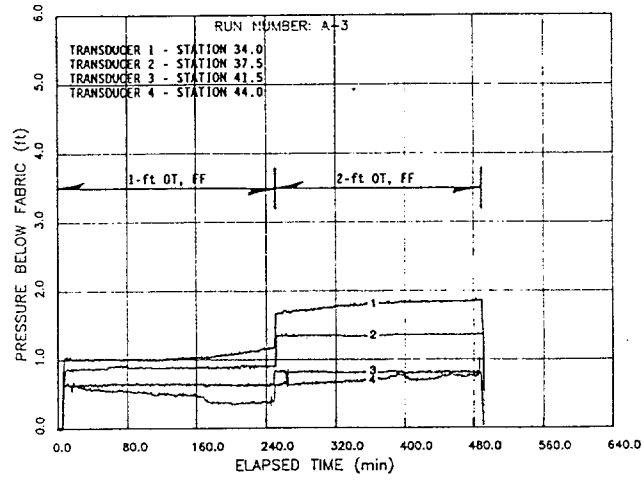


Figure 54. Transducer data for test A-3 (Armorflex Class 30).

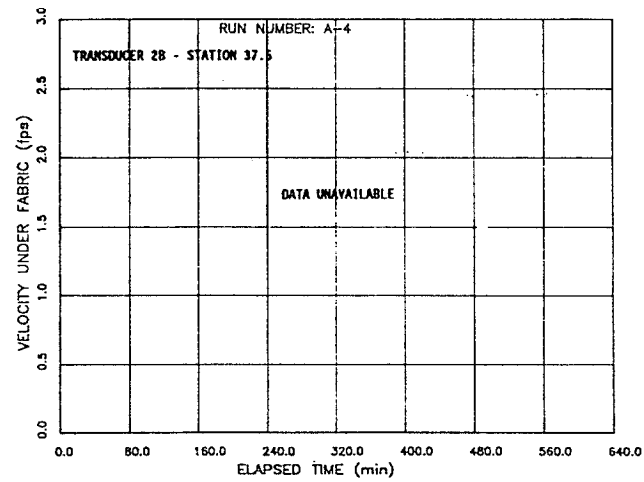
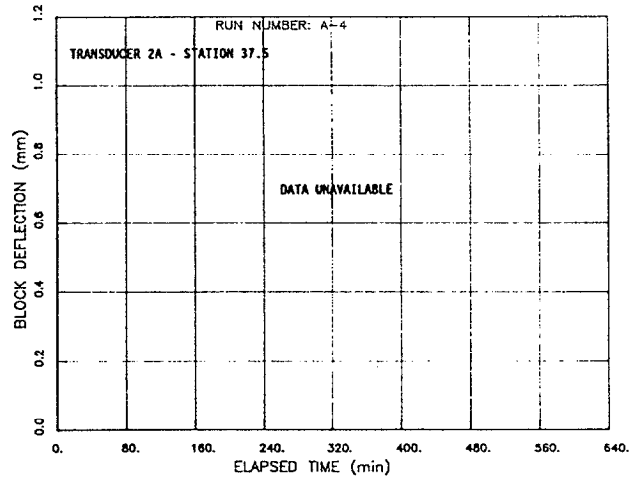
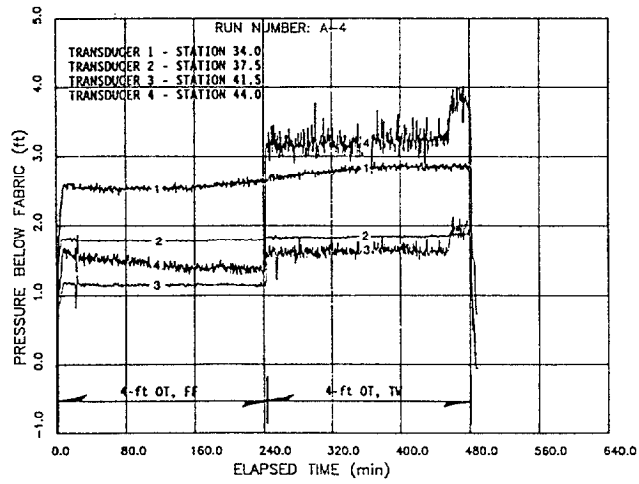


Figure 55. Transducer data for test A-4 (Armorflex Class 30).

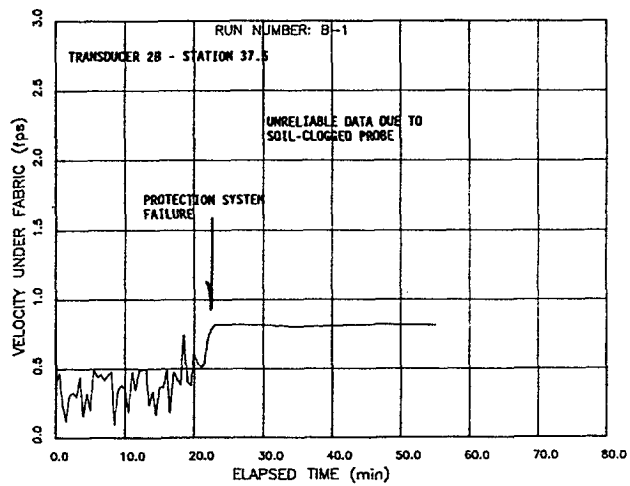
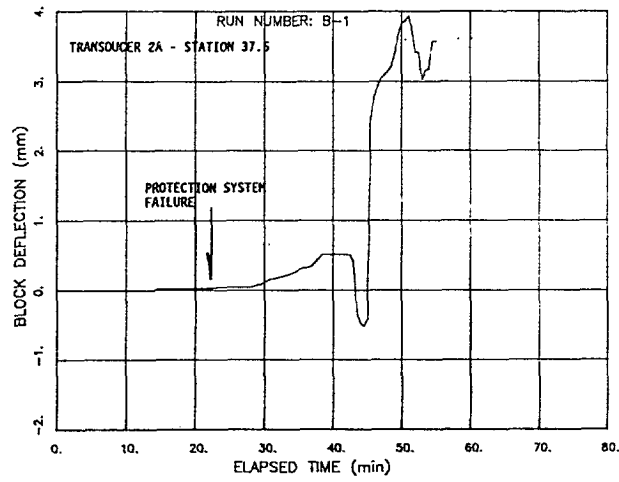
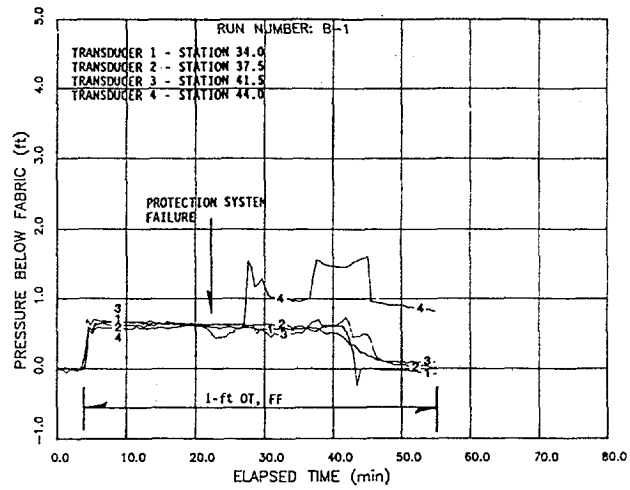


Figure 56. Transducer data for test B-1 (Dycel 100).

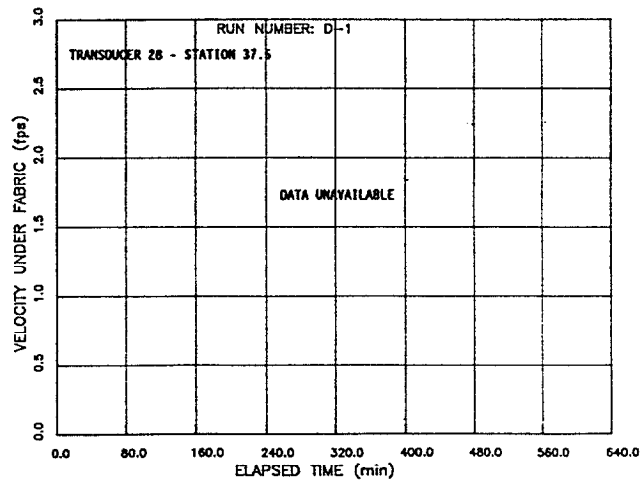
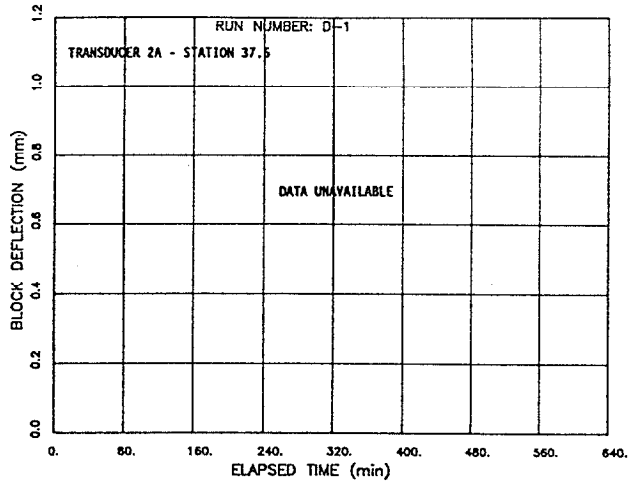
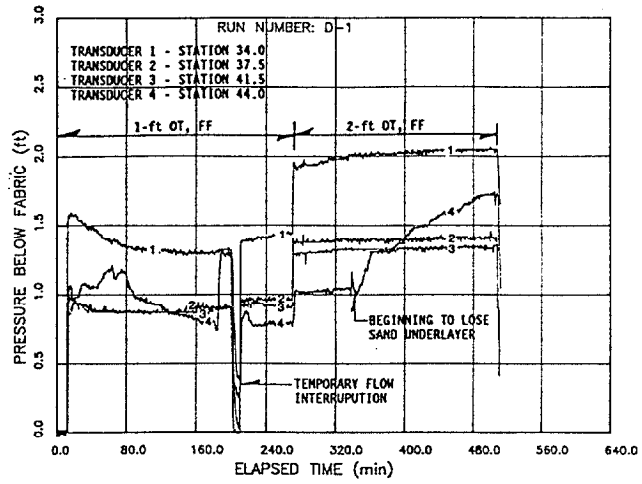


Figure 57. Transducer data for test D-1 (construction blocks).

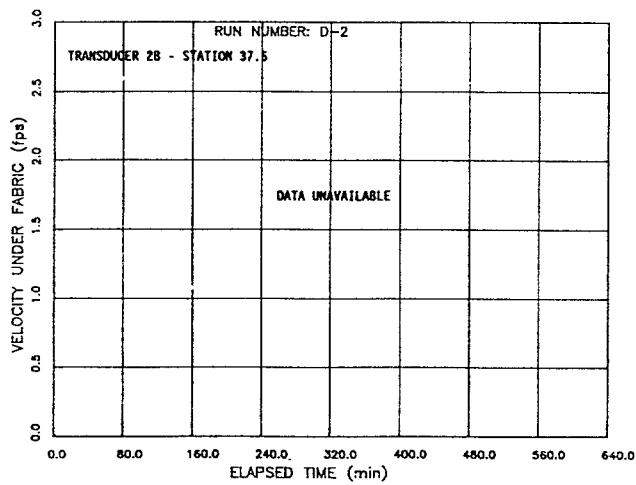
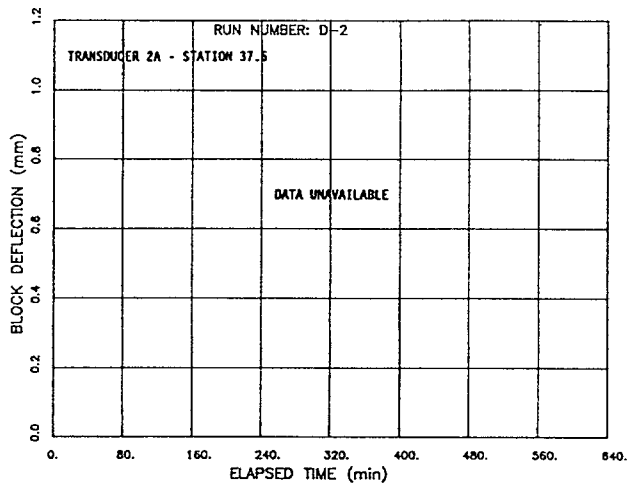
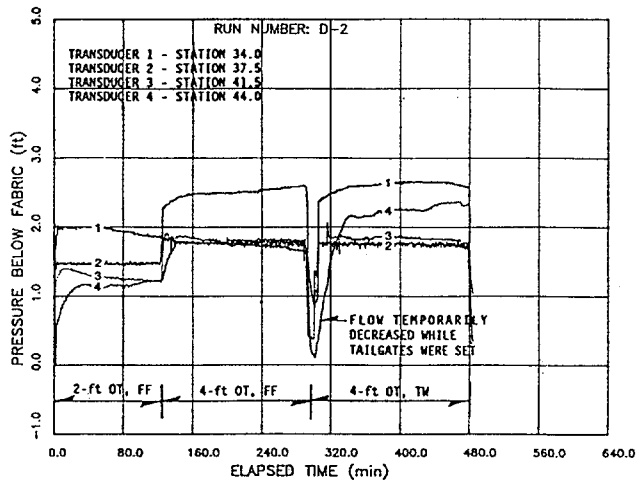


Figure 58. Transducer data for test D-2 (construction blocks).

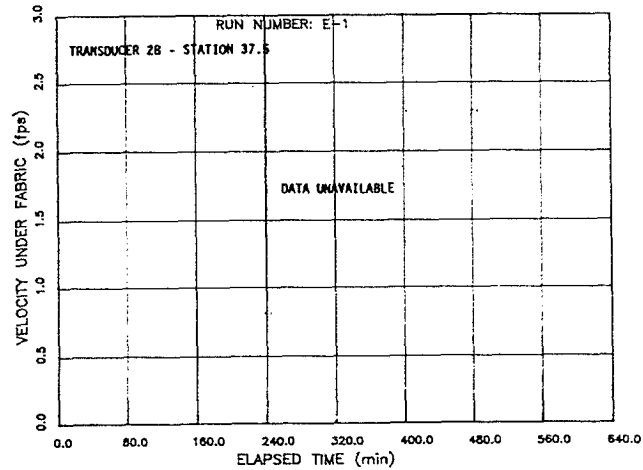
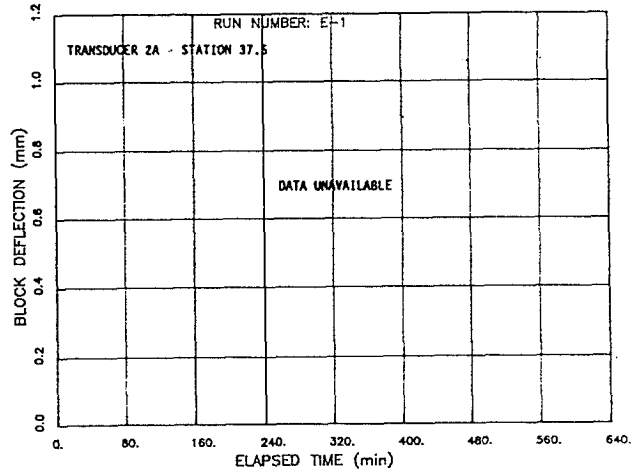
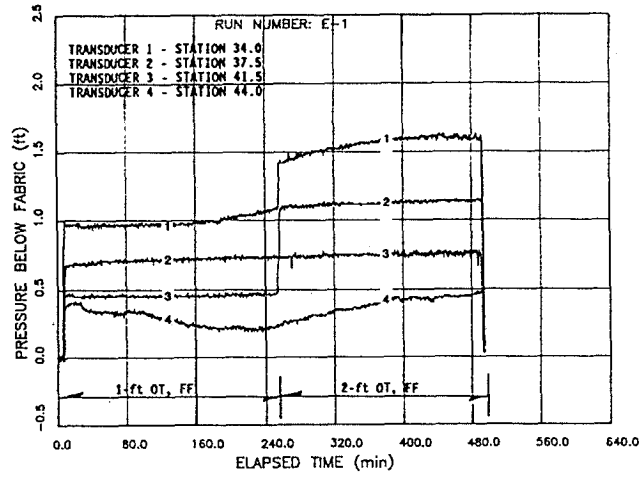


Figure 59. Transducer data for test E-1 (wedge blocks).

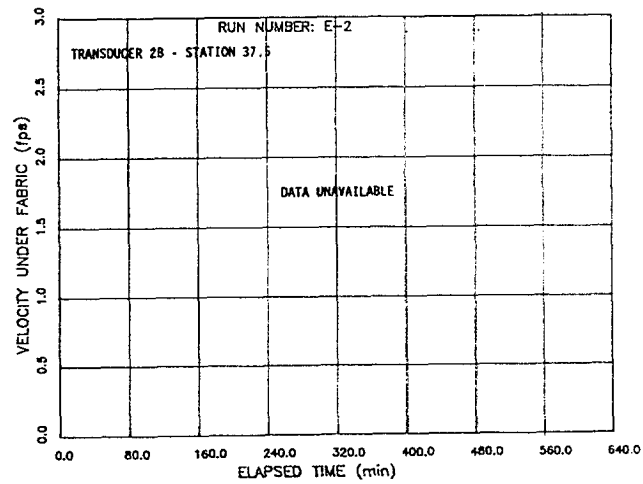
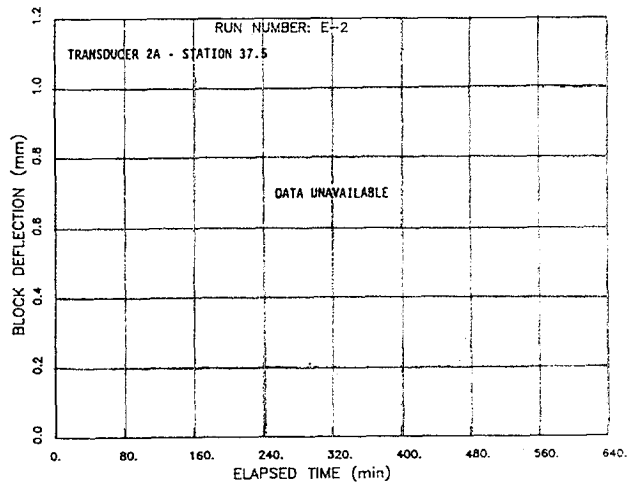
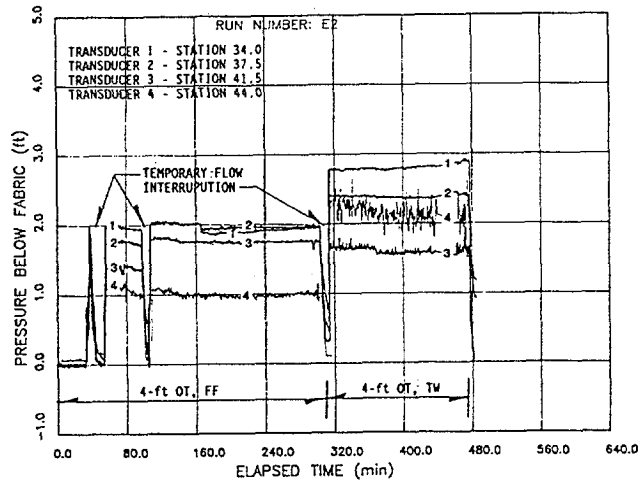


Figure 60. Transducer data for test E-2 (wedge blocks).

transducers tended to return reliable data during the course of the erodible embankment series of tests.

6. Analysis of the Pressure Data

Figures 61 through 64 are plots of observed versus calculated pressure at stations 34.0, 37.5, 41.5 and 44.0, respectively. Observed pressures were mean values determined from the transducer data. Calculated pressures were determined assuming hydrostatic conditions, using the equation:

$$P_{\text{calc}} = (d_{\text{corr}} + t_{\text{block}} + t_g) \cos \theta \quad (7)$$

where d_{corr} is the corrected flow depth, t_{block} is the block thickness, t_g is the thickness of the drainage layer, and θ is the angle of the embankment (to horizontal) at the location under consideration. Data from both rigid and erodible embankment tests are plotted in these figures. Observed subblock pressures were generally lower than calculated pressures. This trend was particularly evident on the embankment slope at stations 37.5 and 41.5 where flow was accelerating.

In figures 61 through 64, points plotting above the 45° line of agreement indicate observations of subblock pressure greater than that expected from hydrostatic forces alone. In general, this was observed primarily for the construction block and Armorflex systems. In the case of the construction blocks, their large cellular dimension (approximately twice that of other systems) may contribute to the transformation of kinetic head to stagnation pressure within the cell. This pressure can then be transmitted to the subblock environment where the pressure transducers were located. In the case of the Armorflex system, it is possible that local stagnation pressures may be transmitted to the subblock environment through the joints, as opposed to through the cells. This condition is brought about through the shouldered profile of the Armorflex block and its stagger pattern of installation, which creates a somewhat lower groove or channel between blocks which then terminates in the raised shoulder of the next downstream block (see figure 31).

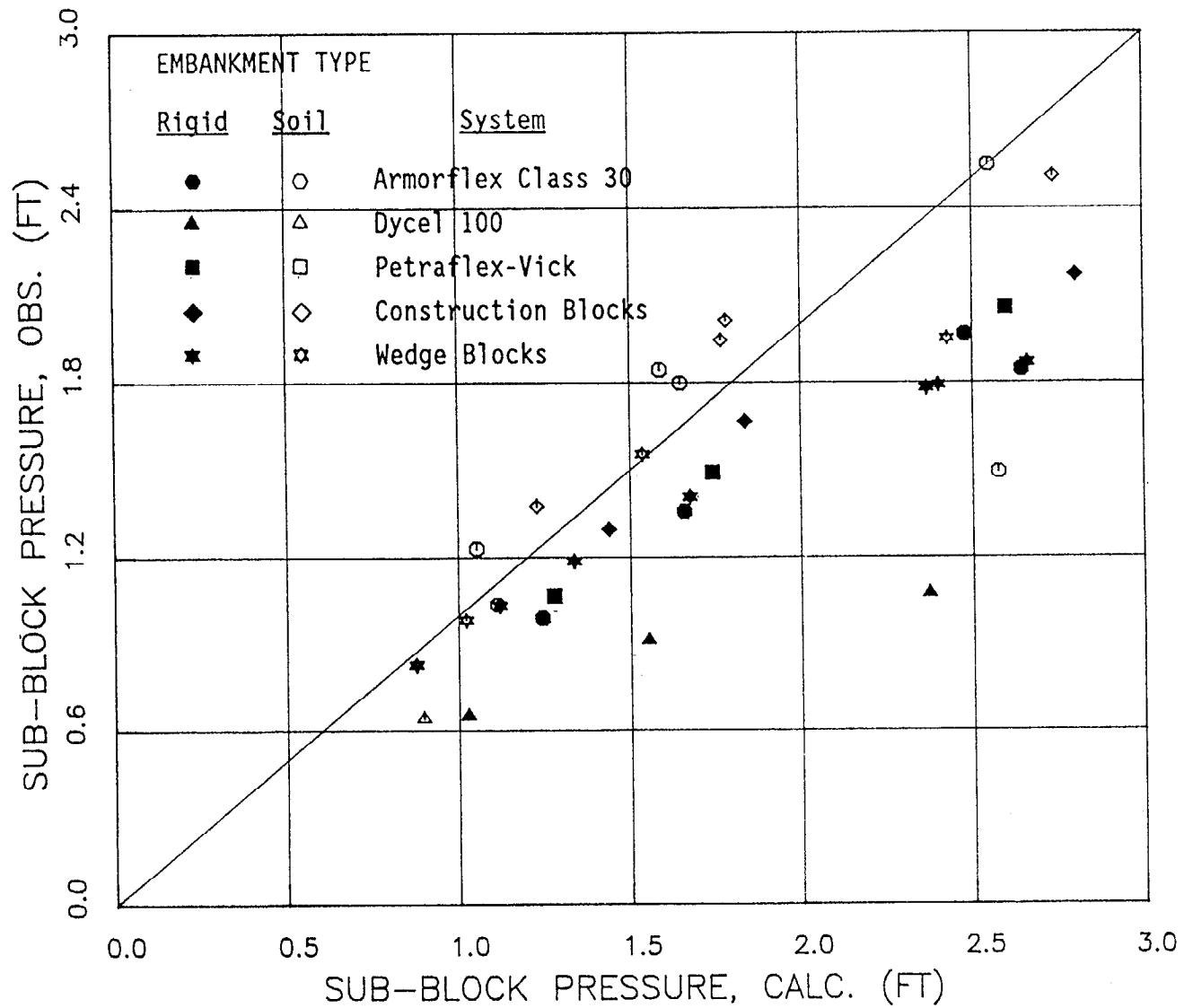


Figure 61. Mean observed sub-block pressure versus calculated sub-block pressure, in feet of water, at station 34.0.

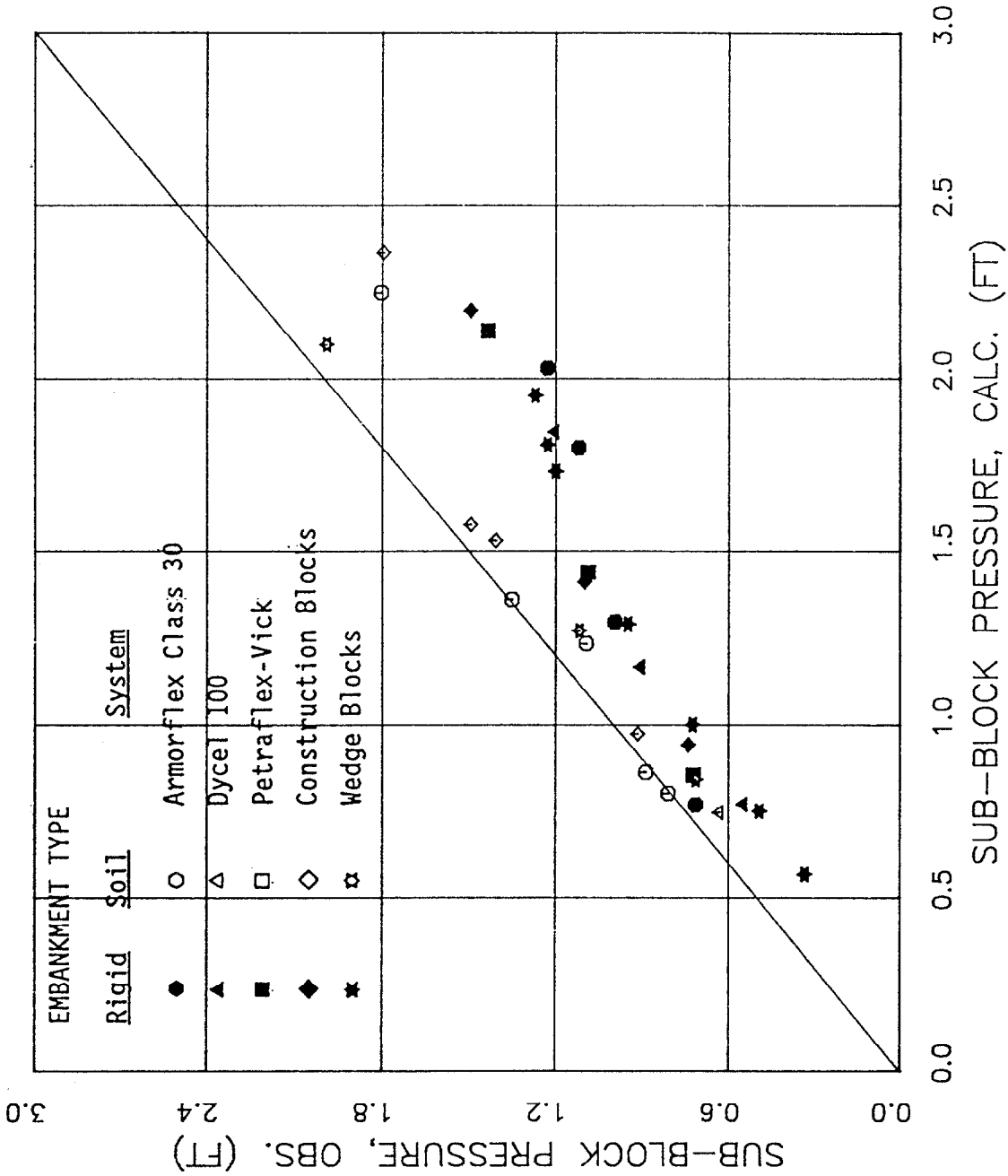


Figure 62. Mean observed sub-block pressure versus calculated sub-block pressure, in feet of water, at station 37.5.

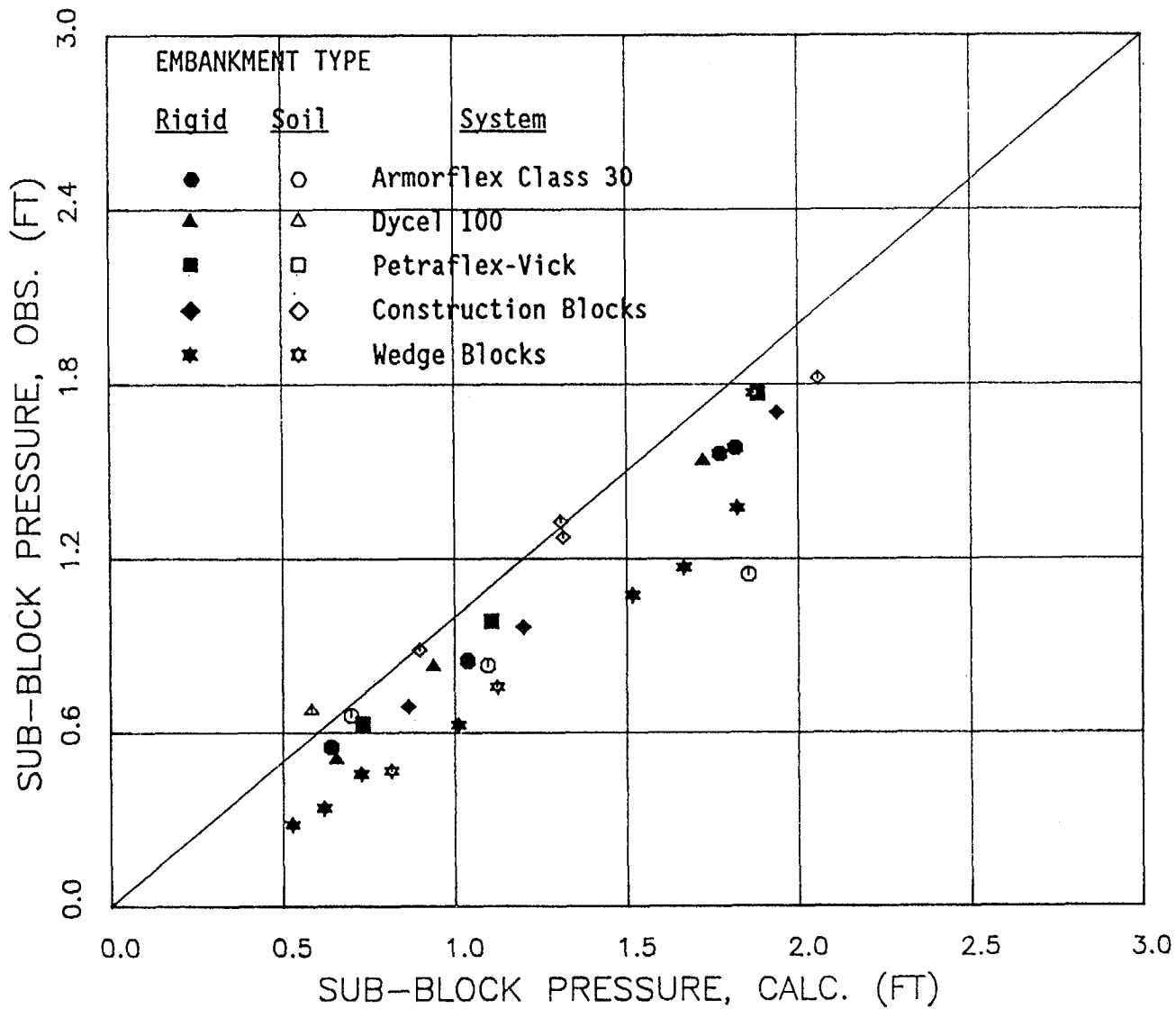


Figure 63. Mean observed sub-block pressure versus calculated sub-block pressure, in feet of water, at station 41.5.

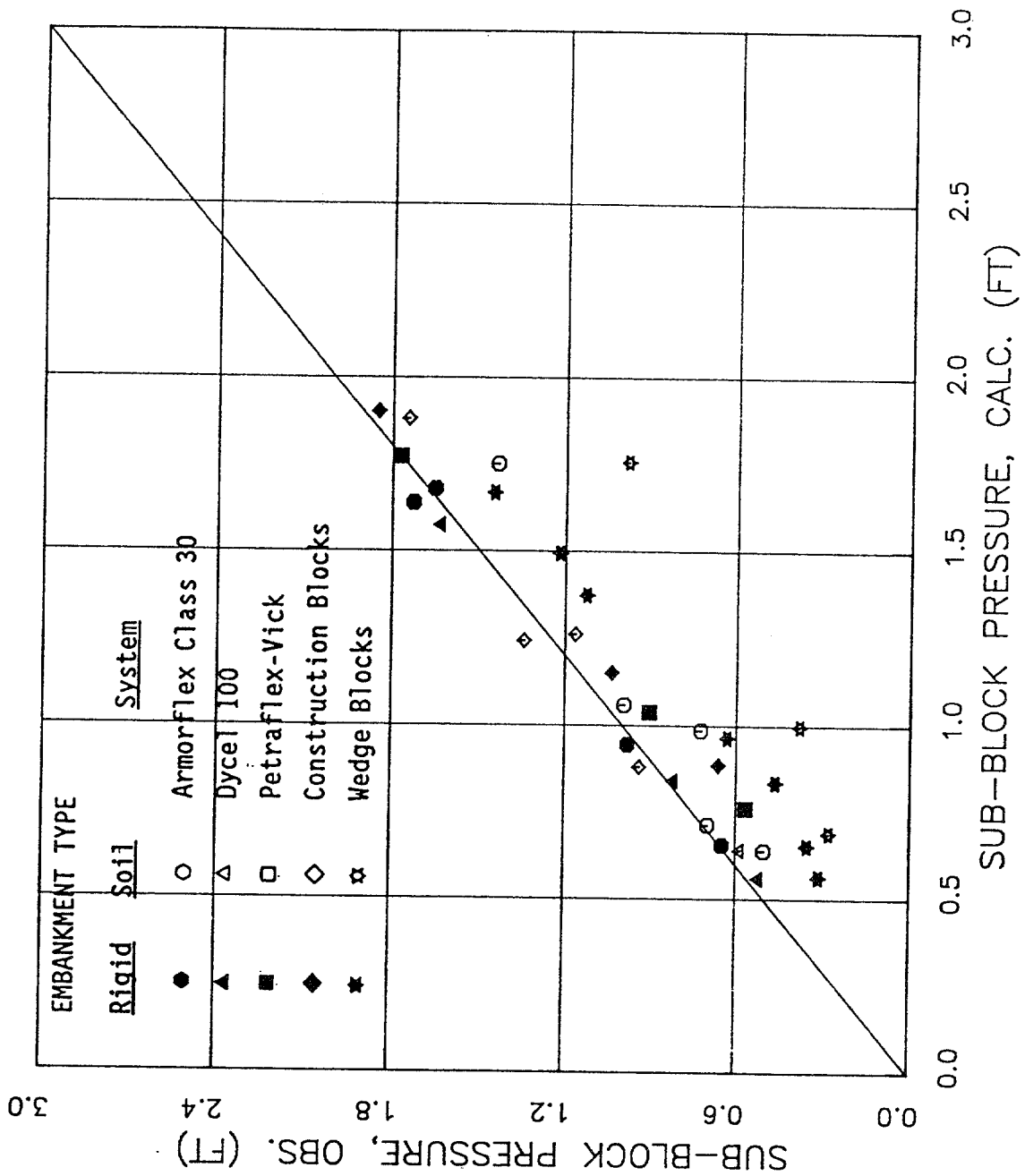


Figure 64. Mean observed sub-block pressure versus calculated sub-block pressure, in feet of water, at station 44.0.

Points falling below the 45° line of agreement in figures 61 through 64 indicate observed subblock pressures which are lower than those expected due to hydrostatic forces. In general, points falling lowest in this region correspond to the wedge-shaped system, particularly for transducer locations on the steep downstream slope. This indicates that the creation of localized zones of flow separation on the upper surface of the blocks is effective in creating a negative pressure field which can communicate with the subblock environment through properly placed drainage slots.

Relationships between subblock pressure and unit discharge were developed at each transducer location. Plots of pressure versus unit discharge at the four transducer locations are given in figures 65 through 68. Pressures plotted in these figures are the measured pressures less the protection system and drainage layer thicknesses as calculated by the equation

$$P_{\text{eff}} = P_{\text{meas}} - (t_{\text{block}} + t_g) \cos \theta \quad (8)$$

where P_{eff} is the effective pressure due to water and P_{meas} is the pressure measured by the transducers. This step was necessary to accommodate the various block thicknesses, which differed for each system. Included in the figures are power curve relationships developed by best-fit regression analysis for each station. All observed data were used to develop these relationships except for the Dycel 100 data at station 34, which did not follow the trend exhibited by the other systems. These relationships are of the form:

$$P_{\text{eff}} = a q^b \quad (9)$$

where P_{eff} is in feet of water and q is the unit discharge in ft^2/s . Envelopes which include 100 percent of the data are indicated by the shaded areas. Note that at stations 41.5 and 44.0 (near the toe of the downstream slope) the Dycel 100 system exhibited relatively high pressures at high unit discharges. This was the result of seepage beneath the system, accumulating in the downstream direction, and expressing itself as excess hydrodynamic pressure when drainage and pressure relief is inhibited.

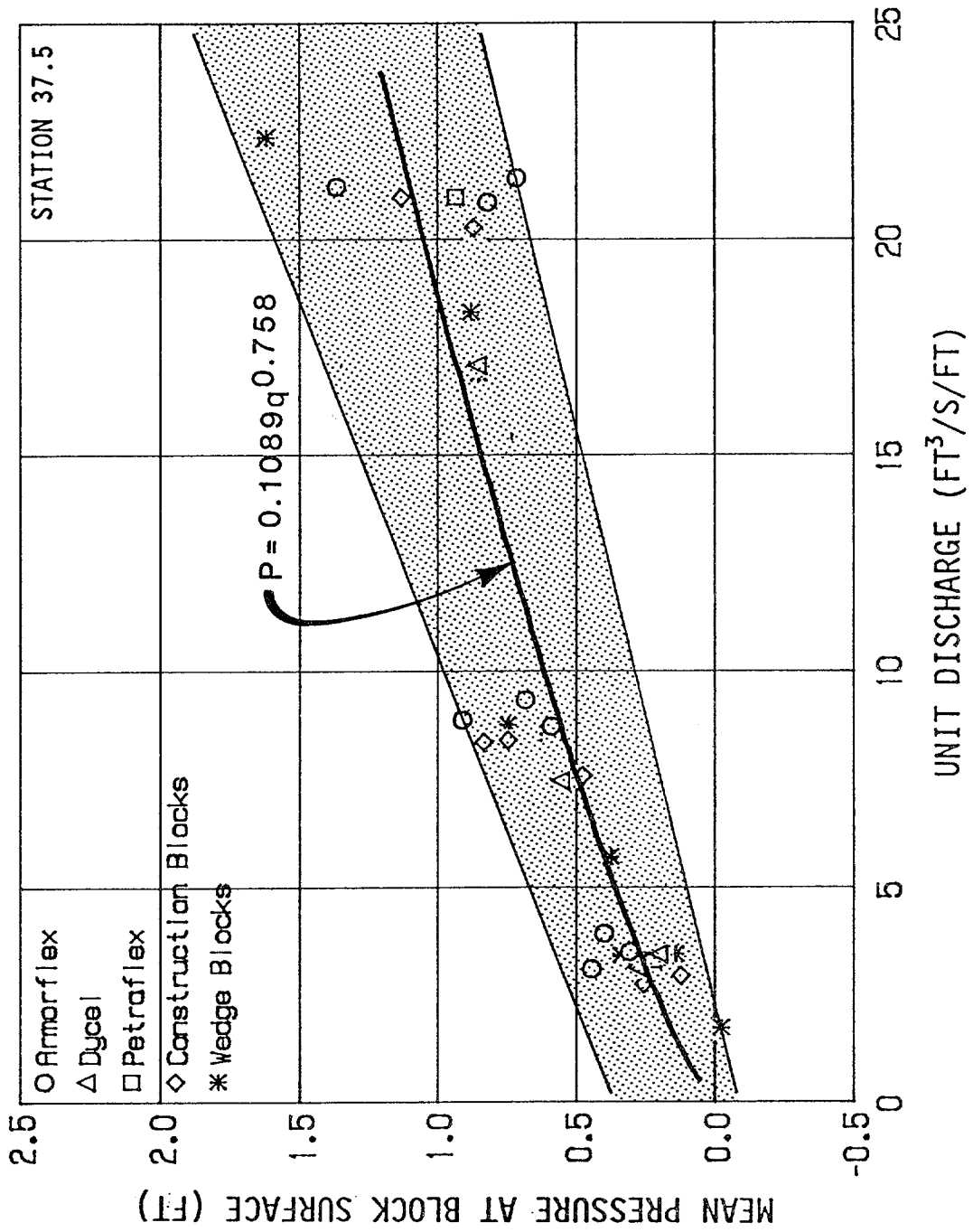
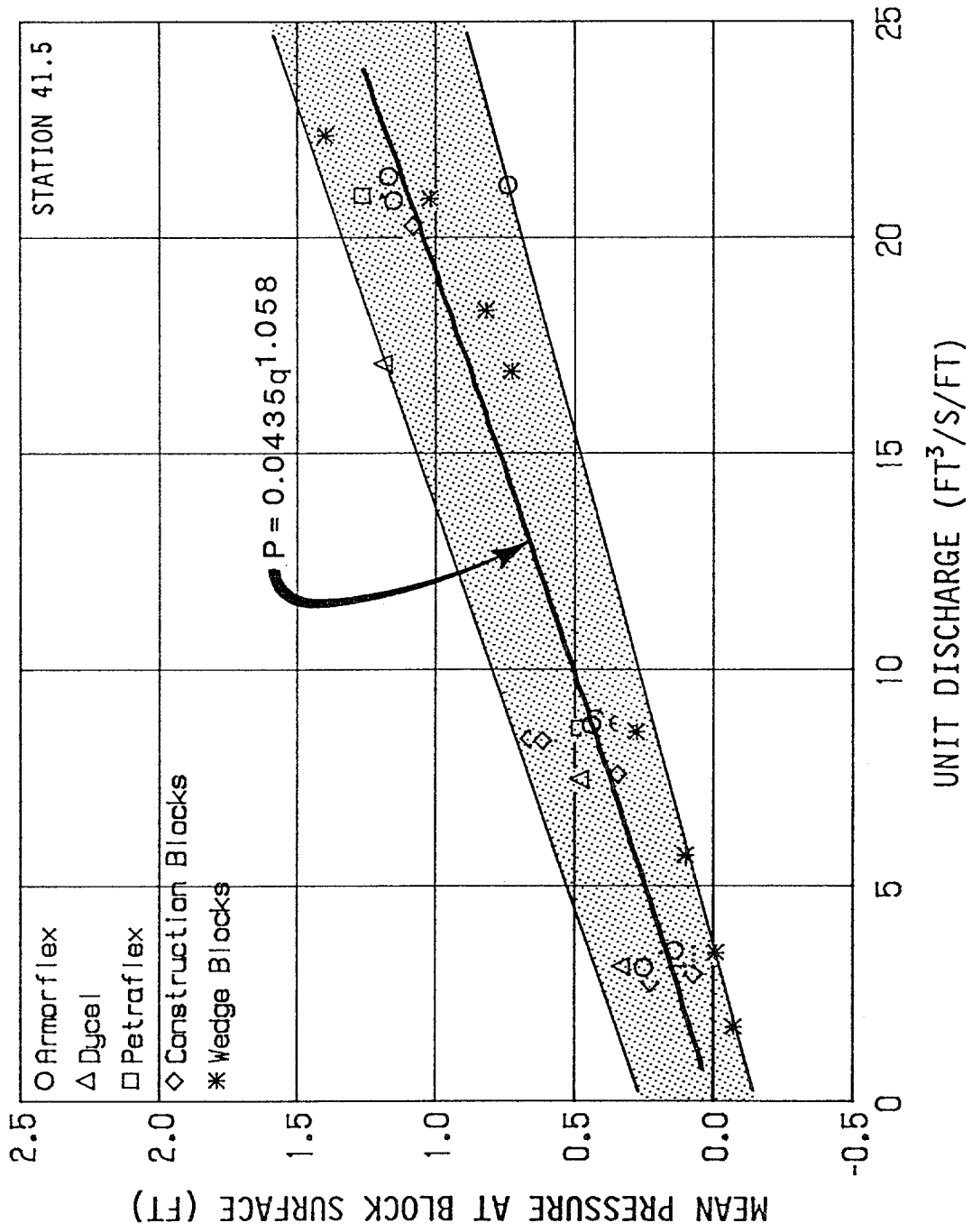


Figure 66. Mean pressure at the block surface versus unit discharge at station 37.5.



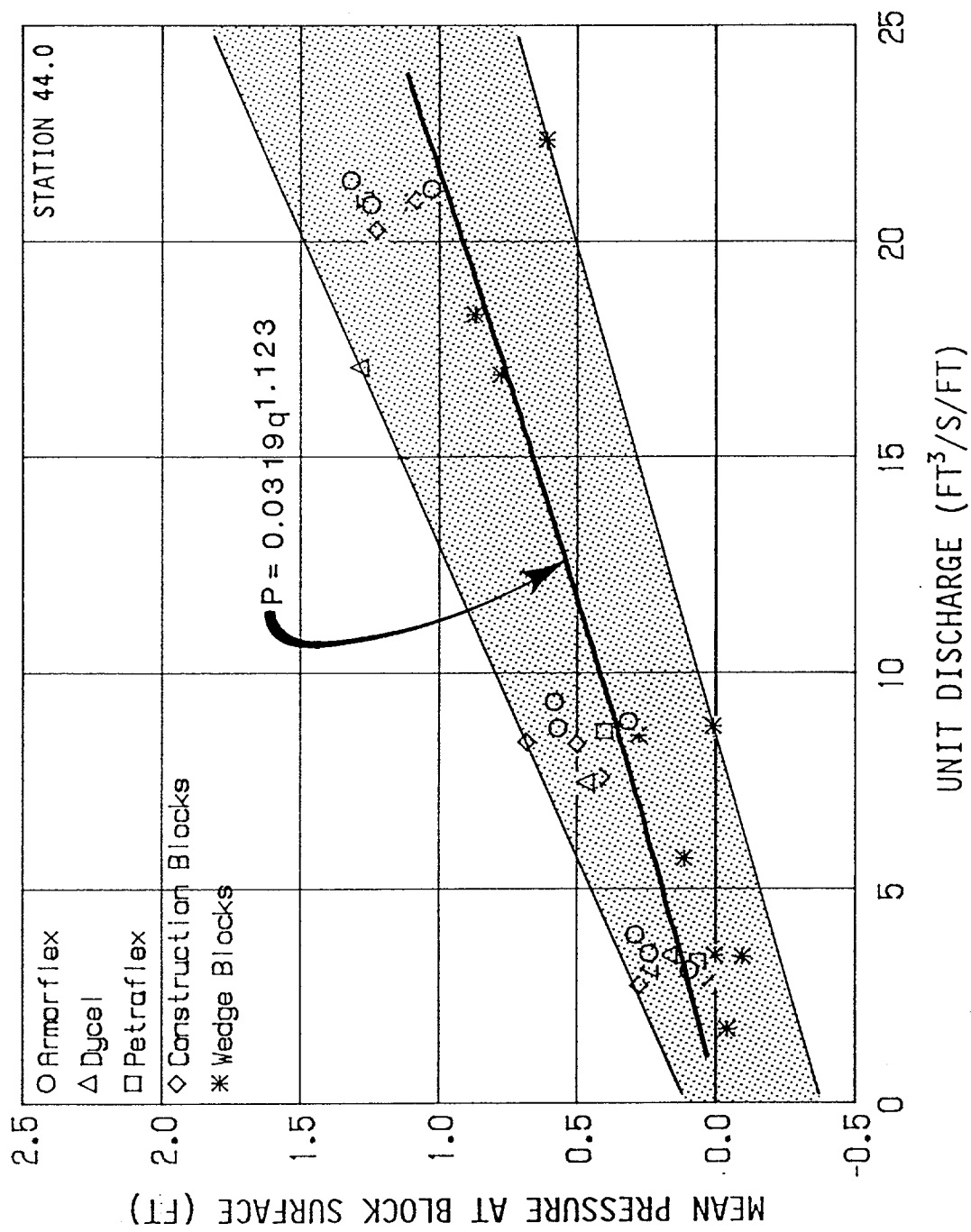


Figure 68. Mean pressure at the block surface versus unit discharge at station 44.0.

Coefficients a and exponents b for the 4 relationships are given in table 6. Note that in this table, the coefficients a are monotonically decreasing in the downstream direction, while the exponents b are monotonically increasing.

7. Analysis of the Flow Resistance Data

As described previously in this section, flow resistance parameters were determined on the steep downstream embankment slope for every freefall discharge examined during the course of the testing program. Resistance parameters were quantified using both the Manning and Darcy-Weisbach methodologies. Figure 69 presents the relationship between the computed Manning's n value and unit discharge for both the rigid and soil embankment series of tests, and clearly indicates a tendency for the apparent resistance to increase with flow rate. Figure 70 presents a similar relationship between the Darcy-Weisbach friction factor f and unit discharge.

The tendency for apparent resistance to increase with discharge, and hence depth, is contrary to the results obtained by researchers working with natural streams. In particular, mountain streams with slopes up to 0.04 (4 percent) were investigated by Bathurst.⁽⁷⁾ He found that resistance was inversely related to the relative submergence and developed an empirical relationship of the form:

$$(8/f)^{1/2} = 5.62 \log (d/D_{84}) + 4 \quad (10)$$

where f = Darcy-Weisbach friction factor

d = depth of flow in feet

D_{84} = bed-material characteristic size for which 84 percent is smaller

Similarly, Mussetter investigated 53 mountain streams in Colorado with gradients ranging from 0.007 to 0.17 and found a similar inverse dependence of resistance on relative submergence:⁽⁸⁾

$$(8/f)^{1/2} = C (d/D_{84})^{n1} (C_u)^{n2} (S_f)^{n3} \quad (11)$$

where C = empirical coefficient, approximately equal to 1.11

Table 6. Coefficients a and exponents b resulting from the pressure versus unit discharge regression analysis.

Station	a	b	r ²
34.0*	0.3521	0.493	0.857
37.5	0.1089	0.758	0.781
41.5	0.0435	1.058	0.814
44.0	0.0319	1.123	0.444

*Regression analysis performed without Dycel data.

Note: The relationship is of the form:

$P = a q^b$ where P is in feet of water (Equation 8)

q is in ft³/s/ft

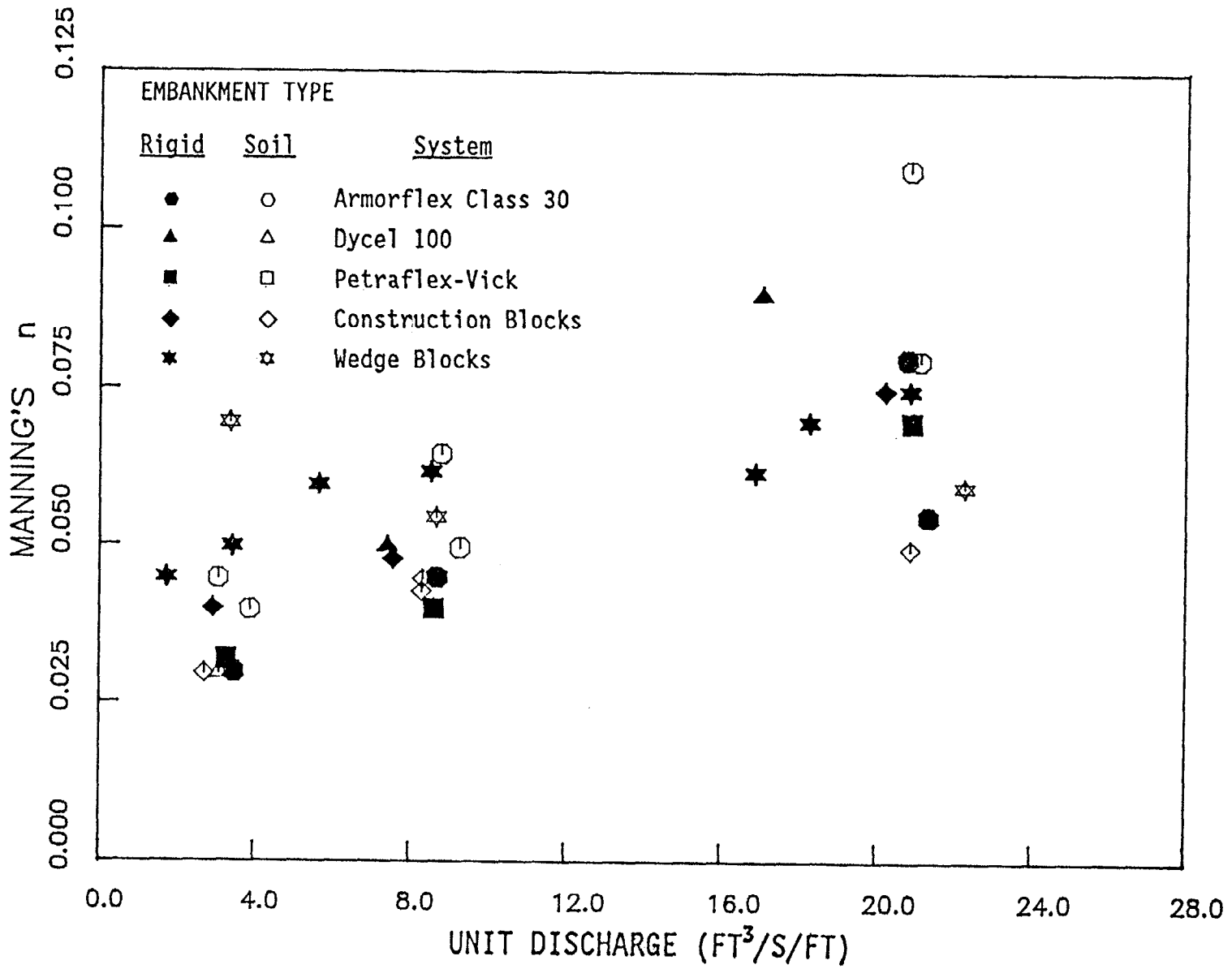


Figure 69. Manning's n versus unit discharge for all freefall tests.

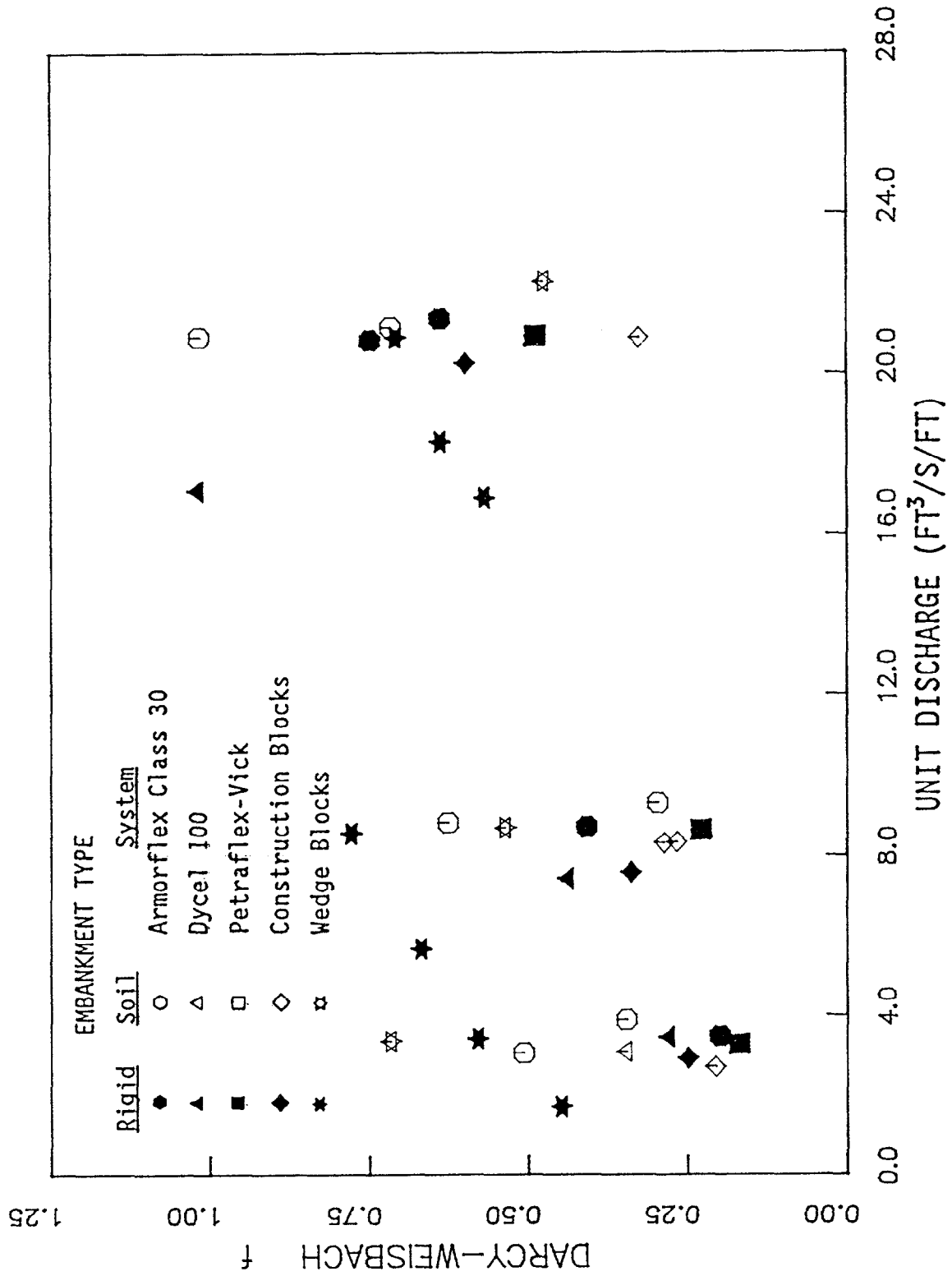


Figure 70. Darcy-Weisbach f versus unit discharge for all freefall tests.

- C_u = uniformity coefficient of bed-material gradation
(assumed equal to 1.0 for concrete blocks)
- n_1 = empirical exponent, approximately equal to 0.46
- n_2 = empirical exponent, approximately equal to -0.85
- n_3 = empirical exponent, approximately equal to -0.39

In the above formulations, the characteristic roughness element size is approximated by the D_{84} size of the graded bed material, and is assumed to be representative of the boundary rugosity k_s . The rugosity is a characteristic of the bed material and is assumed to be independent of the hydraulic condition of the flow. However, with the range of gradients investigated under the current testing program (bed slopes 0.33 to 0.50, with energy slopes ranging from 0.22 to 0.49), the traditional approaches do not appear to accurately account for the high rates of observed energy loss, which are presumably due to extremely high momentum transfer in the turbulent flow field.

The effect of higher rates of energy loss which occur on very steep slopes can be seen by using either equation 10 or 11 to calculate the effective k_s given the hydraulic conditions measured during the tests. This was done, with the results plotted against unit discharge and displayed in figures 71 and 72 for the Bathurst and Mussetter equations, respectively. From these figures it can be seen that the values of k_s calculated using these relationships are not constant for any given block system, instead appearing to depend on discharge (hence, depth). However, it can also be seen that the relative magnitude of the calculated characteristic roughness height is quite different between the two methods. The Bathurst relationship yields values of k_s up to approximately 2.5 ft (0.76 m), while the Mussetter equation gives maximum values of k_s of approximately 0.4 ft (0.12 m) for the same data. Qualitatively, the Mussetter relationship appears to yield more realistic estimates of rugosity, considering block geometry and the actual size of the cells.

The above discrepancy in analytical methodologies is ostensibly the result of Mussetter's incorporation of the friction slope term, whereas Bathurst does not. This conclusion was also reached in steep slope flume studies involving riprap.⁽⁹⁾ In addition, the above analyses indicates that more traditional resistance relationships developed for typical open-channel flow may not be

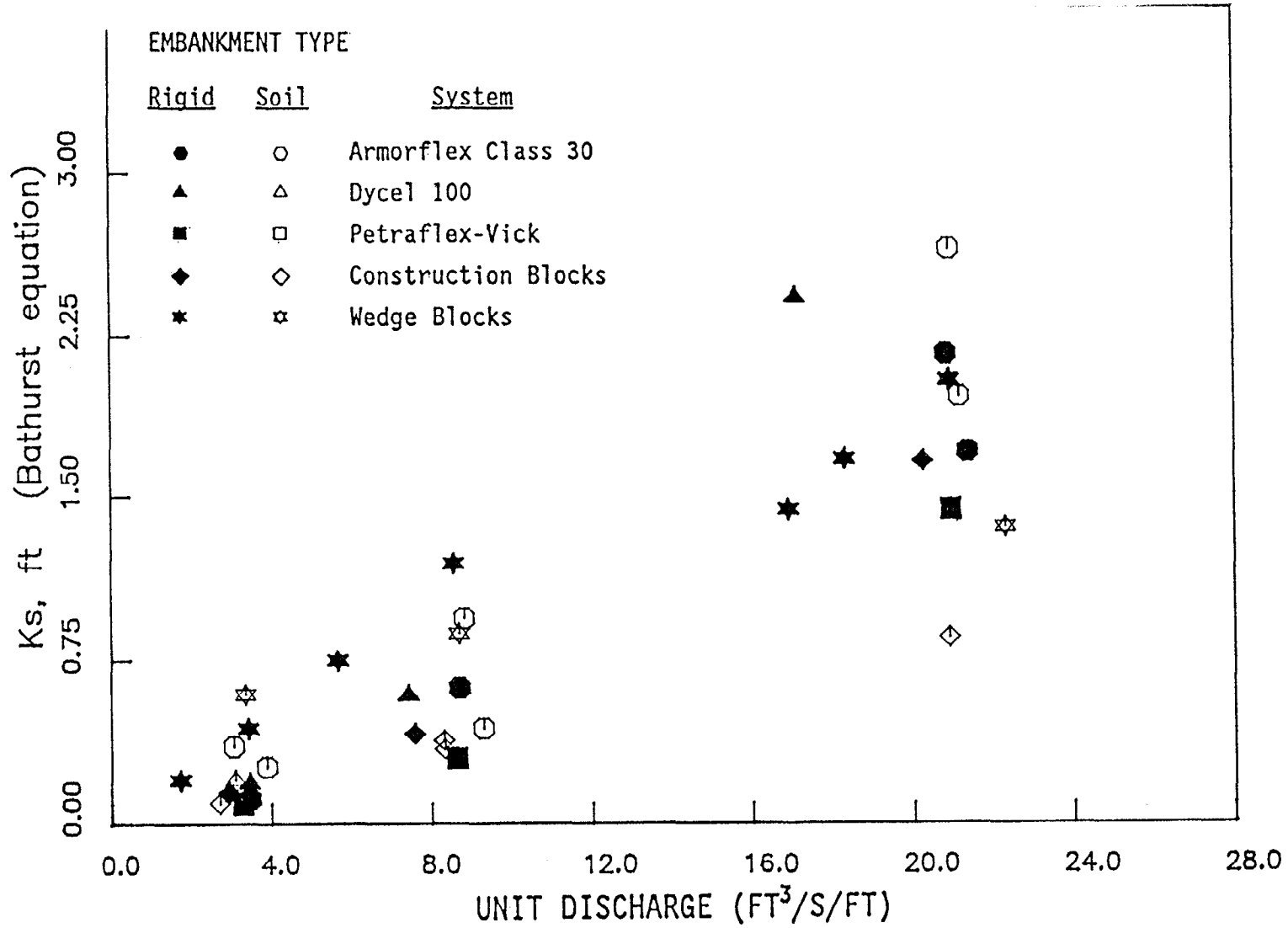


Figure 71. Boundary rugosity k_s calculated using the Bathurst relationship for all freefall tests.

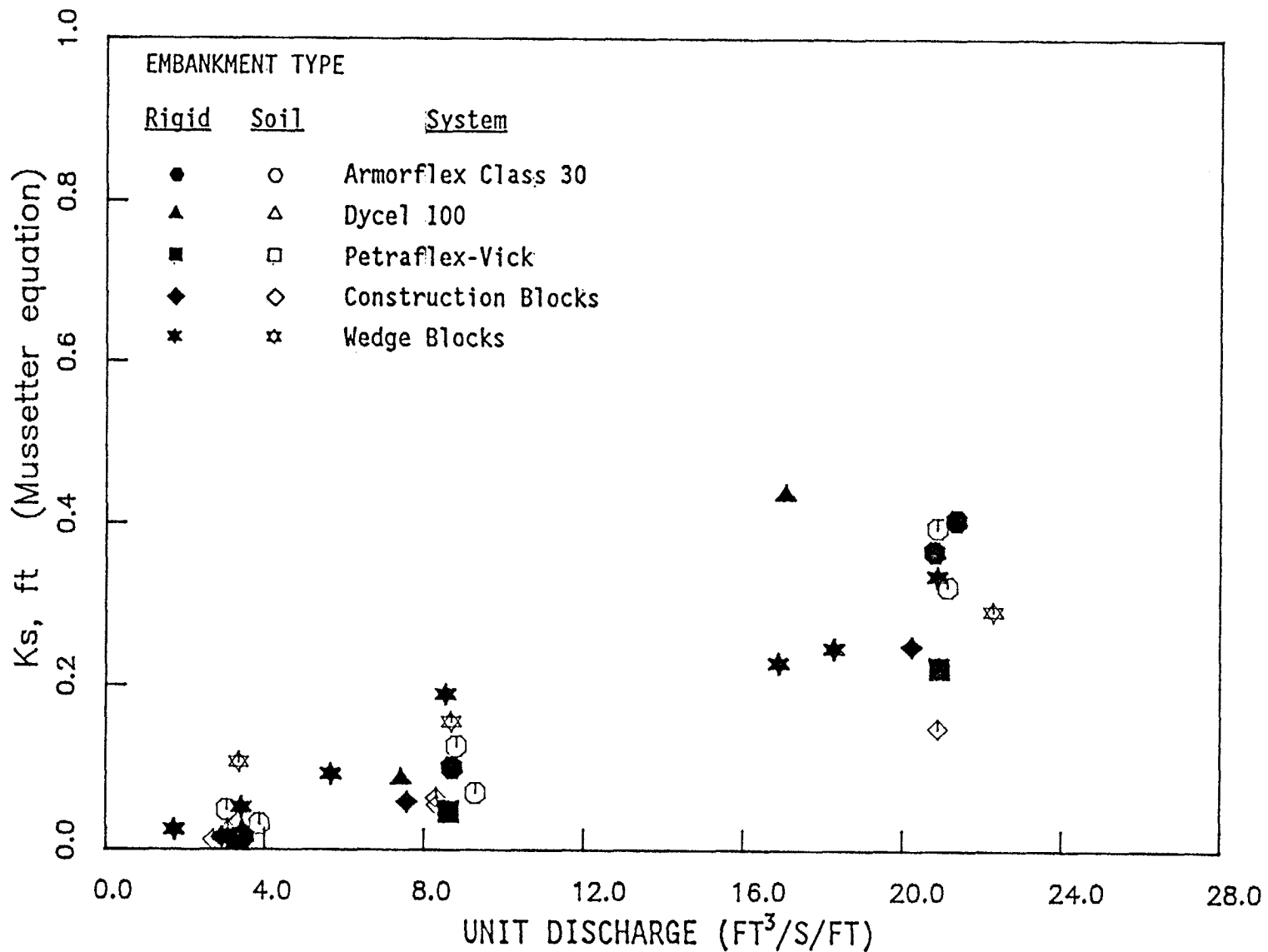


Figure 72. Boundary rugosity k_s calculated using the Mussetter relationship for all freefall tests.

directly applicable to steeply sloped installations with bare (i.e., unvegetated) concrete block revetment; however, it is likely that a resistance function which includes the slope can be developed which will reliably characterize the hydraulics of flow for a wide range of slopes and overtopping depths.

SUMMARY AND CONCLUSIONS

1. Summary

The qualitative results of the 1988 testing program, coupled with the quantitative analysis of the resulting data, has yielded a better understanding of the hydraulics of flow over an embankment and its effect on the stability of articulated concrete block revetment mattresses used to protect the underlying embankment structure from erosion damage and potential breaching.

A total of 17 tests were conducted on 5 different revetment systems. Eight of the 17 tests were conducted on a rigid (concrete) embankment, while the remaining 9 tests were performed with a highly erodible, silty clay soil embankment. Each test consisted of subjecting the revetment system to one or more overtopping depths, up to the maximum capacity of the testing facility which was 4 ft (1.2 m) of overtopping head. Under maximum flow conditions, a unit discharge rate of 20 to 24 ft³/s/ft (1.8 to 2.2 m³/s/m) was attained, which yielded maximum velocities of approximately 16 to 18 ft/s (4.8 to 5.5 m/s) at the toe of the embankment slope. A total of 34 freefall discharge conditions were examined, along with 8 conditions with tailwater held at the midpoint of the embankment slope.

The systems investigated included:

- Armorflex Class 30 open-cell block, 36 lb/ft² (1.73 kN/m²), with lateral and longitudinal cables, with and without slope anchors.
- Dycel System 100, closed-cell block, 42 lb/ft² (2.02 kN/m²), with longitudinal cables and slope anchors.
- Petraflex-Vick open-cell block, 42 lb/ft² (2.02 kN/m²), with lateral and longitudinal cables.
- Concrete construction block system, open-cell block, 40 lb/ft² (1.92 kN/m²), no cables.
- Wedge-shaped block system, closed cell block with drainage slots, 48 lb/ft² (2.30 kN/m²), no cables.

Pressure, velocity, and displacement data were collected beneath the revetment systems through the use of a remote electronic transducer network

installed in the embankment subgrade. In addition, depth and velocity measurements were made in the overtopping flow field above the revetment at 2-ft (0.6 m) intervals along the embankment. These data were analyzed to determine the hydraulic characteristics of the overtopping flow, quantify stress levels imposed on the revetment system, and calculate flow resistance parameters. This information was used to gain insight into the factors controlling the stability of these systems under the conditions imposed by the tests.

All systems were found to be stable up to and including the maximum capacity of the testing facility, given proper subgrade preparation and installation within the confines of the flume walls and floor, with the exception of the Dycel 100 system, which failed during the 1-ft (0.30 m) overtopping run on the soil embankment.

For ease in comparing performance indicators for the various protection systems, table 7 provides a summary of limiting values of velocity and shear stress as documented in the previous FHWA study.⁽¹⁾ Table 7 has been updated to include the results of the hydraulic tests described in this report.

2. Conclusions

The following conclusions are derived from the results of the hydraulic tests and data analyses as presented in this report:

1. Articulated concrete block revetment systems on steep slopes, when properly installed on a well-prepared subgrade, can maintain hydraulic stability under high-velocity flows of approximately 20 ft/s (6.10 m/s) or more, with corresponding bed shear stresses of 30 to 40 lb/ft² (1.44 to 1.92 kN/m²).
2. Failure of a block system can be defined by the following general conditions for unvegetated systems on steep slopes:
 - a. Loss of embankment soil beneath the system by gradual erosion along the slope beneath the system, or washout through joints and open cells.

Table 7. Summary of critical velocity and shear stress for various protection measures.

Source	Protective Cover	Underlying Soil	V_c (ft/s)	τ_c (lb/ft ²)
ARS [see ref. (1)]	Class A Vegetation	Erosion Resistant	6-8	3.7
		Erodible	4-6	3.7
	Class B Vegetation	Erosion Resistant	5-7	2.1
		Erodible	3-5	2.1
	Class C Vegetation	Erosion Resistant	4-5	1.0
Erodible		3-4	1.0	
Class D Vegetation	Erosion Resistant	3.5	0.60	
	Erodible	2.5	0.60	
Class E Vegetation	Erosion Resistant	3.5	0.35	
	Erodible	2.5	0.35	
FHWA phase I study [see ref. (1)]	Woven Paper		N/A	0.15
	Jute Net		N/A	0.45
	Single Fiberglass		N/A	0.60
	Double Fiberglass		N/A	0.85
	Straw w/Net		N/A	1.45
	Curled Wood Mat		N/A	1.55
	Synthetic Mat		N/A	2.00
CIRIA [see ref. (1)]	Plain Grass, Good Cover	Clay	7-15*	N/A
	Plain Grass, Average Cover	Clay	5-12*	N/A
	Plain Grass, Poor Cover	Clay	3-10*	N/A
	Grass, Reinforced w/Nylon Mat	Clay	14-19*	N/A
CIRIA [see ref. (1)]	Dycel w/Grass	Clay	23-26	N/A
	Petraflex w/Grass	Clay	>26	N/A
	Armorflex w/Grass	Clay	23-26	N/A
	Dymex w/Grass	Clay	15	N/A
	Grasscrete	Clay	26	N/A
FHWA phase I study [see ref. (1)]	Gravel D ₅₀ = 1 in D ₅₀ = 2 in		N/A	0.40
			N/A	0.80
	Rock D ₅₀ = 6 in D ₅₀ = 12 in		N/A	2.50
			N/A	5.00
FHWA phase II study [see ref. (1)]	6 in Gabions	Type I	17	35
	4 in Geoweb	Type I	9-10	10
	Soil Cement	Type I	>16.0	>45
	(8% Cement)			
FHWA phase II study [see ref. (1)]	Dycel w/o Grass	Type I	<7.3	<7.0
	Petraflex w/o Grass	Type I	>17	>32
	Armorflex w/o Grass	Type I	12-15	12-20
	Enkammat w/3 in Asphalt	Type I	13	13-16
	Enkammat w/1 in Asphalt	Type I	<8.6	<5

Table 7. Summary of critical velocity and shear stress for various protection measures (continued).

Source	Protective Cover	Underlying Soil	V_c (ft/s)	T_c (lb/ft ²)
FHWA phase II study addendum (see tables 4 and 5)	Armorflex Class 30 with longitudinal and lateral cables, no grass	Type I	>15	>34
	Dycel 100, longitudinal cables, cells filled with mortar	Type I	<9	<12
	Concrete construction blocks, granular filter underlayer	Type I	>17	>20
	Wedge-shaped blocks with drainage slots	Type I	>17	>25

*Critical velocity is dependent on test duration.

ft/s x 0.3048 = m/s

lb/ft² x 47.87 = N/m²

- b. Deformation of the underlying embankment through liquefaction and shallow slip of the embankment soil caused by the ingress of water beneath the system.
 - c. Loss of a block or group of blocks (uncabled systems) which directly exposes the underlayer to the flow.
3. The occurrence of flow beneath the system is detrimental, and can lead to failure if neither limited nor allowed to drain by passive or active mechanisms. Subblock velocities ranging from approximately 1.2 to 2.0 ft/s (0.4 to 0.6 m/s) were recorded for the systems investigated, during the maximum flow condition, at a point near the embankment shoulder.
 4. The effect of cabling on the hydraulic stability in steep-slope applications is probably insignificant. While cables serve an important part in facilitating field placement of large preassembled mats, their overall effect in preventing the ingress of flow beneath the system is likely to be minor. It can be said, however, that the cables, when properly anchored, will serve to keep the system tied together on the slope, even when the embankment beneath is deforming. This may be a secondary benefit of the cables, considering the potential for a rapid progression of block loss in an uncabled system, as demonstrated in laboratory studies.
 5. Providing a drainage layer beneath the block system is considered important for allowing pressure relief to occur. This is probably more important for bare (unvegetated) installations. The drainage layer must have the capacity to conduct water safely out from beneath the system at a rate greater than that at which water is entering the subblock environment. Additionally, pressure buildup beneath the revetment system may exceed the effective system weight when longer slopes or greater unit discharges are examined.
 6. A geotextile should be provided at the interface between the embankment soil and the blocks. Important selection criteria for the geotextile include effective opening size, permeability, and net open area.

7. Providing drainage slots which communicate with the subblock environment with an orientation which promotes self-aspiration appears to function well in the removal of water beneath the system. Maximum benefit is achieved by providing a block geometry which allows the drainage slots to be located in a region of local (small-scale) flow separation, such that a zone of lower pressure is created on the upper surface of the blocks in this region.

8. The resistance to flow on bare (unvegetated) block systems has been quantified for conditions of steep-slope flow, and indicative parameters such as Manning's n value and the Darcy-Weisbach f value appear to be larger than would be expected for the same lining on a mild slope. Additionally, the resistance to flow increases with the discharge and depth of overtopping flow, for the range of conditions examined during the course of testing. Development of a predictive equation to provide more accurate information for design and analysis of these systems is indicated.

GLOSSARY OF TERMS

- ANCHOR** An object placed in the subsoil which is designed to provide restraint against separation of the protection system from the subgrade.
- ASPHALT** Bitumen-bound admixture consisting of tar, oil, and granular soil aggregate commonly used for the surface of roadways.
- ANGLE OF REPOSE** Angle of slope formed by noncohesive soil or rock at the critical equilibrium condition of incipient sliding.
- AUXILIARY SPILLWAY** A secondary spillway designed to operate only during exceptionally large floods.
- COMPACTION** A decrease in the volume of voids within a soil matrix, yielding an increase in density.
- CREST** The horizontal or near-horizontal top of an embankment.
- CRITICAL DEPTH** Depth of flow where the combined kinetic and potential energies are at a minimum. For this condition the ratio of inertial forces to gravitational forces is equal to unity.
- DEPTH OF FLOW** The distance from the channel bed to the water surface measured normal to the direction of flow.
- DEPTH OF OVERTOPPING** The head of water above an embankment crest as measured vertically from the crest to the water surface in the upstream pool.
- DISCHARGE** The volume of water passing a given cross section in a specified length of time, e.g. cubic feet per second.
- DESIGN DISCHARGE** The discharge at a specific location to be used for design purposes, usually associated with a specified return period or frequency of occurrence.
- EMBANKMENT** A raised mound of soil or rock typically used for elevating a roadway or impounding water. Embankments are generally characterized by a length dimension many times greater than either the height or width dimensions.
- EROSION** In the context of this report, the uncontrolled detachment and removal of soil from an embankment by the action of flowing water.
- FABRIC** A woven or nonwoven geotextile.
- FAILURE** In the context of this report, the loss of direct and intimate contact between protection system and subgrade whereby the retention of subgrade soils against the action of flowing water cannot be guaranteed.
- FILTER BLANKET** One or more layers of graded, permeable noncohesive soil material placed between the subsoil and the protection system to prevent soil loss by piping or washout while permitting drainage and pressure relief to occur.

FILTER FABRIC A permeable geotextile used between the subsoil and the protection system to achieve the same results as a filter blanket.

FREEBOARD Vertical distance from the water surface to the top of the protection system at the design discharge.

FREEFALL In the context of this report, the hydraulic condition which exists on the downstream embankment slope whereby supercritical flow reaches the toe of the embankment unconstrained by tailwater.

GABION Compartmented rectangular containers made of galvanized steel hexagonal mesh and filled with stone.

GEOTEXTILE A synthetic fabric specifically designed to be used as a construction material, typically in conjunction with soil placement and compaction in civil engineering applications. Primary purposes include filtration, separation, drainage, soil reinforcement, and erosion control.

HYDRAULIC JUMP Transition zone from supercritical to subcritical flow characterized by turbulent, non-uniform flow with associated head loss due to change from kinetic to potential energy.

HYDRAULIC LOADING The discharge-related parameters of flow which have a bearing on the potential failure of a protection system. These parameters include velocity, depth, duration, shear stress, pressure, and frequency of immersion.

HYDRAULIC RADIUS Cross-sectional area of flow divided by the wetted perimeter.

HYDRAULIC RESISTANCE A measure of channel roughness and form resistance encountered by flowing water, typically described by the Manning's n value.

HYDROSTATIC PRESSURE Pressure at a depth below the water surface for flow at constant, unidirectional velocity or at rest.

INCIPIENT MOTION The threshold of movement for a given particle of soil or rock under the action of flowing water.

LINING, FLEXIBLE Channel protection material or system which exhibits deformability such that adjustment to subgrade settlement can occur. Materials are typically porous in nature to allow infiltration and exfiltration to occur.

LINING, PERMANENT Lining designed for long-term use.

LINING, RIGID Lining material with no capacity to adjust to subgrade settlement. Typically constructed of nonporous material with a smooth finish that provides a large conveyance capacity (e.g., concrete, soil cement).

LINING, TEMPORARY Lining designed for short term utilization, typically to assist in the establishment of a permanent vegetative lining.

MAT A 3-dimensional flexible geotextile typically greater than 10 mm thick.

MESH A 2-dimensional geotextile made of two sets of parallel strands which intersect at a constant angle, typically 0.5 to 5 mm thick with an opening size greater than 2 mm.

NAPPE The shape of the underside of an aerated overfall jet of water, for example as occurring over a sharp-crested weir.

NORMAL DEPTH Depth of flow under uniform flow conditions. See UNIFORM FLOW.

OGEE A particular spillway surface geometry which approximates the shape of an aerated nappe at the design discharge.

PERMEABILITY Property of a soil or geotextile that enables water or air to move through it under an applied gradient.

PROTECTION SYSTEM In the context of this report, a channel lining designed to resist erosion by high velocity flows.

RETARDANCE CLASSIFICATION Qualitative description of the resistance to flow exhibited by various types of vegetation.

REVETMENT A facing of erosion-resistant material which protects the underlying material from erosion damage. This term is typically used to describe heavier, non-vegetated systems or products.

RIPRAP Broken rock, cobbles, or boulders placed on the sides and/or bottom of channels for erosion protection. Often used in conjunction with filter blankets or filter fabrics.

RIPRAP, GROUTED Riprap with all or part of the interstices filled with Portland cement mortar.

RIPRAP, WIRE-ENCLOSED See GABIONS.

ROLLER-COMPACTED CONCRETE (RCC) A no-slump mixture of sand, gravel, portland cement and water placed and compacted by standard earthworking equipment.

SHEAR STRESS Frictional force developed on the wetted area of the channel in the direction of flow; force per unit area.

SHEAR STRESS, PERMISSIBLE Maximum allowable shear stress for a given soil or protection system. Shear stresses exceeding this value invite system failure and erosion damage.

SIDESLOPE Slope of the channel sides, customarily reported as a ratio of the amount of run to the amount of rise, e.g., 3H:1V.

SOIL CEMENT A no-slump mixture of (native) soil and portland cement placed and compacted by standard earthworking equipment. Differs from RCC in that a higher percentage of fines (silts and clays) are present in the mix, resulting in less cement by weight and a correspondingly lower compressive strength.

SUBCRITICAL FLOW Tranquil flow characterized by a flow depth greater than critical depth.

SUBGRADE The soil which comprises the embankment underlying the channel, and which is to be protected from erosion by the protection system.

SUBMERGENCE The presence of tailwater above the embankment crest such that the unit discharge is decreased to a value less than that for freefall conditions.

SUPERCritical FLOW Rapid flow characterized by flow depths less than critical depth.

TAILWATER The elevation of the water surface in the channel downstream from the embankment toe.

TOE The intersection of the downstream embankment slope with the foundation or valley floor.

TRANSDUCER, PRESSURE An electronic instrument whose voltage output is directly related to the pressure at its sensing tip.

UNIFORM FLOW The condition of flow where the rate of energy loss due to frictional resistance is equal to the bed slope of the channel. Where uniform flow exists, the slopes of the energy line, the water surface, and the channel bed are identical.

VELOCITY, MEAN Discharge divided by the cross-sectional area of flow.

VELOCITY, LOCAL Velocity at a specific point within the flow region. May be defined as a direction-dependent vector quantity, e.g., V_x , V_y , V_z .

VELOCITY, PERMISSIBLE Maximum allowable mean velocity for a soil or protection system. Velocities exceeding this value invite system failure and erosion damage.

REFERENCES

1. P. E. Clopper and Y. H. Chen, 1988. "Minimizing Embankment Damage During Overtopping Flow." Report No. FHWA-RD-88-181, Federal Highway Administration, Washington, D.C., November 1988.
2. J. K. Mitchell, J. L. Evans, and J. Kellerman, 1987. "Hydraulic Performance of Concrete Block Chutes." Paper No. 87-2056 presented at the 1987 Summer Meeting of the American Society of Agricultural Engineers, Baltimore, Maryland.
3. L. Wendte, and M. E. Andreas, 1986. "Concrete Block Lined Chutes and Channel Protection." Paper No. 86-2605 presented at the 1986 Winter Meeting of the American Society of Agricultural Engineers, Chicago, Illinois.
4. Soil Conservation Service, 1988. "Concrete Block-Lined Chute Design." Design Chart No. IL-ENG-50, Drawing IL-ENG-122N.
5. R. Baker, 1988. "The Stability of Block Protection Systems in High Velocity Flows." University of Salford, Department of Civil Engineering. Final Report, SERC Grant GR/D/93385. Salford, England.
6. H. W. M. Hewlett, L. A. Borman, and M. E. Bramley, 1987. "Design of Reinforced Grass Waterways." Construction Industry Research and Information Association, Report I16, London, United Kingdom.
7. J. C. Bathurst, 1985. "Flow Resistance Estimation in Mountain Rivers." Journal of Hydraulic Engineering, Vol. III, No. 4, pp 625-643.
8. R. A. Mussetter, 1989. "Dynamics of Mountain Streams." Doctorate Dissertation, Colorado State University, Department of Engineering, Fort Collins, Colorado.
9. S. R. Abt, R. J. Wittler, J. F. Ruff, and M. S. Khattak, 1988. "Resistance to Flow Over Riprap in Steep Channels." Water Resources Bulletin, Vol. 24, No. 6, December.

